CHARACTERIZATION OF BIOPOLYMERS FOR USE AS MATRICES FOR ENCAPSULATION OF HYDROPHOBIC COMPOUNDS

A Dissertation

by

ALEX FRANK PUERTA-GOMEZ

Submitted to the Office of Graduate and Professional Studies of
Texas A&M University
in partial fulfillment of the requirements for the degree of

DOCTOR OF PHILOSOPHY

Chair of Committee,	Maria Elena Castell-Perez
Committee Members,	Rosana Moreira
	Joseph Awika
	Sandun Fernando
Head of Department,	Steve Searcy

May 2014

Major Subject: Biological and Agricultural Engineering

ABSTRACT

The high cost and potential toxicity of biodegradable polymers has increased the interest in natural and modified biopolymers as bioactive carriers. To design particles of small size characteristics, small dextrin (approximately15 nm) were prepared from waxy starches (WS) by enzymatic depolymerization with α-amylase of previous gelatinized WS granules. The small dextrin and phytoglycogen were converted to amphiphilic molecules by 3% and 7% octenyl succinate anhydrate (OSA) modification. Water sorption capability and the glass transition temperature (Tg) were associated with the physical stability of OSA-dextrin, OSA-phytoglycogen, and proteins like whey protein concentrate 80% (WPC), whey protein isolate (WPI), and α-lactalbumin (α-L). Depolymerization of WS incremented their water sorption capability and reduced the Tg at high relative humidity (RH) environment compared to native WS. The OSA modification did not change the adverse effect of depolymerization. The moisture sorption isotherm method could not accurately predict the effect of adsorbed water on the physical characteristics of the proteins, but it was consistent regarding the effect of plasticization by water adsorption on the Tg values of OSA-polysaccharides exposed to higher than 70% RH. The effectiveness of inexpensive encapsulating method based in self-assemble interaction of pure and combination of amphiphilic biopolymers in aqueous system was assessed using both fluorescent spectroscopy and rheological principles. Structure micelle-type formation of WPI (0.6 g/L) and α-lactalbumin (2.5 g/L) was determined by fluorescence. Different types of structure are formed by OSA-

polysaccharides (10-20 g/L). Dynamic oscillatory tests at 0.01Pa, 23°C and neutral pH (7.0) using an analysis of the relaxation time "λ" value (G'/G"*ω), showed high sensitivity to type, concentration and combination of biopolymers. A distinguishable linear reduction of "λ" values (slope) up to a critical frequency value can be used as indicator of structure formation. Absorbance measurements (600 nm) were congruent with OSA-polysaccharides interaction-adsorption by electrostatically precipitated proteins and with the entrapment efficiency based on precipitated protein. The "λ" slope value approach demonstrates the possibility to evaluate the geometric aspect ratio of anisotropic particles formed from electrostatic precipitation of proteins alone or in combination with OSA-polysaccharides. This new rheological evaluation demonstrates the possibility to assess interactions of self-assembled amphiphilic biopolymers in aqueous solution. Electrostatic precipitation (pH=4.5) of protein alone or combined with OSA-polysaccharides was well-suited and it offers a safer alternative to entrap volatile and thermolabile compounds than the commonly used PLGA (poly (lactic-co-glycolic) acid).

DEDICATION

To my beloved wife, Veria, for your love, care, optimism, and unconditional support to achieve all my goals.

To my children, Verita y Alejandro, for the refreshing energy you gave me every day in spite of expending a lot of time on my projects.

To my mother, Elia Rubi, for your words of encouragement and push for tenacity, and your willingness to help in any possible way.

ACKNOWLEDGEMENTS

I would like to thank my committee members for their support and guidance in the completion of this dissertation. Special thanks to Dr. M. Elena Castell-Perez for her friendship, guidance and encouragement to accomplish all my research projects.

In addition, I would also like to thank Dr. Rosana Moreira for her additional guidance on this research. Thanks to Dr. Fernando for welcoming me in his laboratory and to Nalin and Ivantha for their assistance in using the particle size analyzer.

Thanks to Dr. Gomes for welcoming me in her laboratory and let me use the spectrophometer. Thanks to Dr. Gee for his assistance on using the fluorometer. Special thanks to Laura Hills for her technical assistance with the TEM for the microstructure analysis.

Thanks to my colleagues at the Food Engineering Laboratory, Basri, Mustafa, Mauricio, Akhilesh, Taehoon, Isin, Laura, Paulo and Dr. Kim, for helping me in part of this research and being good fellows all these years.

Thanks also go to my friends, colleagues, the department faculty and staff for making my time at Texas A&M University a great experience.

TABLE OF CONTENTS

Page

ABSTRACT ii

DEDICATION iv

ACKNOWLEDGEMENTS v

TABLE OF CONTENTS vi

LIST OF FIGURES ix

LIST OF TABLES xv

CHAPTER I INTRODUCTION 1

CHAPTER II LITERATURE REVIEW 5

2.1 Use of biopolymers as a delivery system of bioactive compounds 5
2.2 Structure of amphiphilic biopolymers 7
2.2.1 OSA-modified polysaccharides 7
2.2.2 Whey proteins 8
2.3 Water sorption isotherm models 9
2.4 Glass transition temperature (Tg) 12
2.5 Self-assembly of amphiphilic molecules 13
2.6 Rheological test for characterization of biopolymeric solutions 14
2.6.1 Viscoelastic properties 14
2.6.2 Creep test 17
2.6.3 Zero-shear viscosity (ZSV) 19
2.6.4 Oscillatory frequency test 21

CHAPTER III CHARACTERIZATION OF THE PHYSICAL STABILITY OF BIOPOLYMERS 27

3.1 Overview 27
3.2 Introduction 28
3.3 Materials and methods 32
3.3.1 Materials 32
3.3.2 Preparation of OSA-modified polysaccharides 33
3.3.3 Percentage of modification (%OSA) 33
3.3.4 Enzymatic treatment of waxy starches 34
3.3.5 Total sugar content 36

3.3.6 Reducing sugar content 37
3.3.7 Microscopic observation 37
3.3.8 Particle size measurement 38
3.3.9 Moisture sorption isotherms 38
3.3.10 Glass transition temperature (Tg) 39
3.3.11 Prediction of glass transition temperature for pure biopolymers 40
3.3.12 Statistical analysis 41
3.4 Results and discussions 41
3.4.1 Waxy starches and phytoglycogen granules size 41
3.4.2 Enzymatic treatment of waxy starch 44
3.4.3 Moisture sorption isotherms 49
3.4.4 Glass transition temperature of biopolymers 56
3.5 Conclusions 64

CHAPTER IV FLUORESCENT AND RHEOLOGICAL METHODS TO ESTIMATE BIOPOLYMER INTERACTIONS FOR ENCAPSULATION PURPOSES 67

4.1 Overview 67
4.2 Introduction 69
4.3 Materials and methods 76
4.3.1 Materials 76
4.3.2 Preparation of OSA-modified polysaccharides 76
4.3.3 Percentage of modification (%OSA) 77
4.3.4 Enzymatic treatment of waxy starches 78
4.3.5 Total sugar content 79
4.3.6 Reducing sugar content 79
4.3.7 Sample preparation 80
4.3.8 Fluorescent method 80
4.3.9 Rheological evaluation 81
4.3.10 Statistical analysis 82
4.4 Results and discussion 82
4.4.1 Fluorescent characterization of biopolymers 82
4.4.2 Linear viscoelastic region (LVR) of diluted solution of proteins 89
4.4.3 Zero shear viscosity (ZSV) of diluted biopolymers by creep test analysis 92
4.4.4 Oscillatory sweep test 100
4.4.5 Relaxation time curve slopes of diluted combination of biopolymer solutions 117
4.5 Conclusions 125

CHAPTER V EVALUATION OF ENTRAPMENT EFFICIENCY, RHEOLOGY AND MICROSTRUCTURE FORMATION OF ELECTROSTATICALLY

PRECIPITATED PROTEINS IN COMBINATION WITH OSA-MODIFIED POLYSACCHARIDES 129

5.1 Overview 129
5.2 Introduction 130
5.3 Materials and methods 135
5.3.1 Materials 135
5.3.2 Preparation of OSA-modified waxy rice starch 135
5.3.3 Percentage of modification (%OSA) 136
5.3.4 Enzymatic treatment of waxy starches 137
5.3.5 Total sugar content (TS) 138
5.3.6 Reducing sugar content 138
5.3.7 Absorbance as indicator of particle formation 139
5.3.8 Polysaccharides adsorption by protein precipitation 140
5.3.9 Bradford protein assay 140
5.3.10 Particle synthesis 141
5.3.11 Entrapment efficiency 142
5.3.12 Rheological test 143
5.3.13 Particle morphology 143
5.3.14 Particle size measurement 144
5.3.15 Statistical analysis 144
5.4 Results and discussion 145
5.4.1 Electrostatically precipitation protein 145
5.4.2 Interaction of protein and OSA-modified polysaccharides in aqueous solution 153
5.4.3 Entrapment efficiency of different combinations of protein/OSA-modified polysaccharides 157
5.4.4 Relaxation time slopes of solution combinations of biopolymers at ratio 1:1 160
5.4.5 Microstructure formation by solutions combination of biopolymers at ratio 1:1 165
5.4.6 Particle size of structures formed by combination of biopolymers at ratio 1:1 171
5.5 Conclusion 173

CHAPTER VI CONCLUSIONS 176

CHAPTER VII RECOMMENDATIONS FOR FURTHER STUDIES 179

REFERENCES 181

APPENDIX A 196

LIST OF FIGURES

Page

Figure 2.1. Relationship of food deterioration rate as a function of water activity.....10

Figure 2.2. Measurement of glass transition temperature (Tg) by differential scanning calorimetry.....12

Figure 2.3. Representation of Maxwell material.....16

Figure 2.4. Creep test for ketchup at constant stress (5 Pa) and 23°C. 19

Figure 2.5. Representation of viscosity as a function of shear rate for a Brookfield standard fluid (4.3 cP) at 23°C. 20

Figure 2.6. Sinusoidal wave forms for stress and strain functions.....22

Figure 2.7. Dynamic oscillatory test for 184 g/L whey protein isolate (WPI) (diluted solution) in aqueous solution. 24

Figure 3.1. Natural waxy corn starch (A), waxy rice starch (B) and phytoglycogen (C) granules. 42

Figure 3.2. Size distribution of waxy corn, waxy rice starch and phytoglycogen granules. Hydrodynamic diameter was measured using a Particle Size Analyzer which determines particle size based on the dynamic properties of particles moving in a solvent.....43

Figure 3.3. Enzymatic treatment 1 (T1) of waxy corn and waxy rice starches during different incubation times at 65°C.....46

Figure 3.4. Size distribution of waxy corn (A) and waxy rice (B) starches after enzymatic treatment 1 (T1) during different incubation times at 65°C.....47

Figure 3.5. Size distribution of (A) waxy corn and (B) waxy rice starches after enzymatic treatment 2 (T2) first incubated at 100°C for 20min and continuing the treatment during different incubation times at 65°C. 48

Figure 3.6. Moisture sorption isotherms at 23°C of native waxy corn starch, with (A) 3% OSA modification and (B) 7% OSA modification at different degree of enzymatic depolymerization (DE=7 - 22). 50

Figure 3.7. Moisture sorption isotherms at 23°C of (A) native phytoglycogen at different percentage of OSA modification (3% and 7%) and (B)

depolymerized waxy corn starch (DWxCn), depolymerized waxy rice starch (DWxRc), phytoglycogen (Phytg) at 7% OSA modification, α-lactalbumin (A-L), whey protein isolate (WPI) and whey protein concentrate 80% (WPC). 52

Figure 3.8. Effect of mass fraction of adsorbed water on the glass transition temperature of (A) depolymerized (DE = 22) waxy corn starch and (B) depolymerized (DE = 24) waxy rice starchat different DE with 3% and 7 % of OSA modification. 59

Figure 3.9. Effect of mass fraction of adsorbed water on the glass transition temperature of (A) phytoglycogen at different percentages of OSA modification and (B) whey proteins : α-lactalbumin, whey protein isolate (WPI) and whey protein concentrate 80% (WPC) 60

Figure 3.10. Effect of water sorption on the physical appearance of depolymerized and OSA-modified waxy corn (D22-WxCn7), waxy rice (D24-WxRc7) starch, α-lactalbumin, whey protein isolate (WPI), and whey protein concentrated 80% (WPC) after 10 days of storage at 23°C and different RH. 63

Figure 4.1. Critical Micelle Concentration (CMC) of (A) α- lactalbumin and (B) whey protein isolate by a fluorescent method using 2 μM of pyrene at 23°C. Pyrene excitation at 337 nm and local polarity based on the intensity ratio of emission at I_1 (373 nm) and I_3 (383 nm). 84

Figure 4.2. Critical Micelle Concentration (CMC) of (A) 3% OSA-modified depolymerized (DE=24) waxy rice starch (DWxRc3) and (B) 7% OSA-modified depolymerized (DE=24) waxy rice starch (DWxRc7) by a fluorescent method using 2 μM of pyrene at 23°C. Pyrene excitation at 337 nm and local polarity based on the intensity ratio of emission at I_1 (373 nm) and I_3 (383 nm). 86

Figure 4.3. Critical Micelle Concentration (CMC) of (A) 3% OSA-modified depolymerized (DE=22) waxy conr starch (DWxCn3) and (B) 7% OSA-modified depolymerized (DE=22) waxy corn starch (DWxCn7) by a fluorescent method using 2 μM of pyrene at 23°C. Pyrene excitation at 337 nm and local polarity based on the intensity ratio of emission at I_1 (373 nm) and I_3 (383 nm). 87

Figure 4.4. Critical Micelle Concentration (CMC) of (A) 3% OSA-modified phytoglycogen (Phytg3) and (B) 7% OSA- phytoglycogen (Phytg7) by a fluorescent method using 2 μM of pyrene at 23°C. Pyrene excitation at 337 nm and local polarity based on the intensity ratio of emission at I_1 (373 nm) and I_3 (383 nm). 88

Figure 4.5. Linear viscoelastic region (LVR) of α-lactalbumin and whey protein isolate at (A) 1.0Hz and (B) 0.1 Hz and 23°C. 90

Figure 4.6. Linear viscoelastic region (LVR) of α-lactalbumin and whey protein isolate at (A) 1.0 Hz and (B) 0.1 Hz and 23°C. 91

Figure 4.7. Zero Shear Viscosity of α-lactalbumin solutions measured by creep test at 0.01Pa and 23°C. (A) Viscosity values influenced by the shear rate. (B) Compliance curve as function of time application of constant stress (0.01 Pa). 93

Figure 4.8. Zero Shear Viscosity of whey protein isolate solutions measured by creep test at 0.01Pa and 23°C. (A) Viscosity values influenced by the shear rate. (B) Compliance curve as function of time application of constant stress (0.01 Pa). 94

Figure 4.9. Zero-shear-viscosity (ZSV) for serial dilutions of (A) α-lactalbumin and (B) whey protein, calculated from creep test at 0.01Pa and 23°C. 97

Figure 4.10. Zero-shear-viscosity (ZSV) for serial dilutions of (A) 3% OSA-modified depolymerized waxy rice (DWxRc3) and (B) 7% OSA-modified depolymerized waxy rice (DWxRc7), calculated from creep test at 0.01Pa and 23°C. 98

Figure 4.11. Zero-shear-viscosity (ZSV) for serial dilutions of (A) 3% OSA-modified phytoglycogen (Phytg3) and (B) 7% OSA-modified phytoglycogen (Phytg7), calculated from creep test at 0.01Pa and 23°C. 99

Figure 4.12. Elastic modulus (G'), viscous modulus (G") (A) and complex viscosity (η*) curves (B) for different concentrations of α-lactalbumin solutions. Oscillatory frequency sweep test was performed at 0.01 Pa and 23°C. 101

Figure 4.13. Elastic modulus (G'), viscous modulus (G") (A) and complex viscosity (η*) curves (B) for different concentrations of whey protein isolate solutions. Oscillatory frequency sweep test was performed at 0.01 Pa and 23°C. 102

Figure 4.14. Elastic modulus (G'), viscous modulus (G") (A) and complex viscosity (η*) curves (B) for different concentrations of 3% OSA-modified depolymerized waxy rice (DWxRc3) solutions. Oscillatory frequency sweep test was performed at 0.01 Pa and 23°C. 104

Figure 4.15. Elastic modulus (G'), viscous modulus (G") (A) and complex viscosity (η*) curves (B) for different concentrations of 7% OSA-modified

depolymerized waxy rice (DWxRc7) solutions. Oscillatory frequency sweep test was performed at 0.01 Pa and 23°C. 106

Figure 4.16. Elastic modulus (G'), viscous modulus (G") (A) and complex viscosity (η*) curves (B) for different concentrations of 3% OSA-modified phytoglycogen (Phytg3) solutions. Oscillatory frequency sweep test was performed at 0.01 Pa and 23°C. 107

Figure 4.17. Elastic modulus (G'), viscous modulus (G") (A) and complex viscosity (η*) curves (B) for different concentrations of 7% OSA-modified phytoglycogen (Phytg7) solutions. Oscillatory frequency sweep test was performed at 0.01 Pa and 23°C. 108

Figure 4.18. Relaxation time (λ) curves for different concentrations of (A) α-lactalbumin and (B) whey protein isolate (WPI) evaluated by oscillatory frequency sweep test at 0.01 Pa and 23°C. 111

Figure 4.19. Relaxation time (λ) curves for different concentrations of (A) 3% OSA-modified depolymerized waxy rice (DWxRc3) and (B) 7% OSA-modified depolymerized waxy rice (DWxRc7) evaluated by oscillatory frequency sweep test at 0.01 Pa and 23°C. 112

Figure 4.20. Relaxation time (λ) curves for different concentrations (A) 3% OSA-modified phytoglycogen (Phytg3) and (B) 7% OSA-modified phytoglycogen (Phytg7) evaluated by oscillatory frequency sweep test at 0.01 Pa and 23°C. 113

Figure 4.21. Comparison of hydrophobic interaction of 3.6 g/L α-lactalbumin with different concentrations of (A) 3% OSA-modified depolymerized waxy rice (DWxRc3) and (B) 7% OSA-modified depolymerized waxy rice (DWxRc7) by relaxation time (λ) values at 0.01Pa and 23°C of different aqueous concentrations. 118

Figure 4.22. Comparison of hydrophobic interaction of 3.6 g/L α-lactalbumin with different concentrations of (A) 3% OSA-modified phytoglycogen (Phytg3) and (B) 7% OSA-modified phytoglycogen (Phytg7) by relaxation time (λ) values at 0.01Pa and 23°C of different aqueous concentrations. 119

Figure 4.23. Comparison of hydrophobic interaction of 3.6 g/L whey protein isolate with different concentrations of (A) 3% OSA-modified depolymerized waxy rice (DWxRc3) and (B) 7% OSA-modified depolymerized waxy rice (DWxRc7) by relaxation time (λ) values at 0.01Pa and 23°C of different aqueous concentrations. 120

Figure 4.24. Comparison of hydrophobic interaction of 3.6 g/L whey protein isolate with different concentrations of (A) 3% OSA-modified phytoglycogen (Phytg3) and (B) 7% OSA-modified phytoglycogen (Phytg7) by relaxation time (λ) values at 0.01Pa and 23°C of different aqueous concentrations. 121

Figure 5.1. Visual observation (A) and absorbance values at 600 nnm (B) for different concentrations of α-lactalbumin precipitation at different pH values measured at 23°C. 147

Figure 5.2. Visual observation (A) and absorbance values at 600 nnm (B) for different concentrations of whey protein isolate (WPI) precipitation at different pH values measured at 23°C. 148

Figure 5.3. Electrostatic precipitation at pH 4.5 of 184 g/L of (A) α-lactalbumin and (B) whey protein isolate. 150

Figure 5.4. Effect of pH on absorbance at 23°C for combination of 3.6 g/L of depolymerized waxy corn and phytoglycogen at different percentages of OSA modification with (A) 1.4 g/L of α-lactalbumin and (B) 3.6 g/L of whey protein isolate. 152

Figure 5.5. OSA-modified polysaccharide (PSC) adsorption after precipitation of (A) 2.8 g/L α-lactalbumin and (B) 3.6 g/L WPI at pH 4.5 and 23°C for different concentration ratios of PSC and protein. 156

Figure 5.6. Relaxation time (λ) curves for different combination of biopolymers at 1:1 weight ratio with a total concentration of 184 g/L in aqueous solutions, evaluated by oscillatory sweep test at 0.01 Pa and 23°C. 162

Figure 5.7. Micrographs of electrostatically precipitated particles formed at a concentration of 184 g/L (A) α-lactalbumin (α-L) and (B) Whey protein isolate (WPI). Images were taken at 50,000x magnification. 167

Figure 5.8. Micrographs of electrostatically precipitated particles formed at 1:1 weight ratio to a total concentration of 184 g/L for different combination of α-lactalbumin (α-L) with (A) DWxRc3, (B) DWxRc7, (C) Phytg3, and (D) Phytg7. Images were taken at 50,000x magnification. 168

Figure 5.9. Micrographs of electrostatically precipitated particles formed at 1:1 weight ratio to a total concentration of 184 g/L for different combination of whey protein isolate (WPI) with (A) DWxRc3, (B) DWxRc7, (C) Phytg3, and (D) Phytg7. Images were taken at 50,000x magnification. 169

Figure 5.10. Particle size of electrostatically precipitated combination of proteins and OSA-modified polysaccharides at 1:1 weight ratio with a total concentration of 184 g/L. 172

LIST OF TABLES

Page

Table 3.1 GAB-model parameters at water activity (Aw) range of 0.11 - 0.97, monolayer value (vm), critical water activity and energy constants CG and k for natural and depolymerized waxy corn starch and waxy rice starch, natural and phytoglycoge with 3% and 7 % of OSA modification, α-lactalbumin, whey protein isolate and whey protein concentrated. 53

Table 3.2. Glass transition temperature (Tg) for depolymerized (DE) OSA-modified (3% and 7%) waxy corn starch, waxy rice starch, phytoglycogen, α-lactalbumin, whey protein isolate and whey protein concentrate 80%. 57

Table 3.3. Glass transition temperature (Tg) values and Gordon-Taylor and Kwei model constants for different biopolymers stored at different relative humidities. 61

Table 4.1. Relaxation time (λ) slope and critical frequency value (CFV) for different concentrations of biopolymers evaluated by oscillatory frequency sweep test at 0.01 Pa and 23°C. 116

Table 4.2. Relaxation time (λ) slope and critical frequency value (CFV) for different biopolymers combinations, evaluated by oscillatory frequency sweep test at 0.01 Pa and 23°C. 123

Table 5.1. Protein concentration and amount of precipitated protein after electrostatic aggregation at pH 4.5 of 184 g/L. 149

Table 5.2. Average entrapment efficiency percentage (EE%) of 10mM trans-cinnamaldehyde for different combination ratios (1:0, 1:1, 1:3, 1:10) of α-lactalbumin and whey protein isolate with OSA-modified depolymerized-waxy rice and phytoglycogen at 23°C. Total mixture concentration of 184 g/L in aqueous solutions. 158

Table 5.3. Relaxation time (λ) slope and critical frequency value (CFV) for α-lactalbumin and WPI alone or in combinations (1:0, 1:1, 1:3, and 1:10) with different OSA-modified polysaccharides, evaluated with oscillatory sweep test at 0.01Pa and 23°C. Total biopolymers concentration in aqueous solution 180 g/L. 164

CHAPTER I

INTRODUCTION

Biodegradable polymers such as poly(alkyl cyanoacrylate), polylactic acid (PLA), poly(ε-caprolactone, PCL), poly(glycolic acid, PGA), polyethyleneglycol (PEG), and the association of two biodegradable polymers consisting on diblock copolymer of PLA-PGA and PLGA (poly (lactic-co-glycolic) acid) have potential as carriers of natural ingredients (Quintanar-Guerrero et al., 1998). In particular, PLGA has been widely used because it is approved by the FDA (Food and Drug Administration) for human therapy (Astete and Sabliov, 2006). However, the major drawbacks restricting the use of these biodegradable polymers in large-scale food applications are their high costs of production and, the potential toxicity of different components (e.g. toxic reagents) involved in the encapsulation manufacture process. Conversely, the use of complexes and conjugates of proteins and polysaccharides as delivery systems for bioactive molecules have many advantages. Most of the proteins and polysaccharides originate from natural food raw materials, and are therefore considered GRAS (generally recognized as safe), are widely available, and are relatively inexpensive (Livney, 2008). The application of proteins and/or hydrocolloids for coating and particle formation purposes may provide a very effective delivery system that integrates into each other the inherent characteristics from both types of biopolymers, so that their performance is enhanced (Sekhon, 2010).

Whey proteins are by-products from cheese preparation and their good gelling and emulsification properties make them a valuable food ingredient (Gunasekaran et al., 2007). Similarly, polysaccharides, the most abundant polymer in the human diet, have relative low cost and the conversion of highly branched phytoglycongen and waxy starch into alkenyl esters by octenyl succinate anhydrate (OSA) modification, turn them into amphiphilic molecules capable to stabilize emulsions (Liu et al., 2008; Tesch et al., 2002) or to entrap and protect hydrophobic compounds from oxidative deterioration (Scheffler et al., 2010b).

Amphiphilic molecules such as surfactants, lipids, copolymers, OSA-modified polysacharides and proteins carry both hydrophilic (polar, water loving) and hydrophobic (nonpolar, lipid loving) properties. These amphiphilic molecules can self-associate into a variety of different structures in aqueous solutions. When the solution conditions are changed (e.g. the ionic strength, type of ions in the solution, the pH, or temperature) the structure can be transformed to a different one (Israelachvili, 2010). Amphiphilic structures are often soft or fluid-like, with the molecules in constant thermal motion within each aggregate: twisting, turning, diffusing, and bobbing in and out of the surface.

Self-assembling structures produce a viscoelastic behavior observed by oscillatory shear (Pätzold and Dawson, 1996). Identification of the linear viscoelasticity for biopolymers diluted in aqueous solution is essential to determine intrinsic properties of the colloidal system, which in turn, will contribute to characterize the structure and interaction between amphiphilic biopolymers. Although linear viscoelasticity of

suspensions has been very difficult to measure at high frequency (Li et al., 2005), the identification of solid-like properties in liquid water at room temperature and at low frequency oscillatory sweep (Noirez and Baroni, 2012) make the possibility to evaluate solid-like behavior in biopolymer solutions. For instance, the solid-like behavior has been previously associated with self-assemble network formation between association of hydrophobic polymer and nonionic surfactant (Talwar et al., 2006). Likewise, the rheological properties of hydrophobically modified polymers of cellulose in aqueous solution were influenced by their molecular structure, hydrophobic association and functionality (Karlson, 2002) and the understanding of intermolecular interactions of biopolymers based on rheological tests would be very helpful in the design of amphiphilic biopolymers as a carrier of bioactive compounds in food and other applications.

The capability of proteins to form aggregates and precipitate at certain conditions of temperature, pH, ionic strength or enzymatically induced by microbial transglutaminase (Jones et al., 2010a; Majhi et al., 2006; Shpigelman et al.; Tang et al., 2006) make these biopolymers suitable materials to prepare and isolate nanoparticles for drug delivery systems. For example, spheroid particles between 100 to 250 nm in diameter were formed by heating 83°C for 15 min β-lactoglobulin solutions in combination with high and low methoxyl pectin (Jones et al., 2010b). Similarly, self-assembled nanotubes of about 20 nm outer diameter have been reported to form partially hydrolyzed α –lactalbumin in combination with calcium (Ipsen and Otte, 2007). These

structures have a good potential to serve as carriers for nanoencapsulated nutrients, supplements, and pharmaceuticals.

There is limited information available about the physical stability and self-assemble capability of OSA-modified polysaccharides, as well as in combination with different proteins in order to encapsulate bioactive compounds. The main goal of this research was to develop a low cost and GRAS encapsulation method by employing natural or modified biopolymers as a delivery system for hydrophobic bioactive compounds. The main hypothesis was that natural abundant polysaccharides could be nanosized and converted into amphiphilic molecules to work alone or in combination with nanosize macromolecules such as proteins to form small self-assembled structures that will be easy to recover and store for further use.

The specific objectives of this research were:

1. To characterize the physical stability of amphiphilic biopolymers at different RH environment to elucidate the possible applications as bioactive carriers.

2. To develop an effective method to determine the type of molecular interaction for better engineering of self-assemble structures according to concentration and combination of different amphiphilic biopolymers.

3. To develop an effective method to understand and predict the entrapment capability and structure-type formation using inexpensive and GRAS synthesis of particles from self-assemble amphiphilic biopolymers.

.

CHAPTER II

LITERATURE REVIEW

2.1 Use of biopolymers as a delivery system of bioactive compounds

The benefits of using bioactive compounds, often extracted from plant roots, leaves, flowers, etc., have been enhanced by their entrapment in special vehicles necessary to retain their performance and maximize their solubilization capacity, bioavailability, and bioefficacy in foods. Encapsulation of bioactive compounds can be prepared from preformed biodegradable polymers such as poly(alkyl cyanoacrylate), polylactic acid (PLA) , poly(ε-caprolactone, PCL), poly(glycolic acid, PGA), polyethyleneglycol (PEG), and the association of two biodegradable polymers consisting of diblock polymers of PLA-PGE and PLGA (poly lactic-co-glycolic acid). In particular, PLGA has been widely used because it is FDA- approved for human therapy (Fanun, 2010). However, the encapsulation methods for biodegradable polymers are in continuous effort to reduce manufacturing cost, and the potential toxicity of different components (e.g. toxic reagents) involved in the process.

Natural polymers have many advantages over their synthetic counterparts for food applications owing to their biodegradable properties and, in many cases, lower cost and free of noxious chemical reagents. For example, proteins and polysaccharides, which are abundant natural food raw materials, are relatively inexpensive and are considered GRAS (generally recognized as safe) for food application (Livney, 2008).

The new advances in bioactive compound delivery have been in the preparation of amphiphilic molecules from polysaccharides as versatile surface active agents. Starch has been hydrophobically modified by reaction with octenyl succinate anhydride (OSA) to become a strongly surface- active compound (Prochaska et al., 2007). Nanoparticles prepared of OSA- modified phytoglycogen in combination with ε-polylysine, a food grade polypeptide, have been proven to enhance the lipid oxidative stability of oil/water emulsions (Scheffler et al., 2010b).

Proteins are natural amphiphilic molecules with polar, ionic, or zwitterionic hydrophilic part and a non-polar hydrophobic part, which make them a surface active agent. Extensive food and pharmaceutical applications have been done by using milk proteins such as β-casein micelle for delivering hydrophobic bioactive potent anticancer and antioxidant natural polyphenol (Esmaili et al., 2011), nanotubes formed from partial hydrolyzed α-lactalbumin as a viscosifier, gelling agent and possible targeted drug release application (Ipsen and Otte, 2007). Moreover, the combination of proteins and polysaccharides for coating and particle formation provide a very effective delivery system that integrates into each other the inherent characteristics to enhance their performance (Sekhon, 2010). For example, edible coating films formed by combination of whey protein, glycerol and hydroxypropylmethylcellulose (HPMC) were stronger with the same oxygen permeability as whey protein and glycerol films and lower oxygen permeability than HPMC films (Brindle and Krochta, 2008). Nanoparticle formation in aqueous combination of anionic high or low methoxyl pectins and β-lactoglobulin was possible to produce at pH 4.75 by thermal denaturation of protein (Jones et al., 2010b).

The reasonable design of encapsulation systems requires a physicochemical understanding of the mechanism by which compounds are encapsulated and released (Madene et al., 2006). There is much more engineering and scientific work to do for the characterization of OSA-modified polysaccharides and integrate it to the current information.

2.2 Structure of amphiphilic biopolymers

2.2.1 OSA-modified polysaccharides

The octenyl succinate is attached to the starch through an ester linkage, which makes OSA-modified starch form strong films at the oil-water interface, giving emulsions that are resistant to agglomeration (Viswanathan, 1999). When a glycosyl unit is a branch point, there is one less hydroxyl group for every branching unit attached to that unit. However, every branch, even if it is a single unit branch, is terminated with a non-reducing end-unit that contains four unsubstituted hydroxyl groups, thus balancing the one lost through branching. No matter how highly branched is a polysaccharide, it has an average number of three hydroxyl groups per glycosyl unit (Dumitriu, 2005). The maximum percentage of hydroxyl group modification of three can be obtained (% OSA = 75).

The hydroxyl groups of the glycosyl units of the starch react with the carboxylic acid anhydride of OSA in the presence of a suitable base. The glucose moiety or residual of starch binds to water while the lipophilic, octenyl part binds to oil; thus, the OSA-modified starch produce stable emulsions.

2.2.2 Whey proteins

β-lactoglobulin is a major constituent with about 58 % of the whey protein, hence tend to dominate the assemble behavior of whey proteins (Hansted et al., 2011). The monomeric unit of β-lactoglobulin consists of 162 amino acid residues and has a molecular mass of about 18.3 kDa. The isoelectric point of the protein is 5.1. β-lactoglobulin monomer contains five cysteine residues, four of which are involved in intramolecular disulfide bridges (Verheul et al., 1999). Secondary structures of β-lactoglobulin are formed by folding up into 8-stranded antiparallel β–barrel structures with a 3-turn lone α–helix located on the surface of the molecule (Kontopidis et al., 2004). The most distinctive feature of this protein is the presence of 8-stranded β-barrel structures which give them the capability to bind and transport small hydrophobic molecules in the beta barrel calix.

α-lactalbumin is a small (MW14,200), acidic (pI 4.5), Calcium binding milk protein (Permyakov and Berliner, 2000). α-lactalbumin is composed of 123 amino acid residues and 4 disulfide bridges. In a native state, α-lactalbumin consists of a large α-helical domain composed of 3 major α-helices and 2 short helical structures and a second small domain β-sheet composed of a 1series of loops, where tree-stranded antiparallel β-pleated sheet are connected by calcium binding and a short helical structure connected by hydrogen bonds (Permyakov and Berliner, 2000).

2.3 Water sorption isotherm models

Water activity (A_w) is directly related to equilibrium relative humidity (RH) of a food, controlling its availability to act as solvent (Figure 2.1). The physical state of powdered food systems depends on the amount of water acting as plasticizer. When water is adsorbed and exceeds the monolayer capacity value of a glassy state powdered food, it becomes rubbery and sticky thus reducing its quality (Labuza, 1980; Levine and Slade, 1986). The water monolayer capacity value and their energy constant are computed from the moisture sorption isotherm curves, which characterizes the relationship between the moisture content and the water chemical potential in foods (Tesch et al., 1999).

An additional function of the sorption isotherm curve is the quantification of the critical water activity that is related to the water monolayer capacity. Although this parameter is a much better predictor of safety and quality than the water monolayer capacity, there are times when it is necessary to know both water activity and moisture content. Critical water activity has also been related to mechanical properties and product stability in low moisture products. When the moisture content related to the critical water activity is reached, a transition from glassy to rubbery occurs, which affects the mechanical properties of the product (Barbosa-Cánovas et al., 2007).

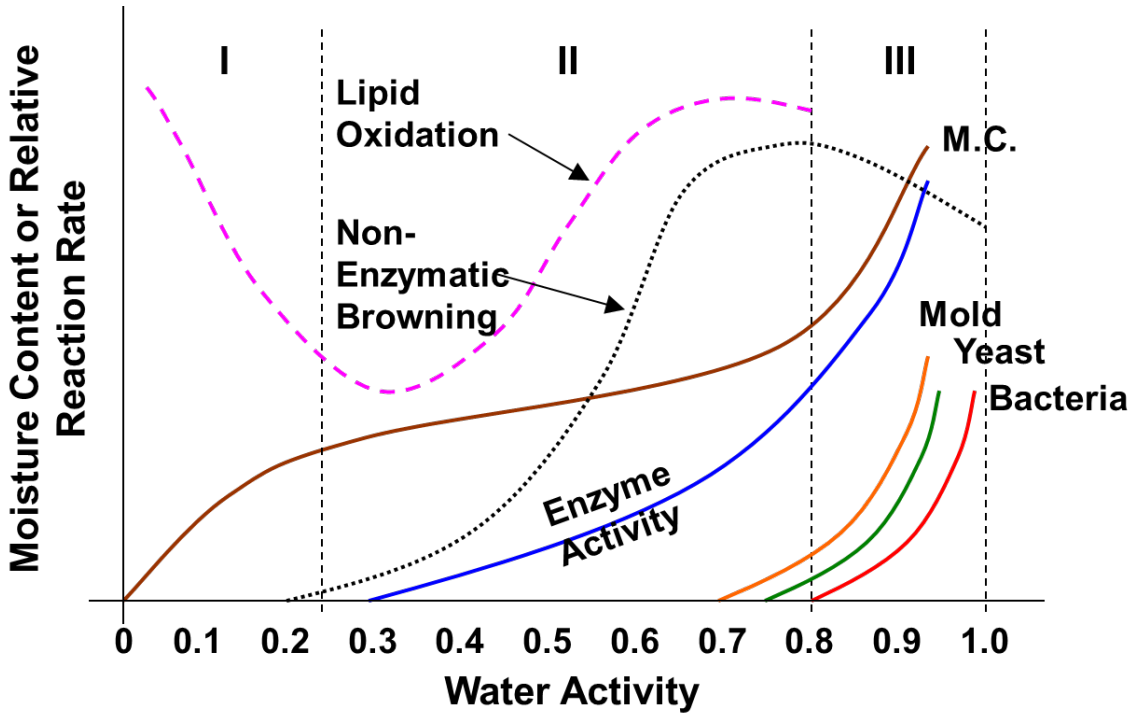

Figure 2.1. Relationship of food deterioration rate as a function of water activity.

The two parameter BET (Brunauer-Emmett-Teller) and the three parameter GAB (Guggenheim-Andersen-de Boer) models are widely accepted to characterize moisture sorption in food materials. (Timmermann, 2003). Unlike the BET equation, that covers only the water activity interval of 0.05< Aw< 0.30, the versatility of the GAB equation allows the use of wider water activity range (0.05< Aw< 0.8 - 0.90) on the analysis. However, the BET and the GAB isotherms are closely related as they come from the same statistical model (Timmermann et al., 2001).

The BET (Brunauer-Emmett-Teller) sorption isotherm model is given in the following equation (Timmermann, 2003) :

$$v(A_w) = \frac{v_m * C_B * A_w}{(1-A_w)(1+(C_G-1)*A_w)} \quad (2.1)$$

Where $v(A_w)$ is the amount of water adsorbed by 100 grams of dehydrated sample at vapor pressure A_w (relative vapor pressure of saturated salt solution), v_m is the BET water monolayer capacity in the same units as $v(A_w)$, C_B is the energy constant related to the differences of the free enthalpy between water molecules in the pure liquid and in the monolayer (Timmermann, 1989).

The Guggenheinm-Anderson-de Boer (GAB) sorption isotherm model is given in the following equation (Timmermann, 2003) :

$$v(A_w) = \frac{v_m * C_G * k * A_w}{(1-k*A_w)(1+(C_G-1)k*A_w)} \quad (2.2)$$

Where v_m is the GAB water monolayer capacity in the same units as $v(A_w)$, C_G is the energy constant and k indicates the difference of free enthalpy between water molecules in the pure liquid and in the layers above the monolayer (Timmermann, 1989).

The differences between the set of values of these two equations have been found to be always the same: v_m (BET) < v_m (GAB); C_B (BET) > C_G (GAB) (Timmermann, 2003).

2.4 Glass transition temperature (Tg)

The glass transition temperature (Tg) is the reversible transition from a hard and relatively brittle state (glass) into a molten or rubber state of amorphous materials (Roos, 2010). Despite the massive change in the physical properties of a material through its glass transition, the transition is not itself a phase transition of any kind; rather it is a change in the physical state extending over a range of temperature and defined by one of several conventions (Abiad et al., 2009).

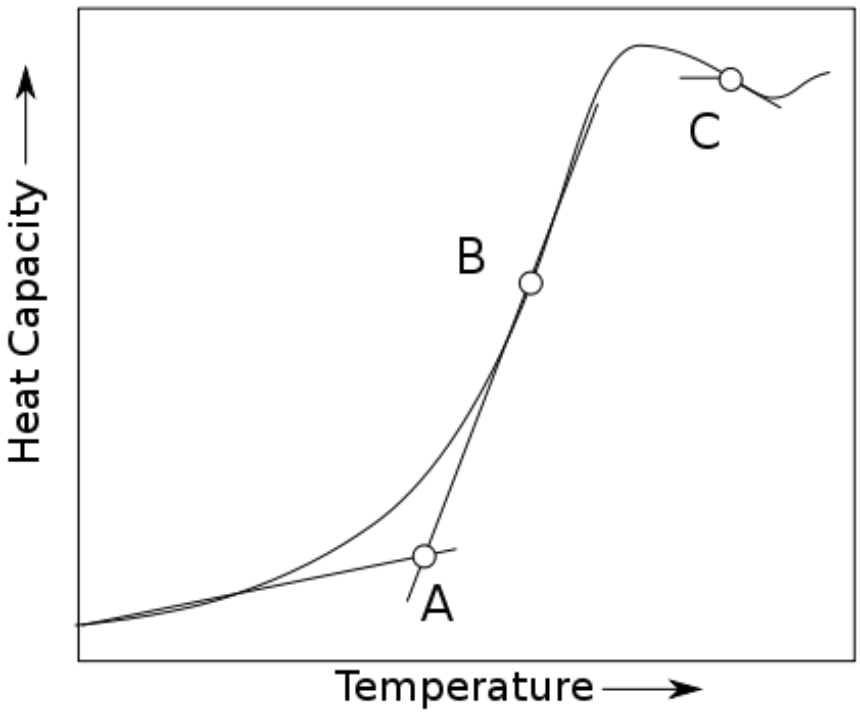

Figure 2.2. Measurement of glass transition temperature (Tg) by differential scanning calorimetry

In the plotting of heat capacity as a function of temperature (Figure 2.2), Tg is the temperature corresponding to point A on the curve. To make this physical characteristic reproducible, the cooling or heating rate must be specified. Water is recognized as a strong plasticizer of amorphous carbohydrates, and when the water content of the carbohydrate increases the glass transition temperature strongly decreases (Slade and Levine, 1995).

2.5 Self-assembly of amphiphilic molecules

Surfactants are amphiphilic molecules with a polar, ionic, or zwitterionic hydrophilic part and a non-polar hydrophobic part. Surfactants reduce the surface tension of water by adsorbing at the liquid-gas interface. They also reduce the interfacial tension between oil and water by adsorbing at the liquid-liquid interface (Rosen and Kunjappu, 2012). Many surfactants can also self-assemble in the bulk solution into aggregates such as micelles, microemulsions, bilayers, and vesicles. These structures and the systems they form depends on the balance of different forces such van der Waals, hydrophobic, hydrogen-bonding, and screened electrostatic interactions, which are influence by the conditions of the surrounding environment. Thus, these structures can interchange from one to another when the solution conditions such as the electrolyte or lipid concentration, pH, or temperature changes (Israelachvili, 2010).

The formation of a particular shape corresponds to specific geometric packing properties of the amphiphilic molecule in the particular environment. This property can be expressed by the so called packing parameter (*v/al*), which is defined as the ratio

between the volume of the hydrophobic chain (v) and the product of the head group area (a) and the chain length (l). The packing parameter lower than unity facilitates the formation of structures where the polar interface is curved towards the hydrocarbon (cone shaped amphiphile) such as micelles, cylindrical micelles and vesicles (Nylander et al., 2008).

2.6 Rheological test for characterization of biopolymeric solutions

2.6.1 Viscoelastic properties

Viscoelasticity is the property of materials that exhibit both viscous and elastic characteristics when undergoing deformation. Viscous materials, like honey, resist shear flow and strain linearly with time when a stress is applied. Elastic materials strain when stretched and quickly return to their original state once the stress is removed. Viscoelastic materials have elements of both of these properties and, as such, exhibit time-dependent strain. Whereas elasticity is usually the result of bond stretching along crystallographic planes in an ordered solid, viscosity is the result of the diffusion of atoms or molecules inside an amorphous material (Meyers and Chawla, 2009)

Viscoelasticity is used in polymer science to characterize the microstructure and chemistry of polymeric materials (Roylance, 2001). Furthermore, determination of the linear viscoelastic region can represent intrinsic properties of the colloidal system. An important point is that not just polymeric liquids show elastic behavior, but all liquids do, at sufficiently small time scales (Sunthar, 2010).

In the case of viscoelastic materials, modified mechanical characterization tests are performed by applying a uniaxial tensile test, similar to that used for elastic solids. Although many viscoelastic tensile tests have been used, the most common are creep, stress relaxation, and oscillatory frequency sweeps (Roylance, 2001).

For viscoelasticity analysis, model substances such as springs (elastic component) and dashpots (viscous component), either single or in combinations have been used to correlate stress or strain applications to the time-dependent deformation reactions. Maxwell and Kevin-Voigt models are two common models that correlate constant stress application with time-dependent deformation reaction, and these models, in comparison with real fluids has been difficult to link to distinct molecular structures, although in the case of molecular melts (high concentration) they have been used to understand their viscoelasticity (Schramm, 2002).

The serial or parallel connection between the mechanical models will define whether one deals with a viscoelastic solid (Kelvin-Voigt solid, parallel connection) or a viscoelastic liquid (Maxwell liquid, serial connection).

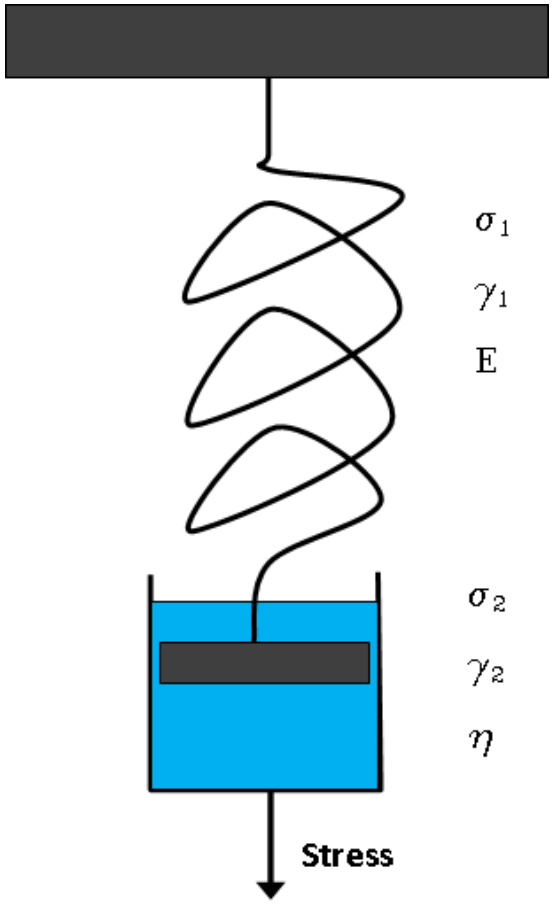

Figure 2.3. Representation of Maxwell material.

The "Maxwell" model (Figure 2.3) is a mechanical representation of a Hookean spring (E) and a Newtonian dashpot (η), which are connected in series. The spring should be visualized as representing the elastic or energetic component of the response, while the dashpot represents the conformational or entropic component.

In a series connection such as the Maxwell model, the stress on each element is the same and equal to the imposed stress: $\sigma = \sigma_1 = \sigma_2$; while the total strain is the sum of the strain in each element: $\gamma_{total} = \gamma_1 + \gamma_2$

Forces applied may lead to tensile or shear stresses and the tensile modulus E (Young's modulus or stiffness) under tension or the shear modulus G (rigidity) under shear torsion are the correlating factors representing the resistance of a solid against being deformed (elastic component).

The dynamic viscosity, η, represents the resistance of the liquid being forced to flow (viscous component) and it can be describes as $\tau = \eta d\gamma/dt$.

The combination of a dashpot and a spring will lead to a time-dependent response single equation relating the constant stress applied to the spring and dashpot strain rates in terms of the stress, σ:

$$\sigma(t) = G\gamma(t) + \eta\frac{d\gamma(t)}{dt} \tag{2.3}$$

Where *t* is time of constant stress applied.

2.6.2 Creep test

In creep tests a constant stress is assigned, σ_0 and the time-related strain, γ is measured as a function of time. The two can be mathematically interrelated by:

$$\gamma(t) = J(t) * \sigma_0 \tag{2.4}$$

This equation introduces the new term of the time-related creep compliance J(t), which is defined as the ratio of measured strain and assigned stress:

$$J(t) = \frac{\gamma(t)}{\sigma_0} \quad ; \ (1/\text{Pa}) \tag{2.5}$$

As long as the test is performed in the linear viscoelastic region, the compliance will be independent of the applied stress. This fact is used to define the limits for the proper creep and recovery testing of viscoelastic fluids within the limits of linear viscoelasticity (Schramm, 2002).

The compliance/time plot is shown in Figure 2.4. During the creep phase, the compliance can be decomposed into two components. Data from the linear portion of the creep curve are related to two parameters: the slope; *dJ/dt*, that is equal to the inverse of the ZSV, and the intercept, sometimes called the steady state compliance, which is equal to $J_0 + J_1$, where J_0 is the instantaneous elastic component due to spring in the Maxwell model, and J_1 is the delayed elastic component.

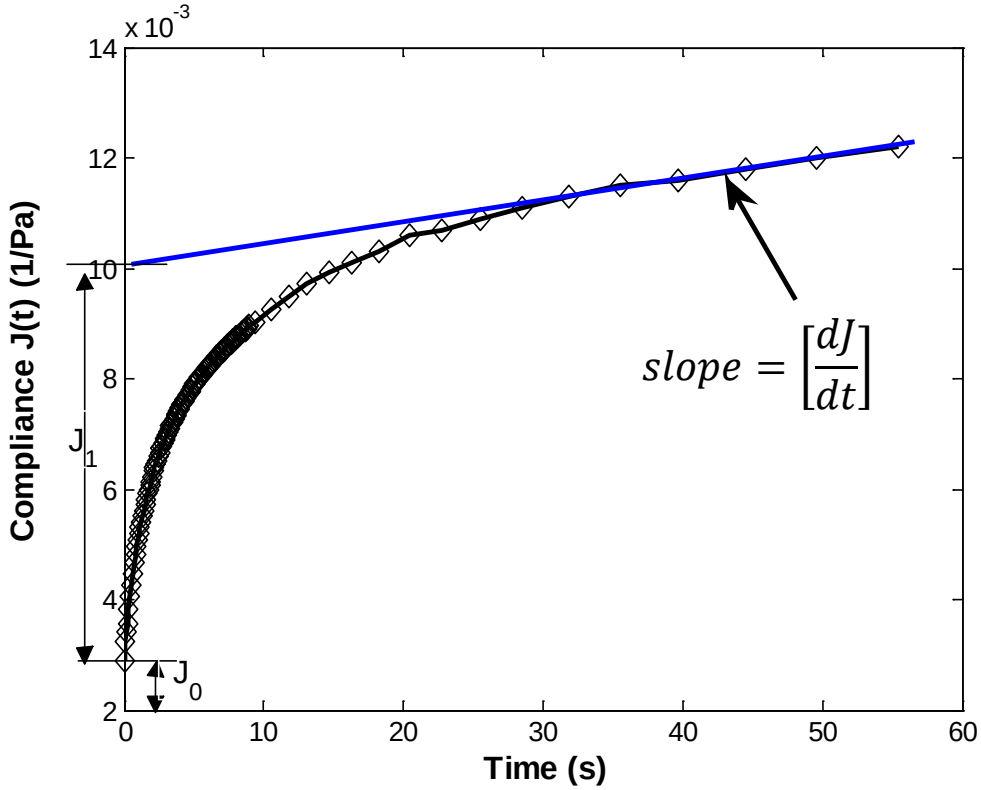

Figure 2.4. Creep test for ketchup at constant stress (5 Pa) and 23°C.
(Adapted from Steffe (1996))

2.6.3 Zero-shear viscosity (ZSV)

In the steady-state part of the creep test (Figure 2.4), the inverse of the slope of the compliance curve gives the Zero Shear Viscosity, ZSV (Desmazes et al., 2000):

$$ZSV = \left[\frac{dJ}{dt}\right]^{-1} \tag{2.6}$$

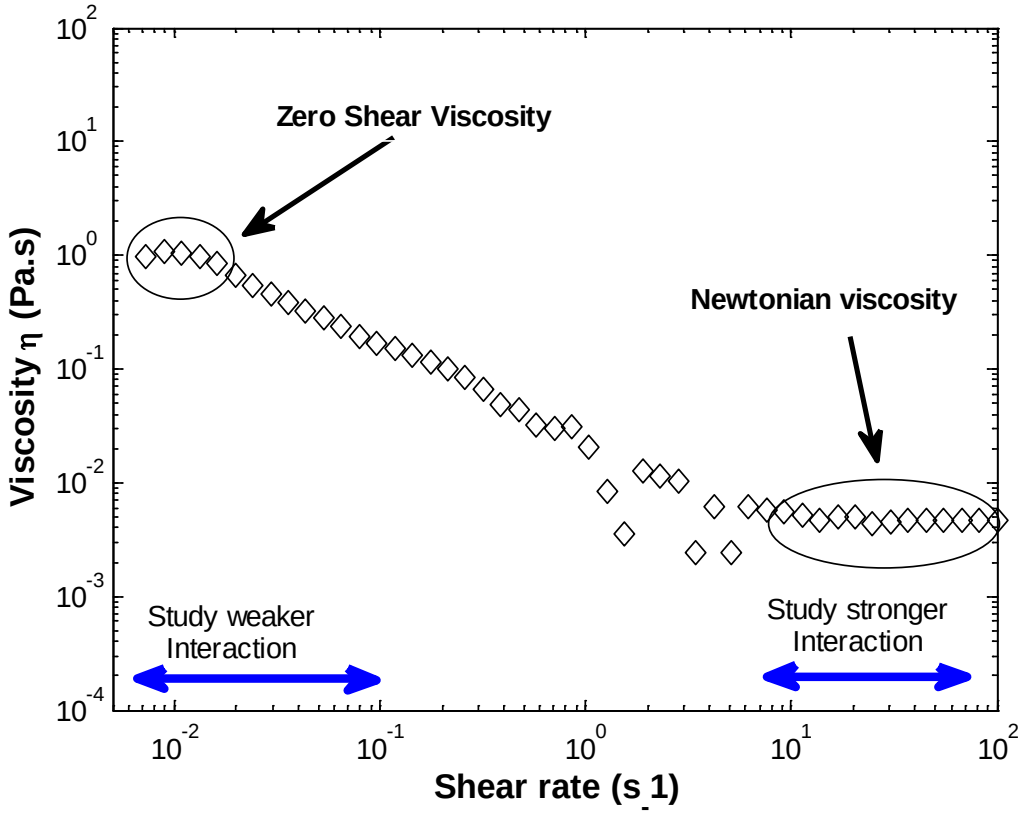

Figure 2.5. Representation of viscosity as a function of shear rate for a Brookfield standard fluid (4.3 cP) at 23°C.

At very low shear rates pseudoplastic liquids composed of polymeric materials behave similarly to Newtonian liquids having a defined viscosity often called the "zero shear viscosity", ZSV, which is independent of the shear rate applied (Figure 2.5).

The ZVS is characterized as the apparent viscosity of a liquid in the limit of zero shear rate (Figure 2.5). In practice, it is not possible to attain very low shear rates for many liquids owing to measurement difficulties. In these cases, the viscosity obtained by extrapolating the viscosities obtained at accessible shear rates.

The ZSV is an important property to characterize the microstructure of polymeric liquids. At rest, all materials suspended in a liquid (e.g. water dilutions) will maintain an irregular internal order and correspondingly they could be characterized by the measure of its internal resistance against flow. At the low shear rate range the Brownian motion of molecules keeps all molecules or particles at random in spite of the initial effects of shear orientation. At increasing shear rate the molecular or particle orientation is induced on a magnitude that exceeds the randomizing effect of the Brownian motion, therefore, decreasing of viscosity at increasing shear rate is the result of the lowered resistant to flow by the oriented arrangement of particles (Krieger and Gougherty, 1959). At this stage more mass can be made to flow, consequently the energy can be reduced to sustain a given flow rate (Schramm, 2002).

Micelle-type structure formation and network association has been characterized with the increment of ZSV values as a function of nonionic surfactant (NPe) concentration in combination with comb-like hydrophobic polymers (Talwar et al., 2006).

2.6.4 Oscillatory frequency test

In dynamic rheological experiments three variables are measured: applied stress (σ), strain (γ) and phase angle (δ) between the stress and strain oscillation (Figure 2.6). A frequency sweep test allows measurement of the viscoelastic properties of a material at different frequencies. Since the rheological behavior is highly time-dependent this method is extremely useful. Because it allows definition of thin film

rheological behavior in different time scales and provides information about whether viscosity or elasticity is the dominating part. The frequency sweep test is characterized by the following equations:

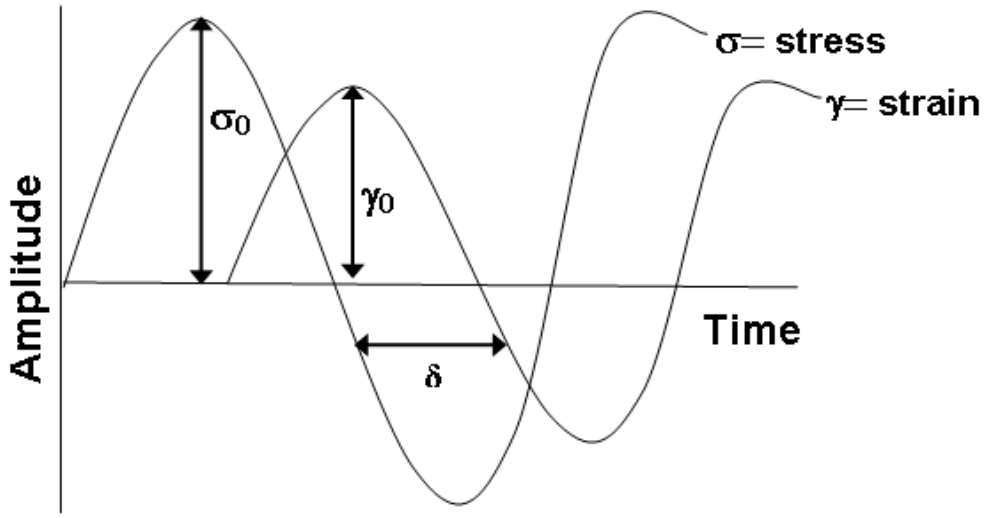

Figure 2.6. Sinusoidal wave forms for stress and strain functions.

$$\sigma = \sigma_0 \cos(\omega t) \tag{2.7}$$

$$\gamma = \gamma_0 \cos(\omega t - \delta) \tag{2.8}$$

Where σ_0 is the stress amplitude, and γ_0 is the strain amplitude. Dynamic viscoelastic modulus G* is obtained as a function of oscillation frequency (ω) from the

measurement, and it can be separated into two components, elastic (or storage) modulus G' and viscous (or loss) modulus G'' as follow:

$$G' = elastic\ modulus = \frac{\sigma_0}{\gamma_0}\ Cos(\delta) \tag{2.9}$$

$$G'' = viscous\ modulus = \frac{\sigma_0}{\gamma_0}\ Sin(\delta) \tag{2.10}$$

Additionally, complex viscosity, η^* which describes the resistance to dynamic shear can be defined as:

$$\eta^* = complex\ viscosity = \frac{G"}{\omega} + i\frac{G'}{\omega} \tag{2.11}$$

Solid-like properties (e.g. deformation) measured in the linear viscoelastic characteristic region (LVR) of the material has shown a different response than measurements at steady shear conditions (e.g. ZSV characterization), however both types of experiments may show similar trends (Chae et al., 2001). When the characteristic equilibrium of a microstructure is disturbed or deformed, thermodynamic forces tend to restore the equilibrium. The energy associated with this restoration process is the elastic energy (Sunthar, 2010).

The short time range produced by a dynamic test (e.g. sinusoidal stress or strain) is often well suited to evaluate a polymer's responses; therefore, oscillatory sweep test responses may be helpful to characterize or classify dispersions as a dilute solution, a concentrate solution (e.g. network formation) or a gel structure (e.g. weak or strong gel) (Steffe, 1996). For instance, gels have significantly higher G' with the modulus practically constant throughout the frequency range (Chamberlain and Rao, 2000; Steffe, 1996).

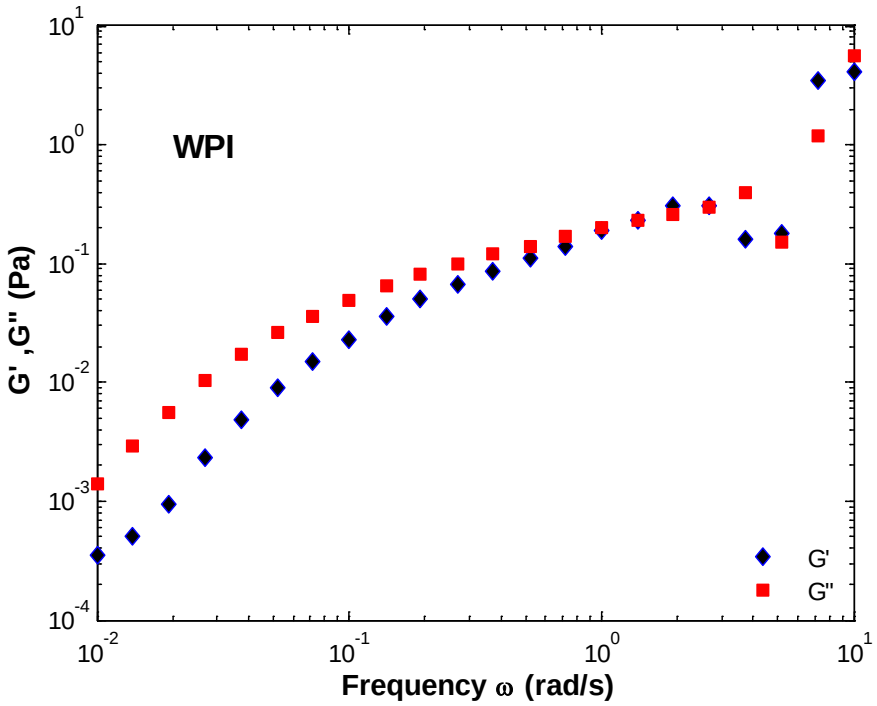

Figure 2.7. Dynamic oscillatory test for 184 g/L whey protein isolate (WPI) (diluted solution) in aqueous solution.

For concentrated solutions, G'' and G' curves intersect at the middle of the frequency range indicating a clear tendency for more solid-like behavior at higher frequencies, which could be assumed as the formation of an entangled network system. In general, diluted solutions of hydrocolloids show viscous (G'') moduli larger than elastic (G') moduli over the entire frequency range but approach each other at higher frequencies (Figure 2.7)

Accordingly to Maxwell fluid element dynamic analysis, the elastic and viscous modulus could be writen as a function of frequency ω (rad/s) and relaxation time λ (s/rad) as follow (Schramm, 2002):

$$G' = \frac{G\omega^2\lambda^2}{1+(\omega\lambda)^2} \tag{2.12}$$

$$G'' = \frac{G\omega\lambda}{1+(\omega\lambda)^2} \tag{2.13}$$

When the term ω * λ becomes very small, the term λ=η/G (dashpot viscosity η/ spring modulus G) is interchanged in equations 2.12 and 2.13, then

$$G' = G\omega^2\lambda^2 \tag{2.14}$$

$$G'' = G\omega\lambda \tag{2.15}$$

When the term ω * λ becomes very high:

$$G' = G \tag{2.16}$$

$$G'' = \frac{G}{\omega\lambda} \tag{2.17}$$

Where G represents the spring modulus from the Maxwell's model. The interrelation between G' and G'' is calculated dividing these two set of equations, 2.15/2.14 or 2.17/2.18:

$$\frac{G\prime}{G\prime\prime} = \omega\lambda \tag{2.18}$$

$$\lambda = \frac{G\prime}{G"\omega} \tag{2.19}$$

The relaxation time "λ" is the time associated with large scale motion (or changes) in the structure of the polymers (Chhabra, 2010; Roland, 2008).The values of λ seem to be sensitive to the frequency oscillatory sweep and polymeric nanocomposite concentration (Utracki et al., 2010). Moreover, the linear decreasing values of λ (slope) have been associated with structure formation and changes in λ slope were related to structure changes for combinations between polyamide-6 and polymeric nanocomposites (Utracki et al., 2010).

$$slope = \left[\frac{dlog\lambda}{dlog\omega}\right] \tag{2.20}$$

An early study on the same combination of polyamide-6 and polymeric nanocomposites showed that the structural changes at a critical frequency have been also associated with an apparent break of the disks-like (or platelet) structure at higher frequencies (Utracki and Lyngaae-Jørgensen, 2002).

CHAPTER III

CHARACTERIZATION OF THE PHYSICAL STABILITY OF BIOPOLYMERS

3.1 Overview

The high cost and potential toxicity of biodegradable polymers like poly(lactic-co-glycolic) acid (PLGA) has increased the interest in natural and modified biopolymers as bioactive carriers. Ambient conditions like temperature and relative humidity (RH) influence the moisture sorption, therefore the physical stability of the encapsulating matrices .To maximize bioactive compound protection and at the same time trigger and control their release, the physical stability of natural encapsulating matrices must be evaluated. Both water sorption capability and the glass transition temperature (Tg) were associated with the physical stability of different octenyl succinate-modified depolymerized waxy corn starch (DWxCn), waxy rice starch (DWxRc) and phytoglycogen, as well as whey protein concentrate (80%, WPC), whey protein isolate (WPI), and α-lactalbumin (α-L). DWxCn and DWxRc showed an increment in water sorption compared to native starch. The level of octenyl succinate anhydrate (OSA) modification (3% and 7%) did not reduce the water sorption of different DWxCn and phytoglycogen samples. According to the GAB (Guggenheim-Andersen-de Boer) model, a significantly ($P < 0.05$) higher water monolayer capacity was observed on natural waxy corn followed by 3% OSA-modified DWxCn and DWxRc, WPI, α-L, and natural phytoglycogen. A significantly lower water monolayer capacity was observed on WPC and dextrin from WxCn and WxRc at different percentage of OSA modification,

limiting their use in lower than 70%RH environments. Water monolayer capacity was directly related to the critical water activity in all natural biopolymers and OSA-modified polysaccharides. For instance, fungi growth was observed at 97% RH on the surface of WPC, which showed a low critical water activity value of 0.25.

The Tg values measured at different RH environments were in good agreement with the solid-like appearance of the biopolymers. Higher values of Tg were observed on natural polysaccharides and whey proteins compared to depolymerized and OSA-modified polysaccharides. Depolymerization of waxy starches significantly reduced their Tg value, though 3 and 7% of OSA modification did not increase them. In most of the biopolymers evaluated the Kwei equation provided better correlation than the Gordon-Taylor equation in order to predict the Tg's sensitivity to water sorption. Depolymerized waxy starches at 7% of OSA modification had a "melted" appearance when they were exposed to over 70% RH after 10 days at 23°C, which indicates that this type of biopolymers could not be used alone as encapsulating matrices for materials that will be exposed to a higher than 70% RH environment.

3.2 Introduction

Natural ingredients such as antioxidants (carotenoids and polyphenols) or colorants (carotenoids and xanthins), sweeteners (stevia), aromas and flavoring agents (essential oils), processing aids (enzymes), and antimicrobials are often used in special vehicles necessary to retain their performance. Effective delivery systems for these natural ingredients become necessary in order to maximize their solubility,

bioavailability, stability and masking of stronger flavors of the enriched foods (Nissim, 2008).

Some biodegradable polymers have potential as promising carriers of natural ingredients. In particular, poly(lactic-co-glycolic) acid (PLGA) has been widely used because it is approved by the Food and Drug Administration (FDA) for human therapy (Astete and Sabliov, 2006). However, there are drawbacks in using biodegradable polymers and their derivatives in foods such as the complex manufacturing procedure, the potential toxicity of different components involved in their manufacturing such as toxic reagents and polymers cost of biodegradable materials (e.g. PLGA).

Today, it is known that many of these synthetic additives that were approved in the past might cause some health concerns. Certainly, humans consume large quantities of polymeric particles from food and pharmaceutical products and the chronic exposure to them remains unknown. It is thought that the ingestion of dietary particles could promote a range of metabolic diseases. For instance, polystyrene nanoparticles investigated in an in vitro model of the intestinal epithelium and an in vivo chicken intestinal loop model showed that a chronic and acute oral exposure to this polymeric particle caused a physiological response that influenced iron uptake and iron transport (Mahler et al., 2012). Similar disruptions in nutrient sorption could be possible in other inorganic elements such as calcium, copper and zinc, as well as other nutrients such as fat-soluble vitamins A, D, E and (Mahler et al., 2012).

On the other hand, several studies have shown that natural ingredients can be good alternatives to synthetic additives with similar performance characteristics. The

most effective coating and microsphere particle formations are biopolymers derived from proteins and/or polysaccharides, and current efforts are in the area of incorporating and integrating these two types of biopolymers for food applications (Sekhon, 2010). Polysaccharides, the most abundant polymer in the human diet, have been converted to alkenyl esters in order to change the physical properties and form films at the oil and water interfaces (Krstonošić et al., 2011; Viswanathan, 1999). However, only starches modified at maximum level of 3% of modification with octenyl succinic anhydrate (OSA) are allowed to be used in food application (JECFA, 2012). In one particular study, phytoglycogen, a plant based high density carbohydrate, and waxy corn starch OSA-modified were combined with ε-polylysine, a naturally occurring homopolyamide, in order to successfully form water in oil emulsions with enhance lipid oxidative stability(Scheffler et al., 2010b). Enzymatic depolymerization of OSA-modified waxy starch have increased in the emulsification capability of resulting OSA-modified dextrin (Liu et al., 2008). Similarly, whey proteins among other milk proteins used alone or in combination with polysaccharides have been extensively investigated for delivery of hydrophobic bioactives compounds(Livney, 2010; Sekhon, 2010)

Therefore, there is unquestionable significant progress on the use of natural carriers to maximize the protection and at the same time trigger and control the release of encapsulated bioactive compounds. However, the physical stability of these promising natural encapsulating matrices must be evaluated. Ambient conditions like temperature and relative humidity (RH) influence moisture sorption, and consequently the physical stability of the matrix material's properties. Water activity (A_w) is related to equilibrium

RH (A_w*100=RH*)* and both glass transition temperature (Tg) and A_w are a function of product moisture content. Furthermore, the interrelations among A_w, RH, Tg and moisture content are important for stability and shelf life of products (Barbosa-Cánovas et al., 2007). Water sorption isotherms and glass transition temperature (Tg) are widely recognized as key characterization methods regarding the stability, functionality and quality of many synthetic and natural polymers (Borde et al., 2002). The two parameters BET (Brunauer-Emmett-Teller) and the three parameters GAB (Guggenheim-Andersen-de Boer) isotherm models are mainly used to analyze moisture sorption in food materials (Timmermann, 2003). Unlike the BET equation, the versatility of the GAB equation allows the use of wider water activity range (0.05-0.90) on the analysis.

Glass transition temperature (Tg) in solids is a function of temperature, time, molecular composition, molecular weight and water sorption (Abiad et al., 2009). The glass transition is referred to as an indication of a change from the physical glassy to rubbery stage and vice versa. Glassy solids are considered to be in a non-equilibrium stage, therefore the stability of the material is greatly sensitive to changes on the surrounding conditions. At temperatures above the glass transition, solids become rubbery, the structure collapses and consequently, the release of entrapped bioactive compounds occurs. Although the Gordon-Taylor equation (Gordon and Taylor, 1952) has been widely used to model Tg values of different pure polymers in food materials exposed to different water activity environments, an extended version of that equation developed by Kwei (Kwei, 1984) has been confirmed to better fit experimental data and modeling of the miscibility influence on the Tg values of synthetic polymer blends

(Brostow et al., 2008; Kalogeras and Brostow, 2009). Thus, the rational design of encapsulation systems requires a physicochemical understanding of how environmental conditions affect the physical stability of the polymer matrix.

The purpose of the present study was to characterize the water sorption and state transition behavior of OSA-modified enzymatic hydrolyzed waxy corn, waxy rice and phytoglycogen, as well as whey protein concentrate (80%), whey protein isolate and α-lactalbumin. The relationship of water sorption and glass transition temperature on the physical stability of these biopolymers could be used to better design encapsulation materials depending on storage environment conditions.

3.3 Materials and methods

3.3.1 Materials

Waxy corn and waxy rice starches (Ingredion, Westchester, IL) were depolymerized with α-amylase-heat stable (Sigma-Aldrich Co., St. Louis, MO) to produce different dextrose equivalent (DE) values (DE= 7 - 24). Depolymerized waxy corn and waxy rice starches as well as phytoglycogen (a highly branched polysaccharide) (Kewpie Corporation, Japan) were modified at different percentage of substitution (approx. 3 and 7%) with Octenyl succinic anhydride (OSA) (Dixie Chemical Co, Houston, TX). Whey protein isolate, whey protein concentrate (80%) and α-Lactalbumin (DAVISCO Foods International, Inc., Eden Prairie, MN) were used without any modifications. Glucose standard, and other reagents and solvents were purchased from Sigma-Aldrich and VWR International, LLC (West Chester, PA).

3.3.2 Preparation of OSA-modified polysaccharides

Twenty five grams of sample was added into distilled water in a glass beaker with agitation. The reaction condition for optimum preparation of OSA-waxy starch was carried out as follows: starch concentration in water 31.5%, temperature 34 °C, pH 8.6, and reaction time 18.7 h (Liu et al., 2008). The pH of the mixture was kept constant adding 0.1N NaOH and the reaction was terminated by reducing the pH to 6.5 using 0.1N HCl. To collect the samples, three volumes of ethanol were added to the mixture and the precipitated material was centrifuged at 3200 x g for 20 minutes (Allegra 25R centrifuge, Beckman Coulter, Fullerton, CA) and subsequently washed with ethanol and centrifuged 3 more times. Afterwards, the sample was dried in a vacuum oven (Squared Lab Line Instruments, Melrose Park, IL) at 60°C overnight.

3.3.3 Percentage of modification (%OSA)

Octenyl succinate modification in waxy starches and phytoglycogen was quantified using a method from the Joint FAO/WHO Expert Committee on Food Additives (JECFA, 2011) with some modifications. The sample (0.5g) was acidified with 3 ml of 2.5 M HCL for 30 minutes. Ten ml of pure isopropanol was added, followed centrifugation at 3200 x g for 20 minutes. Subsequently, the precipitate was washed and centrifuged 3 more times or until the test of chloride ions using one drop of 0.1 M $AgNO_3$ on the supernatant showed negative haze formation. Afterwards, 30 ml of distilled water was added to the precipitate and heated in boiling water for 30 min, and

then titrated using 0.01 M NaOH. The percentage of OSA modification (%OSA) was calculated by the following equations :

$$A = \frac{(V - V_0) * 0.01}{0.5} \quad (3.1)$$

$$\%\, OSA = \frac{210 * A}{1000} * 100 \quad (3.2)$$

Where A (mmol/g) is the molar amount of octenyl succinate groups in one gram of derivative; 210 is the molecular weight of octenyl succinate group (g/mol); V (ml) is the volume of NaOH solution consumed by the octenyl succinate derivative; V_0 (ml) is the volume of NaOH consumed by the native waxy starches or phytoglycogen; 0.5 is the weight of material in grams and 0.01 is the molar concentration of NaOH (JECFA, 2012).

3.3.4 Enzymatic treatment of waxy starches

Waxy corn and rice starch samples (5 g, dry weight) were mixed with water to a 35% suspension by weight containing 200ppm of $CaCl_2$. The pH of mixture was adjusted to 5.9 with 0.1N NaOH and α-amylase at 20 U per gram of starch was added into the mixture (Liu et al., 2008). Two different enzymatic treatment procedures were evaluated in order to minimize the final dextrin size. On treatment 1 (T1) the suspension was heated in a shaking water bath (VWR International, West Chester, PA) set at 65°C

and 100 rpm for different hydrolyzing times (30, 60, 120, 240, 360, 480, and 720 minutes) with agitation. Afterwards, the sample was incubated at 100°C for 20 minutes and cooled down in water at 5°C for 10 min. On treatment 2 (T2) samples (5g) of waxy corn and waxy rice starch were first incubated at 100°C for 20 minutes right after the enzyme addition and then incubated in a shaking water bath (VWR International, West Chester, PA) set at 65°C and 100 rpm for different hydrolyzing times (30, 60, 120, 240, 360, 480, and 720 minutes).

The enzymatic reaction was stopped by reducing the mix pH to 4.0 with 0.5N HCl to get different dextrose equivalent (DE) values. Three volumes of ethanol were added to the mixture, followed by centrifugation at 3200 x g for 20 minutes (Allegra 25R centrifuge, Beckman Coulter, Fullerton, CA) and the precipitate solids were dried in a vacuum oven (Squared Lab Line Instruments, Melrose Park, IL) at 60°C overnight. The DE values were calculated based on the following equation (3.3):

$$DE = \frac{Reducing\ sugar\ content\ (\frac{mg}{g})}{Total\ sugar\ content\ (\frac{mg}{g})} \quad (3.3)$$

The kinetic of starch depolymerization by the α-amylase were determined based on a modified hyperbolic one-site ligand biding equation (Rogers and Gibon, 2009) as follows:

$$DE = \frac{DE_{max} * t}{(K_h + t)} \quad (3.4)$$

Where DE_{max} is the maximum dextrose equivalent achieved by the α-amylase under the experimental conditions and K_h is the time needed to achieve half of the DE_{max}.

3.3.5 Total sugar content

The phenol-sulfuric acid assay method was carried out (Fournier, 2001). This method is very general, and can be applied to many classes of carbohydrates including oligosaccharides where reducing and non-reducing sugars are present. The phenol-sulfuric acid method is based on the absorbance at 490 nm of colored aromatic complex formed between phenol and the carbohydrate. The amount of sugar present was determined by comparison with a calibration curve of D (+) glucose using a spectrophotometer (Thermo Scientific Genesys 10S UV-Vis, Waltham, MA). One hundred mg of sample was diluted in 10 ml of distilled water. One ml of the previous dilution was subsequently diluted in 9 ml of distilled water. A blank was prepared using 50 µl of distilled water. Five hundred µl of 4% phenol was added to 50 µl of later dilution and followed by 2.5 ml 96% sulfuric acid. The mixture was allowed to cool down at room temperature for 15 minutes and its absorbance measured in a spectrophotometer (Thermo Scientific Genesys 10S UV-Vis, Waltham, MA) at 490 nm.

3.3.6 Reducing sugar content

Quantification of reducing sugars was determined by the Somogyi-Nelson method (Fournier, 2001). This method utilizes the reducing properties of certain types of carbohydrates based on the absorbance at 500 nm of a colored complex formed between a copper-oxidized sugar and arsenomolybdate. The amount of reducing sugar present was determined by comparison with a glucose calibration curve using a spectrophotometer (Thermo Scientific Genesys 10S UV-Vis, Waltham, MA). One hundred mg of sample was diluted in 10 ml of distilled water. One ml of the previous dilution was subsequently diluted in 9 ml of distilled water. A blank was prepared using 50 µl of distilled water. One ml of low-alkalinity copper agent was added to the 50 µl of later dilution and heated in boiling water for 10 min. Then, 1 ml of arsenomolybdate reagent was added with an extra 2900 µl of distilled water and the mixture was allowed to cool down at room temperature for 15 minutes and its absorbance measured in a spectrophotometer (Thermo Scientific Genesys 10S UV-Vis, Waltham, MA) at 500 nm.

3.3.7 Microscopic observation

Samples (10 mg) of native and depolymerized waxy starches and phytoglycogen were placed in a precleaned glass slide (3 x 1x 1 mm) and suspended with one drop of 50% glycerol/water solution. The suspension was covered by a microscope cover glass (24 x 60 mm) and the sample was observed under a Nikon Eclipse TS100 microscope (Nikon Instruments Inc., Melville, NY, USA) with 40 x objective and 10x eyepiece

magnification lenses. The micrographs acquisition was performed with a NIS-Elements BR-3.2 software.

3.3.8 Particle size measurement

The sample was dissolved in distilled water at a concentration of 10 mg/ml and vortex for 30 seconds. Thereafter, the particle size was measured at room temperature using a Particle Size Analyzer (Delsa™ Nano C, Beckman Coulter, Pasadena, CA). This machine uses photon correlation spectroscopy (PCS), which determines particle size based on the dynamic properties of particles moving in a solvent. Thus, the hydrodynamic diameter is calculated based at the rate of fluctuations in laser light intensity scattered by equivalent spherical particles as they diffuse through the solvent.

3.3.9 Moisture sorption isotherms

Dehydrated samples (approx. 0.5g) of natural, hydrolyzed, and OSA-modified (3 and 7%) waxy corn, waxy rice starches and phytoglycogen were weighed into tin flat containers (5.08cm width x 2.03 cm height) and placed in a desiccator containing a saturated salt solution of known water activity levels (A_w*100= RH) in the range of 0.113 to 0.973. The desiccators with the samples were kept at ambient temperature (23°C). After ten days, equilibrium was considered to be reached and the amount of water adsorbed on the samples was determined by re-weighing the containers and the contents. The weight data were fitted to the Guggenheinm-Anderson-DeBoer (GAB) (Timmermann, 2003) sorption isotherm model given in the following equation:

$$v(A_w) = \frac{v_m * C_G * k * A_w}{(1 - k * A_w)(1 + (C_G - 1) k * A_w)} \quad (3.5)$$

Where $v(A_w)$ is the amount of water adsorbed by 100 grams of dehydrated sample at vapor pressure A_w (relative vapor pressure of saturated salt solution), v_m is the GAB water monolayer capacity in the same units as $v(A_w)$, C_G is the energy constant and k indicates the difference of free enthalpy between water molecules in the pure liquid and in the layers above the monolayer (Timmermann, 1989). The k constant takes characteristic values for different types of biopolymers (Chirife et al., 1992). For example, non-porous materials such as starchy material presented a narrow range between 0.65-0.75, $k \approx 0.78$-0.85 for proteins and 0.92 for electrolytes and polyelectrolytes (Chirife et al., 1992).

3.3.10 Glass transition temperature (Tg)

Differential scanning calorimetry (DSC) was performed with a Perkin Elmer differential scanning calorimeter (Perkin Elmer, DSC-6, Boston, MA). Indium was used for enthalpy calibration. Samples were weighed with an accuracy of 10 ± 0.01 mg, placed in 40-µl closed aluminum pans, and scans were conducted under nitrogen between 5 and 100^{o}C at 10^{o}C/min rate. DSC curves of samples were obtained. Two individual measurements were carried out to ensure reliability of measurements. Glass

transition temperature (Tg) was determined as the inflection point of the specific heat increment at the glass-rubber transition by running an immediate rescan for each sample.

3.3.11 Prediction of glass transition temperature for pure biopolymers

The models proposed by Gordon and Talor (Gordon and Taylor, 1952) and Kwei (Kwei, 1984) have been developed to predict the Tg of binary polymer blends based on the Tg of pure polymers and the mass fraction of their components (Brostow et al., 2008); however, these models could also be used to predict the Tg of a pure polymer, based on the experimental values of Tg at different mass fraction of water sorbed into the polymer at different water activity environments . The Gordon–Taylor equation (Gordon and Taylor, 1952) (equation 3.6) and its extended version developed by Kwei (Kwei, 1984) (equation 3.7) were used for modeling the influence of water adsorption on the Tg values of different pure polymers according to the following equations:

$$T_g = \frac{w_1 T_{g1} + K_{GT} w_2 T_{g2}}{w_1 + k w_2} \tag{3.6}$$

$$T_g = \frac{w_1 T_{g1} + K_{Kw} w_2 T_{g2}}{w_1 + k w_2} + q w_1 w_2 \tag{3.7}$$

Where Tg is the glass transition of the mixture in °C, w_1 and Tg_1 are the mass fraction (g/g) and glass transition of water (Tg of amorphous water = -135°C), respectively. The

values of w_2 correspond to the mass fraction (g/g) at different water activity, Tg_2 is the glass transition temperature (°C) of dehydrated polymer, whereas K_{GT}, and K_{Kw} are model constants that are function of the coefficient of expansion of components as the change from the glassy to the rubbery state. Kwei (1984) introduced a quadratic term in the Gordon-Taylor equation, with a q constant in the role of an interaction-dependent parameter.

3.3.12 Statistical analysis

All experiments were replicated two or three times, and their results were reported as average. Statistical analysis software (IBM SPSS Statistics, Version 14, IBM Corporation, Armonk, NY) was used to perform Duncan mean comparison analysis among samples with a p-value <0.05 being considered to be a significant difference between samples means.

3.4 Results and discussions

3.4.1 Waxy starches and phytoglycogen granules size

Waxy corn and rice starch granules present asymmetrical spheres of different granule size (Figures 3.1.A and 3.1.B). In general, waxy corn starch granules present the largest granule size compared to waxy rice and phytoglycogen granules as it is observed in Figure 3.1C.

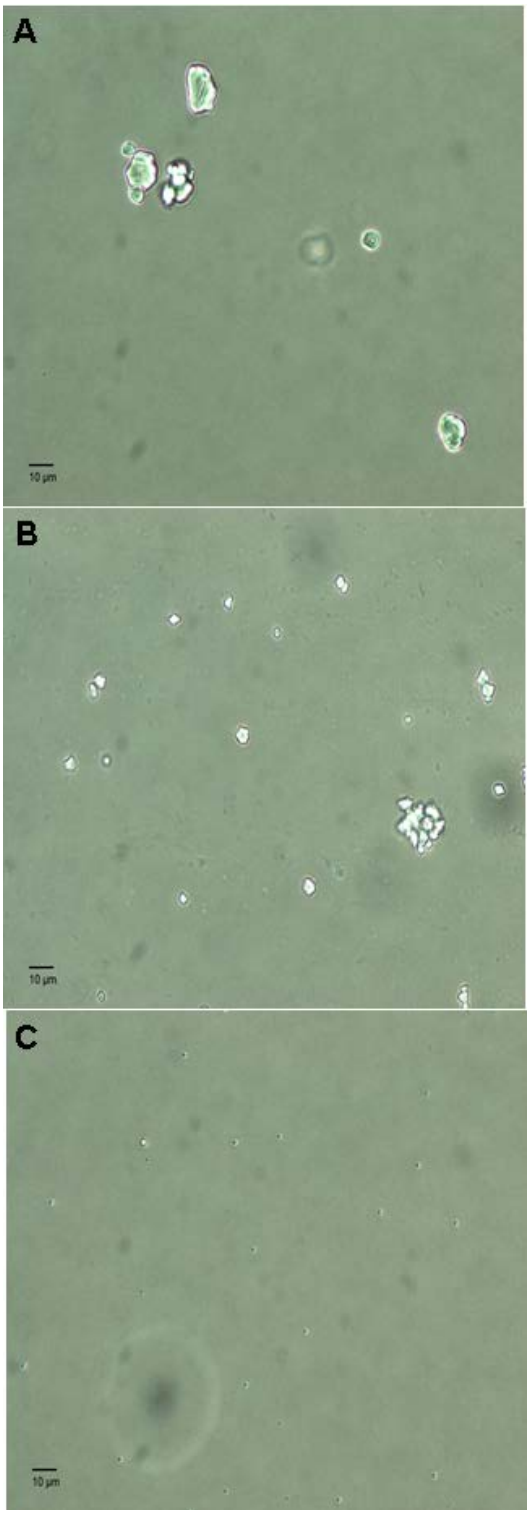

Figure 3.1. Natural waxy corn starch (A), waxy rice starch (B) and phytoglycogen (C) granules.

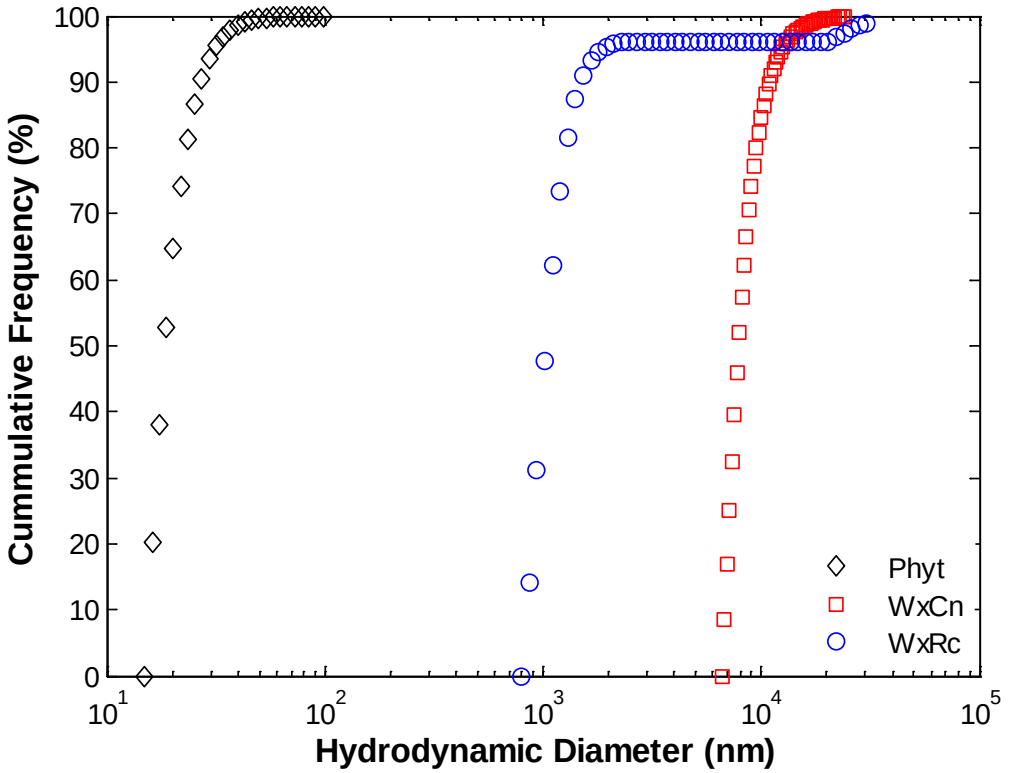

Figure 3.2. Size distribution of waxy corn, waxy rice starch and phytoglycogen granules. Hydrodynamic diameter was measured using a Particle Size Analyzer which determines particle size based on the dynamic properties of particles moving in a solvent.

Starch granules come in wide variety of size, the predominant (> 90%) hydrodynamic diameter of waxy corn granules measured about 20 μm, while wazy rice and phytoglycogen granules were about 2 and 0.04 μm (40 nm), respectively, under the same percentage of predominant hydrodynamic diameter (> 90%) (Figure 3.2). On other words, waxy corn starch granules presented 10 times and 200 bigger size compared to waxy rice and phytoglycogen, respectively.

3.4.2 Enzymatic treatment of waxy starch

Enzymatic depolymerization of waxy starch seems to be affected by the size of the granules. Waxy rice starch granules, which present predominant smaller size than waxy corn starch granules showed higher depolymerization kinetic than waxy corn starch for enzymatic treatment 1(T1) (Figure 3.3).

Although the time to achieve maximum dextrose equivalent (DE) of waxy corn starch is shorter (52.24 minutes) than for waxy rice starch (63.73 minutes), both types of waxy starches achieved a maximum degree of dextrose equivalent (DE) at 6 hours of depolymerization with α-amylase at 65°C during treatment 1(T1). No significant increment of DE was obtained at longer times (Figure 3.3).

Waxy rice starch could achieve a maximum 22.93 DE under T1, which is higher than the maximum 18.11 DE achieved from waxy corn starch under the same enzymatic treatment. Hence, waxy corn starch has a more complex structure than waxy rice starch, which could be reducing the enzyme's capability to penetrate and rapidly hydrolyze the inner amylose molecules due to the length and rigidity of amylopectin spacers and branches (Blazek and Gilbert, 2010). Previous studies indicate that not only the size and shape of granules control the access of the enzyme to its substrate, but also the release of reaction products is influenced by many more factors including granule integrity, crystallinity, and porosity of granules, amylose to amylopectin ratio, structural homogeneities, phosphate content, proteins, and lipids on the surface of starch granules and hydrolysis products such as malto-oligosaccharides have been shown to inhibit the action of amylase enzymes (Blazek and Gilbert, 2010; Copeland et al., 2009).

The predominant diameter of waxy corn dextrin measured after enzymatic treatment 1 (T1) was approximately 300 and 600 nm (Figure 3.4.A), for 12 and 6 hours of incubation at 65°C, respectively, where the waxy starch samples were first incubated during different times at 65°C and then treated at 100°C for 20min. On the other hand, waxy rice dextrin presented a predominant diameter between 100 and 300 nm for 12 and 6 hours of incubation at 65°C, respectively (Figure 3.4.B).

The smaller the native waxy starch the smaller the size of dextrin obtained from the enzymatic treatment 1(T1), which indicates that the size of the granules is clearly a controlling factor to allow access of the enzyme to its substrate and the consequent release of reaction products such as dextrin.

A smaller predominant dextrin size was achieved when either waxy corn starch or waxy rice starch samples were first treated at 100°C for 20 minutes and subsequently incubated during different times at 65°C (treatment 2, T2).The predominant dextrin size from waxy corn starch achieved after 1 hour of incubation at 65°C was about 80nm (Figure 3.5.A). However, a smaller predominant dextrin size around 15 nm was achieved from waxy rice starch after 1 hour of incubation at 65°C (Figure 3.5.B). The exposure of waxy starch granules to 100°C caused the gelatinization of the granule, expanding and breaking the granule to maximum exposure of amylose molecules; hence, an extensive depolymerization process by the α-amylase enzyme was achieved.

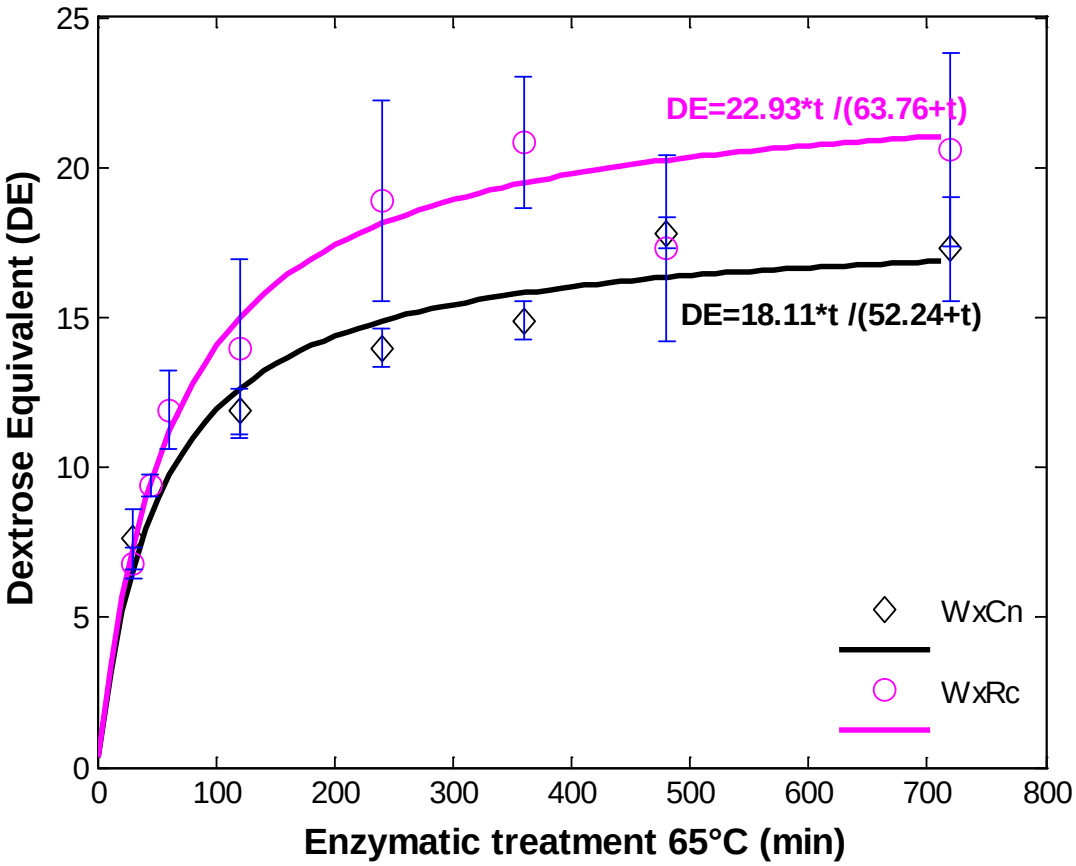

Figure 3.3. Enzymatic treatment 1 (T1) of waxy corn and waxy rice starches during different incubation times at 65°C.

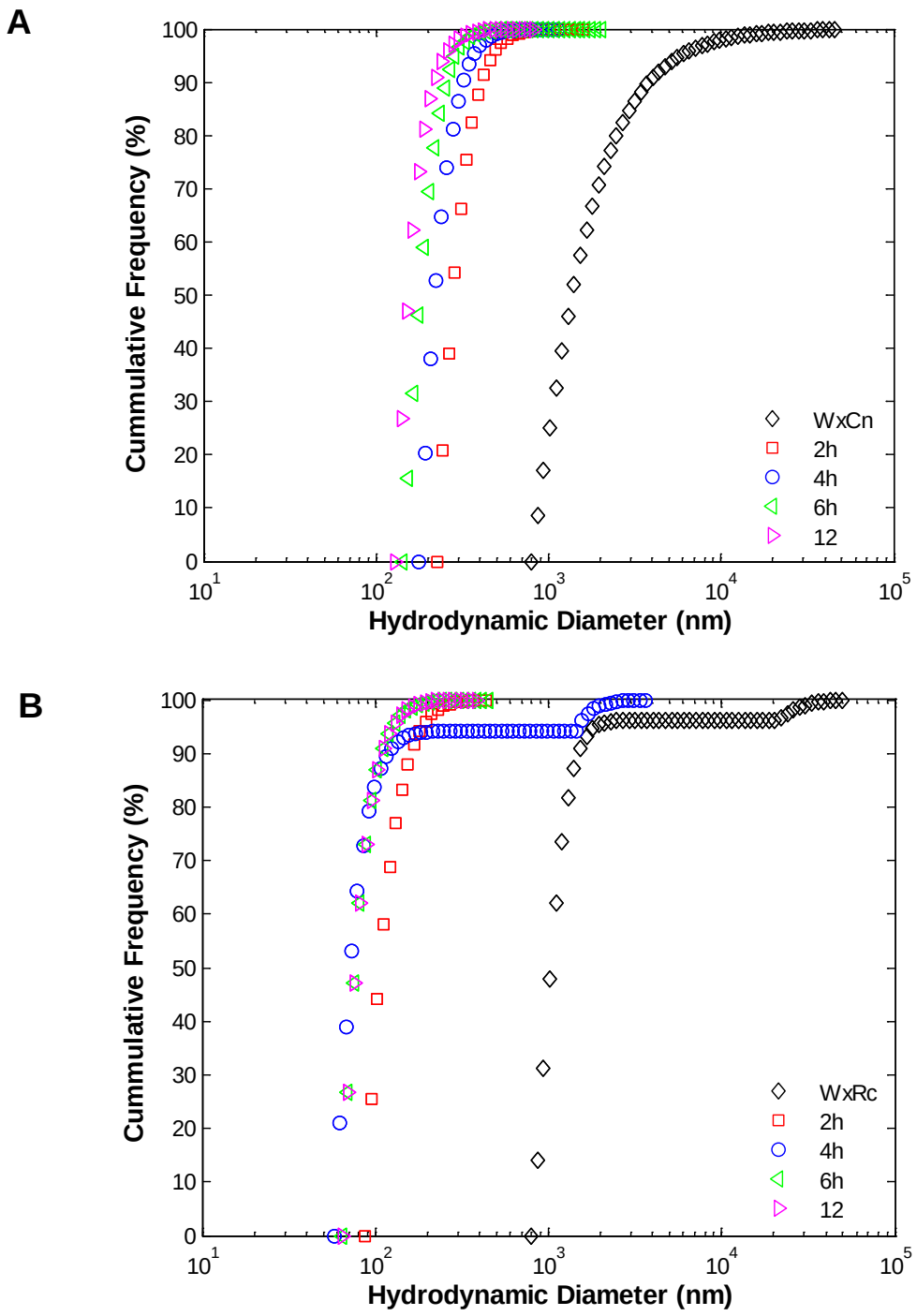

Figure 3.4. Size distribution of waxy corn (A) and waxy rice (B) starches after enzymatic treatment 1 (T1) during different incubation times at 65°C.

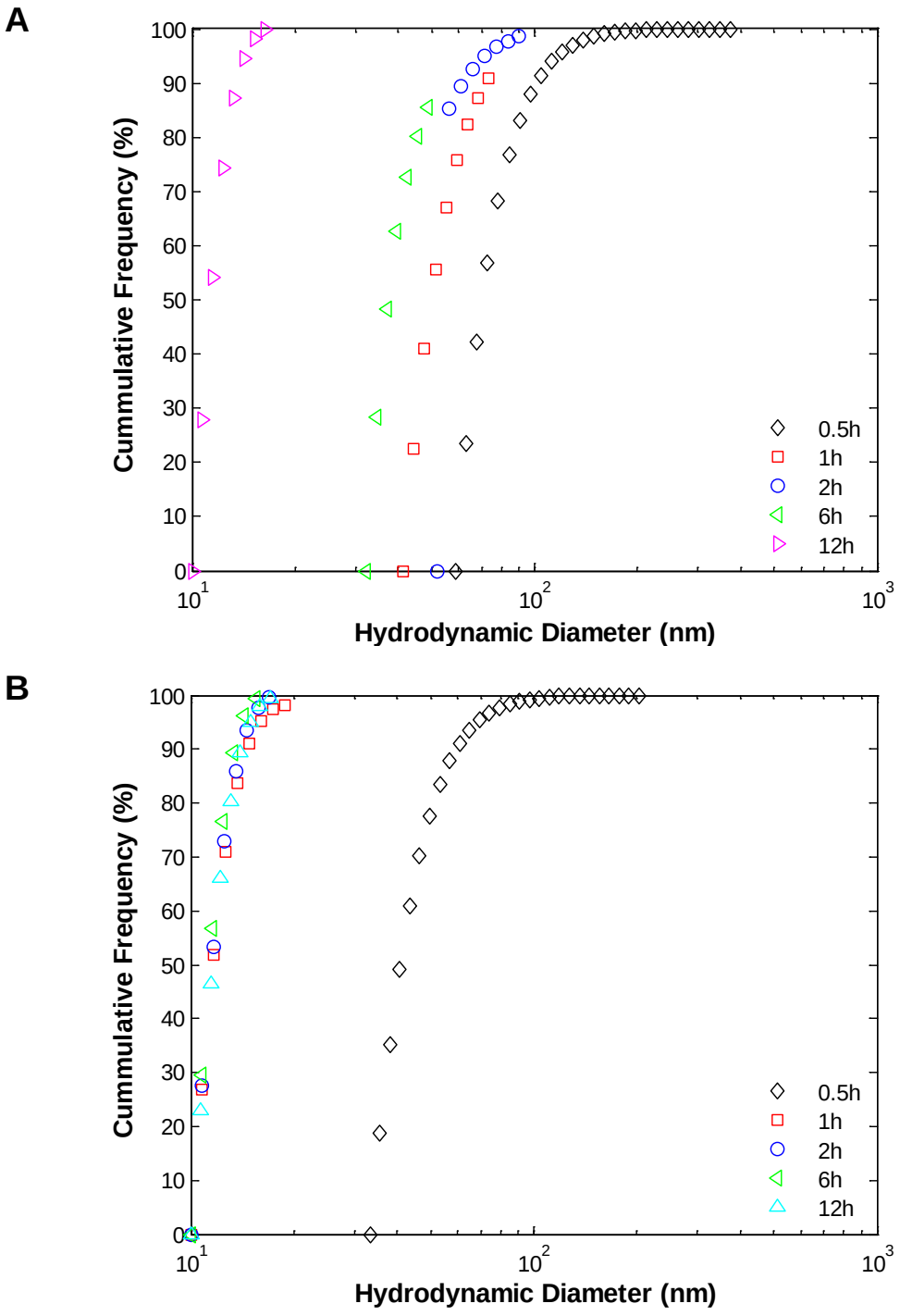

Figure 3.5. Size distribution of (A) waxy corn and (B) waxy rice starches after enzymatic treatment 2 (T2) first incubated at 100°C for 20min and continuing the treatment during different incubation times at 65°C.

These results highlight the capability of α-amylase enzyme to withstand at 100°C for 20 minutes and show a similar trend on dextrin size as it was observed on T1, and the smaller the native waxy starch the smaller the size of dextrin it was obtained from T2. The smaller the dextrin size the more feasible will be to engineer particles of nanosize characteristics. Small dextrin could be converted to small amphiphilic molecules at low cost and be capable to encapsulate hydrophobic active compounds.

3.4.3 Moisture sorption isotherms

The sorption isotherms (Figure 3.6 A and B) show an increment of water sorption in all the depolymerized OSA-modified waxy corn starch (DWxCn) compared to native waxy corn starch (WxCn) (Figure 3.6.A, 3.6.B), except in the highest DE WxCn. A higher degree of OSA reaction efficiency has been related to a higher level of depolymerization treatment for waxy corn starch (Bai, 2008). The OSA modification seems to reduce the water adsorption of high DE WxCn at low water activity (A_w*100 = RH) levels. The reduction of water sorption in high DE WxCn seems to be affected by the level of OSA modification in samples only exposed to low RH environments; however, greater water adsorption (~50% more) ocurred under the environment that provided the highest RH (97%). Similarly, water sorption reduction was observed on OSA-modified phytoglycogen (Figure 3.7.A) stored at lower than 80% RH. However, the higher the percentage of OSA modification (7%), the more the water adsorption under the environment that provided the highest RH (97%) compared to the behavior of native phytoglycogen.

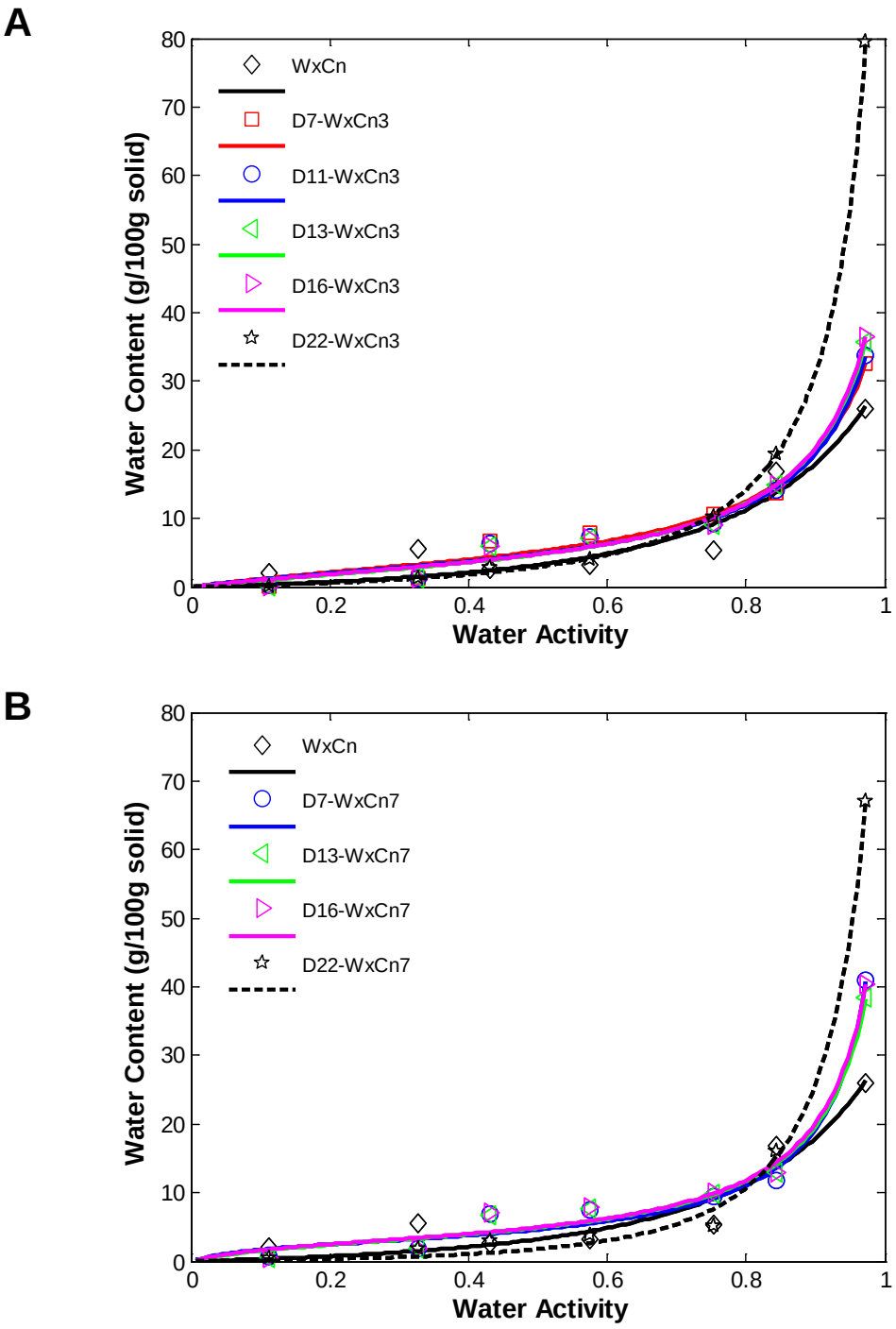

Figure 3.6. Moisture sorption isotherms at 23°C of native waxy corn starch, with (A) 3% OSA modification and (B) 7% OSA modification at different degree of enzymatic depolymerization (DE=7 - 22).

The alkaline conditions for OSA reaction (pH 8.6) of higher OSA modification could produce more glucosidic bond cleavage to form more functional groups (Tharanathan, 2005) on the surface of phytoglycogen granules, increasing the available hydroxyl groups to cross-link with more OSA reagent. However, the percentage of OSA modification seems to reduce the water adsorption only at low RH environment (< 80%). Therefore, the unbounded hydroxyl groups would increase the affinity to moisture (Wurzburg, 1972) at high RH conditions.

In general, higher water adsorption at all water activity levels, except at 97% RH, was observed for the whey protein concentrate (80%), whey protein isolate and α-lactalbumin samples, compared to 7% OSA-modified highly depolymerized waxy starch and phytoglycogen (Figure 3.7B). However, at the highest RH (97%) the OSA-modified polysaccharides adsorbed 40% more water than the proteins.

The GAB model parameters for different natural and OSA-modified polysaccharides, as well as whey proteins are summarized in Table 3.1. A significantly ($P < 0.05$) higher water monolayer capacity ($\boldsymbol{v_m}$) was observed on native waxy corn; followed by depolymerized waxy corn starch at 3% OSA modification (D22-WxCn3) , depolymerized waxy rice starch at 3% OSA modification (D24-WxRc3), whey protein isolate, α-lactalbumin, and natural phytoglycogen.

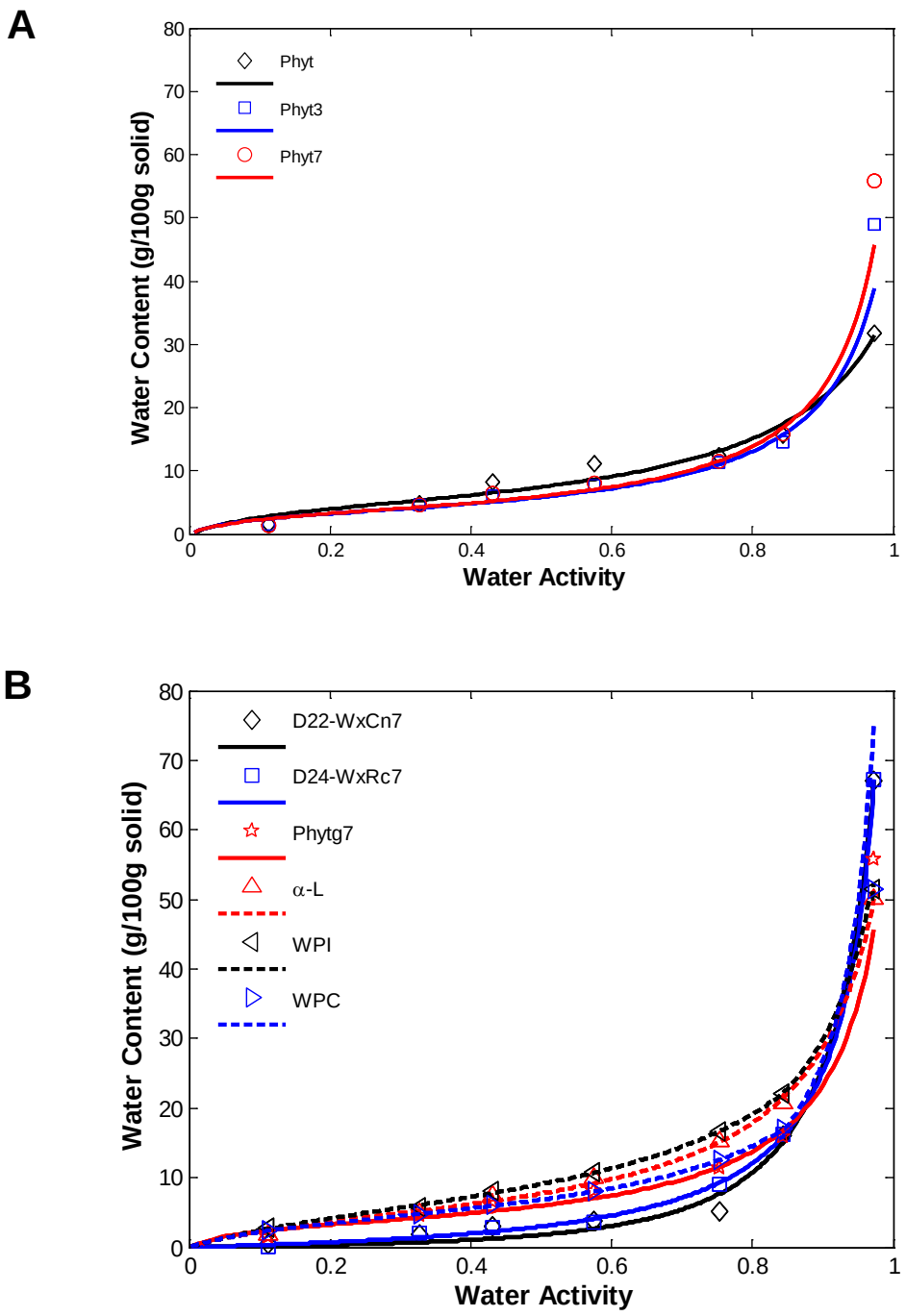

Figure 3.7. Moisture sorption isotherms at 23°C of (A) native phytoglycogen at different percentage of OSA modification (3% and 7%) and (B) depolymerized waxy corn starch (DWxCn), depolymerized waxy rice starch (DWxRc), phytoglycogen (Phytg) at 7% OSA modification, α-lactalbumin (A-L), whey protein isolate (WPI) and whey protein concentrate 80% (WPC).

Table 3.1 GAB-model parameters at water activity (Aw) range of 0.11 - 0.97, monolayer value (vm), critical water activity and energy constants CG and k for natural and depolymerized waxy corn starch and waxy rice starch, natural and phytoglycoge with 3% and 7 % of OSA modification, α-lactalbumin, whey protein isolate and whey protein concentrated.

Polymer Type	v_m ***(g/100gsolid)***	***Critical Aw***	C_G	***k***	R^2
WxCn	6.29 ± 1.08^{a}	0.66	7.64 ± 0.53^{de}	0.77 ± 0.04^{c}	0.987
D7-WxCn3	3.62 ± 0.91^{c}	0.36	4.15 ± 0.55^{f}	0.92 ± 0.03^{abcd}	0.982
D11-WxCn3	3.34 ± 0.73^{c}	0.36	4.13 ± 0.51^{f}	0.93 ± 0.02^{ab}	0.987
D13-WxCn3	3.45 ± 0.76^{c}	0.38	3.22 ± 0.35^{f}	0.93 ± 0.02^{ab}	0.989
D16-WxCn3	3.36 ± 0.70^{c}	0.37	3.54 ± 0.391^{f}	0.94 ± 0.02^{ab}	0.998
D22-WxCn3	5.71 ± 0.83^{abc}	0.63	0.39 ± 0.01^{g}	0.97 ± 0.01^{a}	0.999
D7-WxCn7	2.60 ± 0.50^{c}	0.22	13.49 ± 3.44^{b}	0.96 ± 0.01^{a}	0.984
D13-WxCn7	2.90 ± 0.52^{c}	0.27	8.90 ± 1.51^{cde}	0.95 ± 0.01^{ab}	0.986
D16-WxCn7	2.90 ± 0.54^{c}	0.26	9.89 ± 1.82^{cd}	0.96 ± 0.01^{a}	0.985
D22-WxCn7	3.42 ± 0.31^{c}	0.53	1.08 ± 0.34^{g}	0.98 ± 0.01^{ab}	0.999
D24-WxRc3	5.07 ± 0.40^{bc}	0.57	0.67 ± 0.01^{g}	0.96 ± 0.004^{a}	0.999
D24-WxRc7	3.59 ± 0.38^{c}	0.54	0.79 ± 0.02^{g}	0.98 ± 0.004^{ab}	0.999
Phytg	4.68 ± 0.82^{bc}	0.27	10.87 ± 1.45	0.88 ± 0.02^{b}	0.979
Phytg3	3.28 ± 0.26^{c}	0.21	16.72 ± 1.82^{a}	0.94 ± 0.01^{ab}	0.996
Phytg7	3.35 ± 0.26^{c}	0.21	15.38 ± 1.68^{ab}	0.95 ± 0.01^{a}	0.997
α-L	4.78 ± 0.65^{bc}	0.29	3.49 ± 1.01^{e}	0.93 ± 0.01^{ab}	0.9997
WPI	5.16 ± 0.49^{bc}	0.26	5.56 ± 0.72^{cd}	0.93 ± 0.04^{ab}	0.999
WPC 80%	3.56 ± 0.50^{c}	0.25	8.80 ± 0.65^{cd}	0.96 ± 0.004^{a}	0.999

Values represent mean ± standard deviation of three replicates per sample.
[a-g] Means values with same letter in same column are not significantly different ($P > 0.05$)
Critical A_w was calculated from GAB curve based on the monolayer value.

In general, water monolayer capacity is related to the critical water activity (Barbosa-Cánovas et al., 2007); as it is observed on Table 3.1. Above the critical moisture content; a detrimental effect on the product stability occurs. Consequently, determination of product critical water activity level is important for evaluation of product stability under different RH storage conditions. Higher water monolayer values were directly related to the critical water activity, except for whey proteins. Critical water activity has also been related to mechanical properties and product stability in low moisture product. When the moisture content related to the critical water activity is reached, a transition from glassy to rubbery occurs, which affects the mechanical properties of the product (Barbosa-Cánovas et al., 2007), therefore, high critical water activity is associated with better sample stability. Significantly lower ($P < 0.05$) water monolayer capacity and consequently lower critical water activity was observed on WxCn at lower degree of depolymerization than DE=22 at different percentage of OSA modification levels. On the other hand, no significant differences ($P > 0.05$) on the water monolayer capacity were observed on native and OSA-modified phytoglycogen compared to the different whey proteins.

The limitation of the GAB equation (equation 3.5) to explain and represent the sorption of materials at very low water activity levels is well known. Compared to GAB monolayer, BET monolayer values have been referred to provide a more physical meaning and acceptability to considered for food stability (Rahman, 1999); however the monolayer values calculated by the GAB equation seems more reasonable according to Timmermann's results (Timmermann, 2003). These results highlight the very low

critical water content on depolymerized and OSA-modified waxy starch, OSA-modified phytoglycogen and whey protein concentrated (80%), limiting these products stability at water activity values less than 0.6 (~60 % RH).

The GAB energy constant $\boldsymbol{C_G}$ determines the more or less pronounced form of the `knee' at the lower water activity range (Timmermann et al., 2001), but this value has not been taken in consideration (Timmermann, 2003) based on its vast range of values for similar food stuff. Although $\boldsymbol{C_G}$ values seem to decrease with the increment in the level of depolymerization, higher values of $\boldsymbol{C_G}$ were observed on 7% OSA-modified waxy corn at DE = 7, compared to native waxy corn starch. On the other hand, the energy constant *k* value has a more applicable physical interpretation. This constant describes the characteristic capability of the sorbent (e.g. biopolymers) in relation to the energy bound to the sorbate (e.g. water) beyond the first layer of bounded sorbent-sorbate molecules. The values of *k* are always less than 1, because a molecule on the top layer of molecules directly sorbed by the solid has less bounded energy than the molecules in a pure liquid sorbate. Therefore, the water molecules from these upper layers are easier to desorb than from the pure liquid sorbate. In other words, the water molecules in the upper sorbed layers have higher vapor pressure than of the liquid (Timmermann, 2003).The *k* values presented in Table 3.1 show no significant differences ($P > 0.05$) among depolymerized WxCn, OSA-modified phytoglycogen and whey proteins. The only significant differences were observed for natural phytoglycogen and natural WxCn. The average *k* value of natural WxCn (0.77) is characteristic of non-porous solid (Timmermann, 2003), and this result is in agreement with values presented

for other starchy materials such as potato, corn wheat, rice, flours that follow in the narrow range between 0.70-0.77 (Chirife et al., 1992). However, the values for whey proteins are out of the range of 0.82-0.88 previously published for these type of biopolymers (Chirife et al., 1992). This discordance occurs because the *k* values are also affected by the sorbate sorption capability at higher water activity levels (>0.85), where the sorption curves present a noticeable upswing characteristic as it is observed for all depolymerized waxy starches, OSA-modified phytoglycogen and whey proteins (Figure 3.7). In the mathematical analysis all data points were considered including the water sorption values at RH of 97%; however, when fitting the GAB equation in a narrow range to RH 84% (A_w=0.84), the *k* values for all whey proteins fell within the relative range of 0.84-0.89, which is considered characteristic for proteins, *k*~0.8 (Timmermann et al., 2001). In this study, all the moisture sorption data were incorporated based in our interest to evaluate the sorption behavior of the different biopolymers for use as potential encapsulation matrices exposed to high RH environments.

3.4.4 Glass transition temperature of biopolymers

WxCn of different dextrose equivalent (DE= 7-22) and different OSA modification (3 and 7%) had lower Tg (35-42^{o}C) compared to the native WxCn (56°C) (Table 3.2). No significant differences (P > 0.05) on Tg were observed among native WxCn, native WxRc, and the different whey proteins (Table 3.2). Similarly, no significant difference was observed among the different DE dextrin obtained from WxCn, WxRc, at different percentage of OSA modification.

Table 3.2. Glass transition temperature (Tg) for depolymerized (DE) OSA-modified (3% and 7%) waxy corn starch, waxy rice starch, phytoglycogen, α-lactalbumin, whey protein isolate and whey protein concentrate 80%.

Polymer Type	Range Temperature (°C)	Tg(°C) Average ± Stdev
WxCn	5-100	53 ± 0.96^{a}
DE7-WxCn3	5-100	40 ± 0.82^{fgh}
DE11-WxCn3	5-100	40 ± 0.58^{fgh}
DE13-WxCn3	5-100	41 ± 1.00^{efg}
DE16-WxCn3	5-100	43 ± 3.56^{defg}
D22-WxCn3	5-100	42.5 ± 0.71^{defg}
DE7-WxCn7	5-100	35 ± 3.71^{ghi}
DE11-WxCn7	5-100	39 ± 1.26^{ghi}
DE13-WxCn7	5-100	36 ± 1.96^{ghi}
DE16-WxCn7	5-100	40 ± 3.74^{fgh}
DE22-WxCn7	5-100	41.3 ± 1.77^{efg}
WxRc	5-100	49 ± 3.51^{abc}
D24-WxRc3	5-100	40.5 ± 4.9^{fg}
D24-WxRc7	5-100	43.5 ± 0.70^{def}
Phytg	5-100	46 ± 2.16^{bcd}
Phytg3	5-100	45 ± 0.58^{cde}
Phytg7	5-100	41 ± 1.71^{efg}
α-Lactalbumin	5-100	54.0 ± 1.41^{a}
Whey Protein Isolate	5-100	50.5 ± 0.71^{ab}
Whey Protein Concentrate 80%	5-100	54 ± 2.83^{a}

Values represent mean ± standard deviation of three replicates per sample.
[a-i]Means values with same letter are not significantly different ($P > 0.05$)
Values were measured by DSC performed between 5 and 100°C at 10°C/min rate.

The Tg of natural phytoglycogen (46°C) was not different ($P > 0.05$) to that of 3% OSA-modified phytoglycogen (45°C), while the 7% percentage of OSA modification on phytoglycogen significantly reduced the value of Tg (41°C). The opposite effect occurred for DWxCn, which showed higher Tg (41.3°C) with increasing

DE value at higher percentage of OSA modification (7%), although no significant differences were observed among them.

The sensitivity to water adsorption of the different waxy starches was greatly influenced by the enzymatic treatment, lowering the Tg of DWxCn and DWxRc at higher relative humidity compared to native starch (Figure 3.8). These results suggest that these enzymatic depolymerized waxy starches become plasticized when adsorbing low quantity of water, as it is observed in Figure 3.8. The drastic reduction of the Tg value occurred at very low mass fraction of adsorbed water per solid sample (0.1). Therefore, careful attention must be taken when using depolymerized waxy starches as encapsulating matrices that will be exposed to high RH environments.

On the other hand, phytoglycogen at different percentage of OSA-modification, as well as the different whey proteins showed less reduction of the Tg values (Figure 3.9), thus showing better stability at higher water adsorption levels compared to depolymerized waxy starches.

The models proposed by Gordon and Taylor (Gordon and Taylor, 1952) and Kwei (Kwei, 1984) were tested for the prediction of Tg of different biopolymers at different water sorption ratios (g of water adsorbed per g of solid biopolymer at different RH environments). In general, Tg values calculated by the Kwei equation were a little higher than the values calculated by Gordon-Taylor Equation 3.6 (Table 3.3).

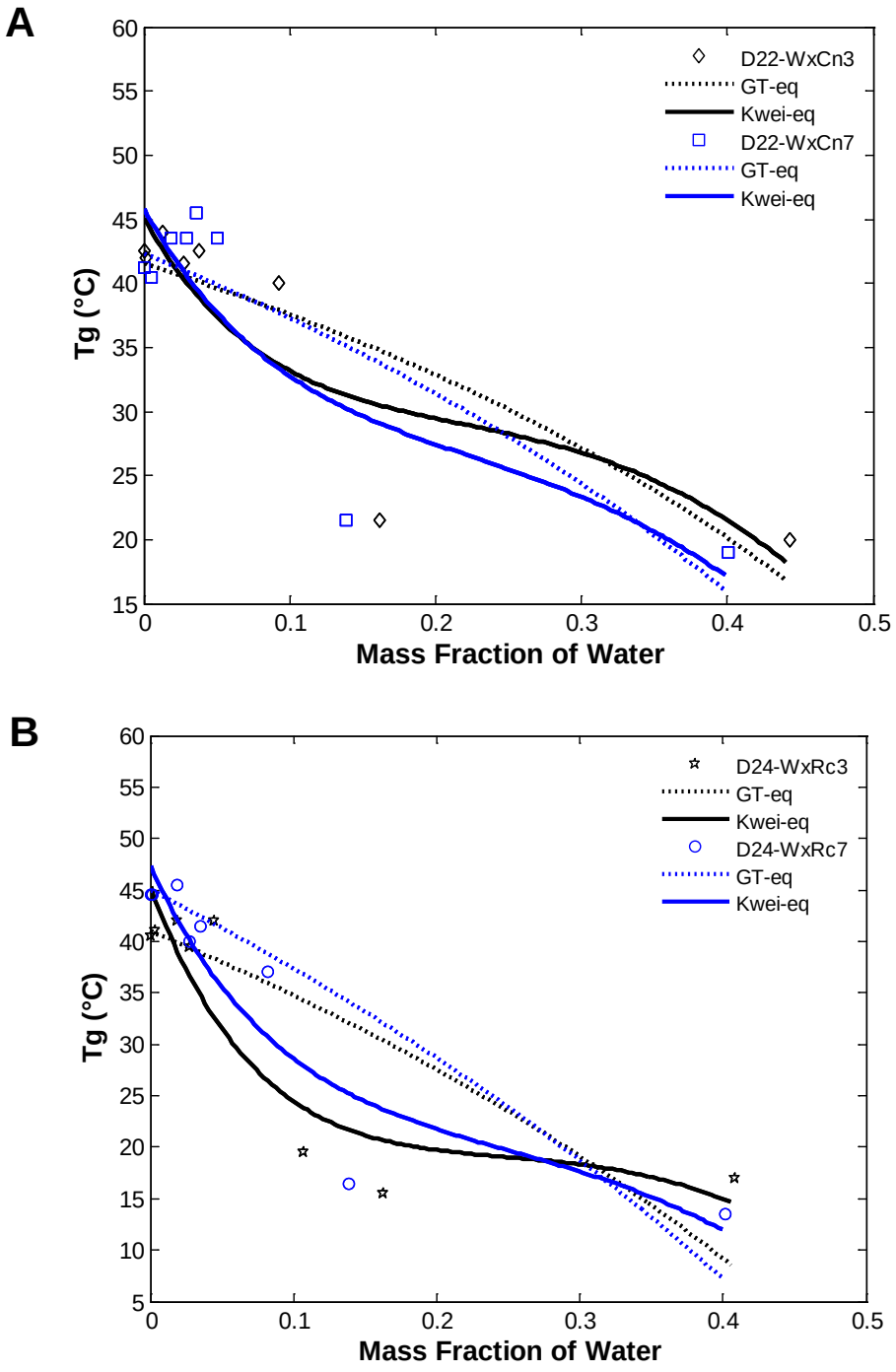

Figure 3.8. Effect of mass fraction of adsorbed water on the glass transition temperature of (A) depolymerized (DE = 22) waxy corn starch and (B) depolymerized (DE = 24) waxy rice starchat different DE with 3% and 7 % of OSA modification.

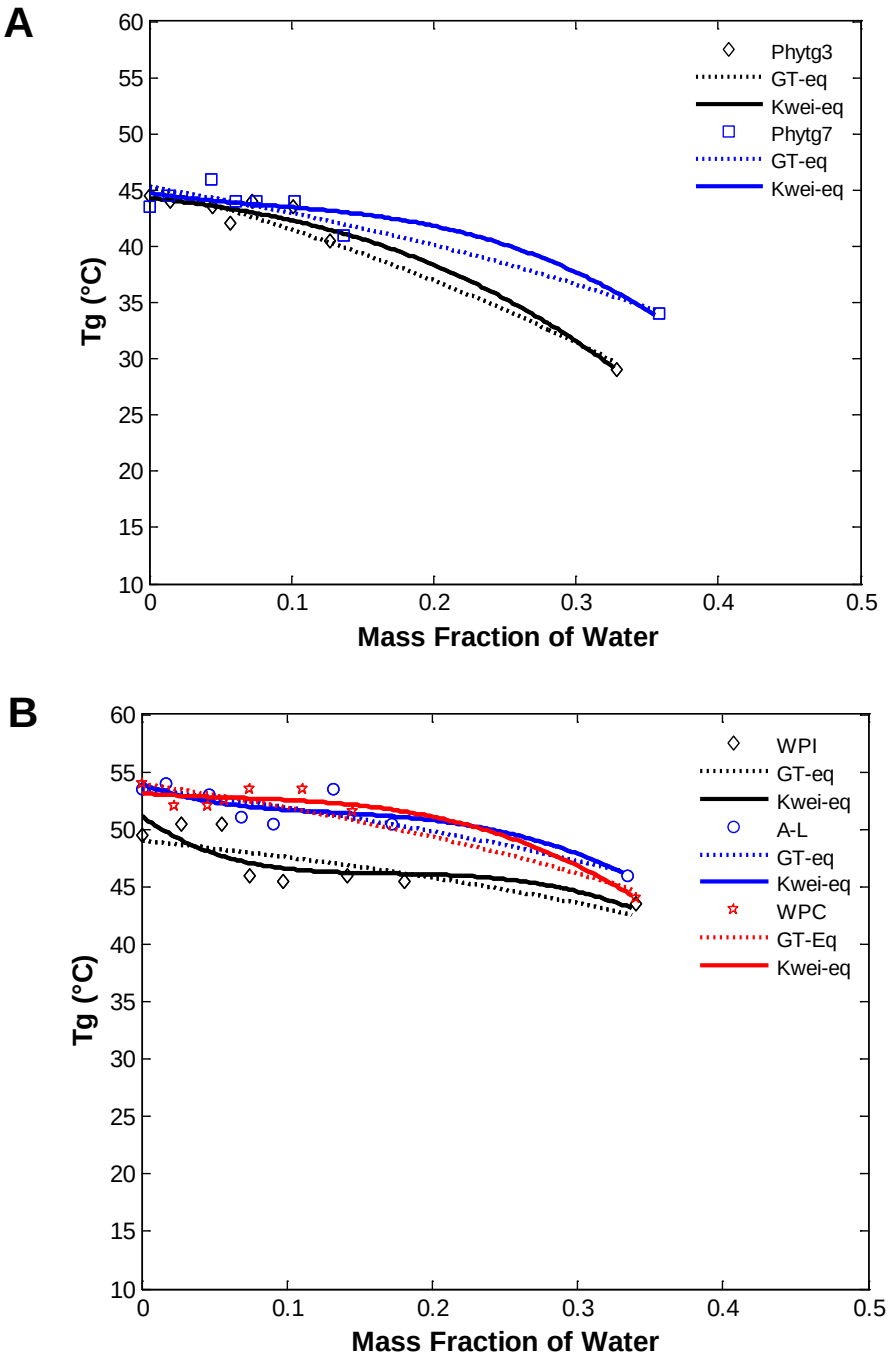

Figure 3.9. Effect of mass fraction of adsorbed water on the glass transition temperature of (A) phytoglycogen at different percentages of OSA modification and (B) whey proteins : α-lactalbumin, whey protein isolate (WPI) and whey protein concentrate 80% (WPC).

Table 3.3. Glass transition temperature (Tg) values and Gordon-Taylor and Kwei model constants for different biopolymers stored at different relative humidities.

Polymer Type	***RH (%)***	**Gordon-Taylor Equation**			**Kwei Equation**			
		T_{g2} (°C)	**K_{GT}**	**R^2**	**T_{g2} (°C)**	**K_{Kw}**	**q**	**R^2**
D22-WxCn3	11 – 97	41.54 ± 1.73^{h}	4.83 ± 1.01^{d}	0.670	45.06 ± 2.17^{ef}	0.287 ± 0.042^{de}	426.4 ± 30.01^{ab}	0.742
D22-WxCn7	11 – 97	42.33 ± 1.79^{gh}	3.81 ± 0.79^{d}	0.680	45.86 ± 2.50^{ef}	0.297 ± 0.057^{cde}	401.3 ± 38.58^{b}	0.741
D24-WxRc3	11 – 97	41.00 ± 0.01^{h}	3.02 ± 0.63^{d}	0.487	45.35 ± 2.54^{ef}	0.222 ± 0.030^{e}	437.5 ± 29.17^{ab}	0.799
D24-WxRc7	11 – 97	45.00 ± 0.01^{ef}	2.51 ± 0.39^{d}	0.673	47.35 ± 2.16^{def}	0.259 ± 0.035^{de}	399.4 ± 29.00^{b}	0.857
Phytg3	11 – 97	45.30 ± 0.63^{ef}	5.15 ± 0.56^{d}	0.876	44.29 ± 0.95^{fg}	0.545 ± 0.089^{a}	315.2 ± 34.70^{c}	0.895
Phytg7	11 – 97	45.26 ± 0.72^{ef}	8.51 ± 1.50^{c}	0.719	44.74 ± 1.24^{efg}	0.439 ± 0.055^{b}	389.4 ± 27.09^{b}	0.701
α-L	11 – 97	53.54 ± 0.58^{ab}	12.46 ± 2.46^{ab}	0.661	53.90 ± 0.90^{ab}	0.385 ± 0.029^{bc}	444.5 ± 17.96^{ab}	0.689
WPI	11 – 97	49.01 ± 0.66^{cd}	14.06 ± 3.84^{a}	0.549	51.16 ± 1.05^{bc}	0.331 ± 0.022^{cd}	468.9 ± 15.77^{a}	0.613
WPC 80%	11 – 97	53.98 ± 0.84^{ab}	9.95 ± 2.35^{bc}	0.582	53.14 ± 1.38^{ab}	0.452 ± 0.066^{b}	405.9 ± 33.05^{b}	0.625

Values represent mean ± standard deviation of three replicates per sample.
Means values with same letter are not significantly different (P > 0.05)
RH = Relative humidity

These results showed that the Kwei equation is better model to predict the Tg sensitivity to water sorption in biopolymers exposed to different relative humidity environments. Kwei model (Equation 3.7) was better than the Gordon-Taylor model (Equation 3.6) for those biopolymers that had a large reduction on Tg at low water sorption ratios (e.g. 0.15), which suggests the strong sensitivity of these biopolymers (e.g. depolymerized waxy starches) to a little amount of adsorbed water. Therefore, the radical reduction of Tg at low adsorbed water ratio indicates the poor stability of depolymerized waxy starches under high relative humidity environments.

The Tg values related well to the physical appearance of the different solid biopolymers stored under different RH environments. The effect of adsorbed water at different RHs on the physical appearance of the different biopolymers is shown on Figure 3.10. Depolymerized waxy starches at 7% of OSA modification appeared to have melted when exposed to over 75% RH and 23°C for 10 days.That melted appearance of depolymerized waxy starches is an indication of their structure failure, which make them ineffective as an encapsulating matrix, thus reducing their capability to hold a bioactive compound at high RH environments.

Critical A_w has also been related to mechanical properties and product stability in low moisture product. When the moisture content related to the critical A_w is reached, a transition from glassy to rubbery will change the mechanical properties of the product (Barbosa-Cánovas et al., 2007). This general assumption was not observed for α-lactalbumin, whey proteins isolate and whey protein concentrate 80% which presented a critical A_w of 0.29, 0.26 and 0.25, respectively (Figure 3.10).

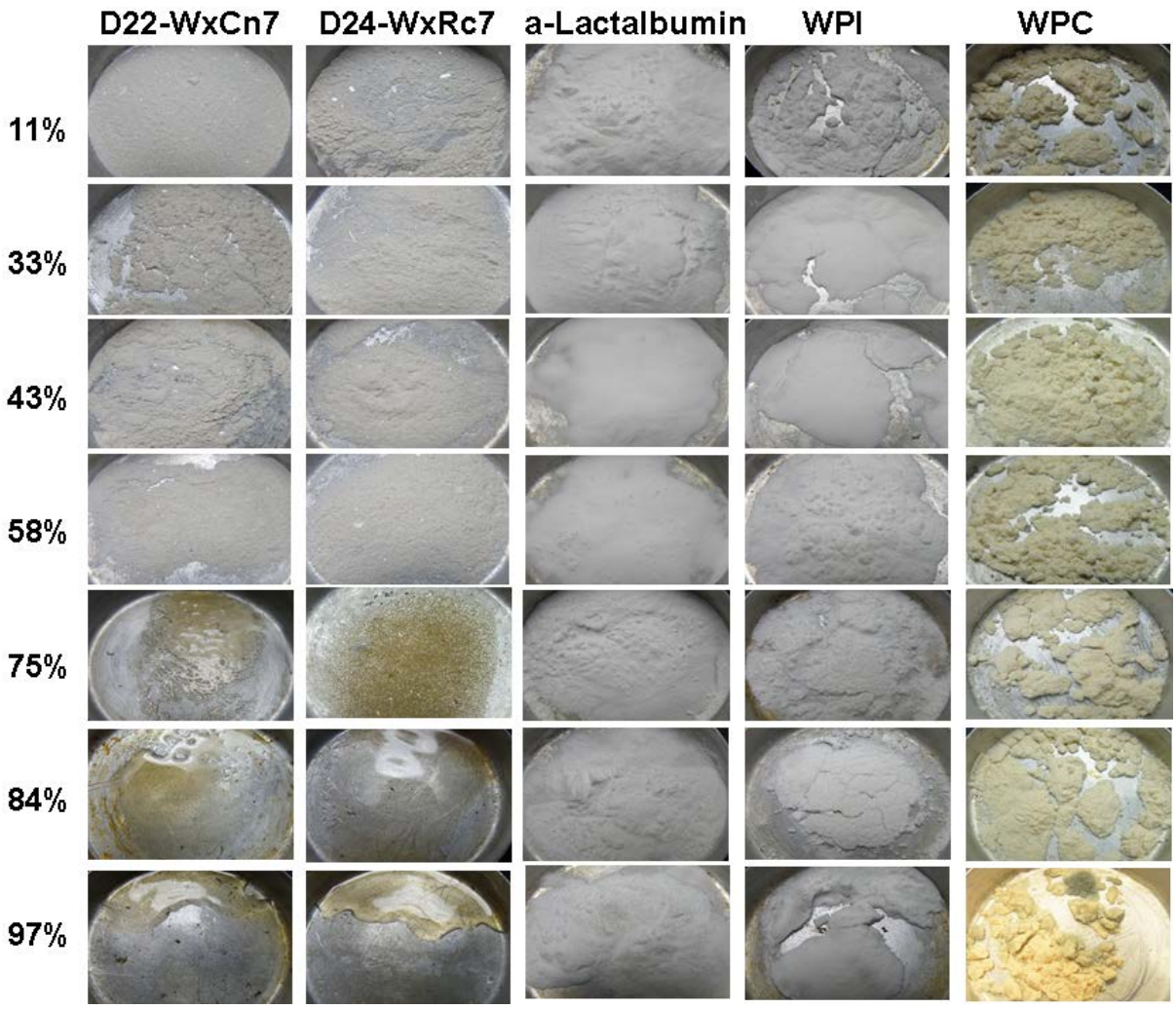

Figure 3.10. Effect of water sorption on the physical appearance of depolymerized and OSA-modified waxy corn (D22-WxCn7), waxy rice (D24-WxRc7) starch, α-lactalbumin, whey protein isolate (WPI), and whey protein concentrated 80% (WPC) after 10 days of storage at 23°C and different RH.

All whey proteins presented a more stable (solid-like) appearance and had higher Tg values even under very high RH environment (97% RH) (Figure 3.9B). Proteins have a hydrophobic domain, built from secondary structural units connected by loops regions. The packing of the polypeptide is usually much tighter in the interior than exterior of the protein structure producing a solid-like core and a fluid-like surface (Zhou et al., 1999). This protein's characteristic structure may be the reason for the more stable physical appearance of the whey proteins, even when exposed to very high RH environments. On the other hand, the formation of more hydrophilic groups, as a result of more free hydroxyl groups formed at each terminal unit of dextrin, increased the affinity to moisture and water solubility (Wurzburg, 1972). The percentage of OSA modification was not high enough to revert the hydrophilic domain of the dextrin.

Fungi growth was observed only on the surface of whey proteins concentrate 80% at 97% RH. This observation is consistent with the microbial stability of the whey protein concentrate (80%) that was predicted by its critical Aw (0.25). The presence of fungi is probably due to the fact that the whey protein concentrate contains about 5.5% of sugar (product manufacturer's specification), which could be the source of carbon for microbial growth.

3.5 Conclusions

The production of small size dextrin from waxy corn and rice starches by enzymatic depolymerization with α-amylase was optimized with preliminary gelatinization of starch granules at 100°C for 20 minutes and subsequently incubated

during 6 hours at 65°C. The smallest predominant dextrin diameter size of 15 nm was obtained from waxy rice starch, which showed smaller native size granule (2μm) compared to those of waxy corn (20μm). The smaller the dextrin size the more feasible will be to engineer particles of nanosize characteristics using that biopolymer. Small dextrin could be converted into small amphiphilic molecules at low cost and capable to encapsulate hydrophobic active compounds.

Depolymerized waxy corn and rice starch (DWxCn and DWxRc) presented an increment in water adsorption compared to native waxy starch (WxCn). Although the percentage of octenyl succinate anhydrate (OSA) modification of different depolymerized waxy starches did reduce the water adsorption sensitivity at low RH (<70%), an opposite effect was observed at high RH (97%). The different whey proteins (α-lactalbumin, whey protein isolate and whey protein concentrate 80%) presented higher water adsorption sensitivity at most RH compared to 7% OSA-modified D22WxCn, D24WxRc and phytoglycogen, an opposite effect was observed at RH of 97%, indicating more water adsorption of the OSA-modified polysaccharides than the whey proteins at high RH environments.

Although the microbial stability of the whey protein concentrate (80%) was predicted by its critical A_w (~0.25), the moisture sorption isotherm method could not fully explain the effect of adsorbed water on the physical characteristic of the biopolymers. However, water plasticization was well established with the measurement of Tg values of the biopolymers exposed under different RH environments The different whey proteins were more stable (solid-like) and had higher Tg values even under very

high relative humidity environment (97%). Moreover, large reduction of Tg at low adsorbed water ratios in depolymerized waxy starches denote poor structure stability at high RH environments (>70%). These results suggest that depolymerized and OSA-modified polysaccharides become unstable and should not be used alone as encapsulating matrices for materials that will be exposed to an environment with RH > 70%.

The combination of different methods to characterize the stability and physical characteristic of biopolymers is necessary to determine future application and handling of these materials. More studies should be carried out on the use of depolymerized and OSA-modified dextrin in combination with proteins to create more stable blends of biopolymers. This information is helpful for future design of encapsulation materials depending on storage environment conditions.

CHAPTER IV

FLUORESCENT AND RHEOLOGICAL METHODS TO ESTIMATE BIOPOLYMER INTERACTIONS FOR ENCAPSULATION PURPOSES

4.1 Overview

An increased interest in the use of inexpensive and natural biopolymers as carriers has motivated research on the use of octenyl succinate-modified polysaccharides and whey proteins. The objective of this study was to evaluate the self-assembly interaction of aqueous diluted biopolymers such as enzymatic depolymerized waxy corn starch (DWxCn), waxy rice (DWxRc) starch, and phytoglycogen modified at different percentage levels with octenyl succinic anhydride (OSA), as well as whey protein isolate (WPI), and α-lactalbumin using fluorescent spectroscopy, creep and dynamic oscillatory tests. Structure micelle-type formation of WPI (0.6 g/L) and α-lactalbumin (2.5 g/L) was determined with a fluorescent method, using 2 μM-Pyrene as the fluorescent probe. Results suggest that another type of structure seems to be formed between 10 to 20 g/L for the different OSA-modified polysaccharides. The linear viscoelastic region (LVR) was observed within range of 0.001 and 0.01 Pa for different concentrations of diluted proteins (0.18, 1.80, and 18.0 g/L) at 0.1 Hz and 23°C. Thus, creep and dynamic oscillatory tests were performed at 0.01 Pa and 23°C. The variability on the Zero Shear Viscosity (ZSV) values estimated from the creep test at each biopolymer concentration makes this method unreliable. The relationship of the elastic (G') and viscous (G") moduli as a function of the angular frequency, called relaxation time "λ" was influenced

by the frequency and polymer concentration. A distinct linear reduction of λ values (slope) up to a critical frequency value (CFV) was established as an indicator of structure formation. Higher values of λ were in agreement with the solid-like behavior observed (G'> G"). Proteins and OSA-modified DWxRc showed a well define slope at all concentrations, while dilutions of OSA-modified phytoglycogen only showed a defined slope at 18.0 g/L, indicating the absence of self-assembly at lower concentrations. With the exception of WPI (0.18 g/L) and 7% OSA-modified DWxRc (1.8 g/L), there were no significant differences ($P > 0.05$) among λ slopes values, which suggests the formation of similar structures at these different concentrations of biopolymers. The self-assembly interaction of α-lactalbumin (3.6 g/L) in combination with OSA-modified polysaccharides was only observed with 18.0 g/L of 7% OSA-modified DWxRc, at a CFV of 0.08 Hz (0.5 s/rad). However, WPI (3.6 g/L) presented self-assembly with all different OSA-modified polysaccharides at the different concentrations evaluated (0.18, 1.8, and 18.0 g/L) independently of the percentage of OSA modification. In summary, the intermolecular interactions among amphiphilic biopolymers are strongly influenced by the structure type and to a lesser extent by the percentage of OSA modification. Dynamic oscillatory testing of intermolecular interactions among biopolymers is a good method to help understand their structure type for practical applications as natural carriers.

4.2 Introduction

Some of the drawbacks of using biodegradable polymers and their derivatives in foods such as PLGA or poly (lactic-co- glycolic acid), which is approved by the Food and Drug Administration for human therapy are the polymers cost, the simplification of manufacturing procedure to allow economic scale-up, and the reduction of the potential toxicity of different components involved in their manufacturing such as toxic reagents. Additionally, synthetic additives such as potassium bromate, BHA and BHT approved as a food additives in USA have been banned in other countries because might cause some health concerns and there is strong pressure to ban them. For instance, it is thought that the ingestion of dietary particles could promote a range of metabolic diseases. In a vitro and in a vivo study using intestinal epithelium and chickens, respectively, have shown a physiological response that influenced iron uptake and iron transport during chronic and acute expose to polystyrene nanoparticles (Mahler et al., 2012). Similar disruptions in nutrient sorption could be possible in other inorganic elements such as calcium, copper and zinc, as well as other nutrients such as fat-soluble vitamins A, D, E and K and need to be investigated (Mahler et al., 2012).

On the other hand, proteins and polysaccharides originate from natural food raw materials, are considered GRAS (generally recognized as safe), widely available, and relatively inexpensive (Livney, 2008). Polysaccharides are the most abundant macromolecules in nature. The complex carbohydrates which consist of monosaccharides joined together by glycosidic bonds are often one of the main structural elements of plants and animals exoskeleton (e.g. pectin, cellulose,

carrageenan, chitosan, chitin) or have a key role in plant energy storage (e.g. starch, phyroglycogen) (Aminabhavi et al., 1990). Polysaccharides such as waxy corn starch and phytoglycogen have been converted to alkenyl esters in order to impart functional application as rheology modifiers (Krstonošić et al., 2011), emulsion stabilizers (Liu et al., 2008), surface modifiers and nanoparticles as drug delivery vehicles (Gurruchaga et al., 2009; Krstonošić et al., 2011; Liu et al., 2008; Scheffler et al., 2010b). Starches modified at maximum level of 3% of modification with Octenyl succinic anhydrate (OSA) are allowed for use in food applications. Similarly, among milk proteins, whey proteins either used alone or in combination with polysaccharides have been extensively investigated for delivery of hydrophobic bioactive compound (Livney, 2010; Sekhon, 2010), as well as rheology modifiers, emulsion stabilizers, and surface modifiers.

β-Lactoglobulin (BLG) is a major constituent of the whey protein (about 58 %), hence tending to dominate the assembly behavior of whey proteins (Hansted et al., 2011). It is a globular protein with 18.3 kDa of g/mol of about 3 nm in length and its functionality as lipid transporter make this protein part of the lipocalin family (Kontopidis et al., 2004). The primary sequence of β-lactoglobulin contains 162 amino acid residues with two disulphide bonds and on free cysteine (Hansted et al., 2011). The secondary structures are formed by folding up into 8-stranded antiparallel β–barrel structures with a 3-turn lone α–helix located on the surface of the molecule (Kontopidis et al., 2004). The most distinctive feature of lipocalin proteins is the presence of 8-stranded β-barrel structures which give them the capability to bind and transport small hydrophobic molecules in the beta barrel calix.

α-lactoalbumin (α-L) is the second higher constituent of total whey protein (about 20%). It has a molecular weight of 14.18 kDa with 5 nm size and is composed of 123 amino acid residues and 4 disulfide bridges. This protein is rich in amino acids tryptophan and cysteine, which form disulfide bonds, and the main structural differences with BLG is that does not have any free thiol group (-SH) that can serve as the starting-point for a covalent aggregation reaction under heat or acid denaturation on the presence of calcium, which make this protein more stable in the presence rather than the absence of calcium (Engel et al., 2002). In a native state, α-L consists of a large α-helical domain composed of 3 major α-helices and 2 short helical structures and a second small domain β-sheet composed of a 1series of loops, where tree-stranded antiparallel β-pleated sheet are connected by calcium binding and a short helical structure connected by hydrogen bonds (Permyakov and Berliner, 2000).

Surface active molecules like proteins and OSA-modified polysaccharides possess both hydrophilic (polar, water-loving) and hydrophobic (nonpolar, lipid loving) properties that make them to be called amphiphilic molecules. Most of these amphiphilic molecules form structures in aqueous solution by their spontaneous self-assembly (Israelachvili, 2010). These structures and the systems they form, instead of arising from strong covalent or ionic bonds are influenced from weaker van der Waals, hydrophobic, hydrogen-bonding, and screened electrostatic interactions. The surrounding characteristics of the medium, such as electrolyte concentration, pH, and temperature exert strong influence on these forces interactions (Nylander et al., 2008). Thus, modifying the size and the shape of the structures (Israelachvili, 2010). On the boundary

layers between lipids and water, surface active substances may saturate at certain concentration forming structures called micelles. Above the minimum concentration that amphiphilic molecules can form micelles, no more molecules can enter the boundary layer and this critical micelle concentration (CMC) becomes an important design parameter for application such as an emulsifier. At higher solution concentrations, micelles of various sizes and shapes pack together and form other characteristic symmetries (Parfitt and Rochester, 1983).

High interest on the diverse interaction between amphiphilic molecules, such as proteins (e.g β-lactoglobulin, α-lactalbumin) and different types of surfactants (e.g. Tween 20 or sodium dodecylsulphate, SDS), has motivated several studies for potential application in the food industry. Different techniques have been used to study the interaction between amphiphilic molecules, such as surface tension, surface rheology (Dickinson and Hong, 1994; Maldonado-Valderrama and Patino, 2010), fluorescent spectroscopy, circular dichroism spectroscopy (Engel et al., 2002; Hansted et al., 2011), differencial scanning calorimetry (Hegg, 1980), and nuclear magnetic resonance (Konuma et al., 2007). Surface tensions measurements have been found to be inaccurate in the presence of impurities, which could bound the protein and have a drastic effect on the interfacial behavior (Clark et al., 1995). Scanning calorimeter has been useful to understand the concentration of SDS and solution conditions in the heat stabilization of BLG (Hegg, 1980), which was not the purpose of the this work. Thus, spectroscopic and rheological methods were used.

The critical micelle concentration (CMC) of proteins and OSA-modified carbohydrates is an indication of self-assembly by ionic and hydrophobic interactions in aqueous solutions. Fluorescent spectroscopic technique is among the most common method to investigate the formation of micelle-type structures. Fluorescent spectroscopy is based on the solubility that a chromophore undergo significant shift spectra inside micelles (Hoiland and Blokhus, 2003). Pyrene is a highly popular fluorescent probe used to investigate polarity changes in micro-organized systems, commonly used to characterize micelle formation by non-ionic surfactant (Wolszczak and Miller, 2002) and water soluble copolymers of poly(ethylene oxide-propylene oxide) (Turro and Kuo, 1986), as well as different types of surfactants alone and their interaction with BLG (Hansted et al., 2011). Monitoring the intensity ratio of the first (373 nm) and the third (383 nm) vibrational bands of pyrene is an indication of microenvironment polarity and can be used to determine the CMC.

Binding between pure or combination of different amphiphilic molecules not only depends on hydrophobic interactions but it is also mediated by ionic forces (Israelachvili, 2010). Unlike low molecular weight surfactants, proteins can saturate the liquid/liquid or gas/liquid interface with relative low concentrations, therefore it is easy to displace other small surface active substances, which could be presented in higher quantities (Dickinson and Woskett, 1989). Because of this relative low concentration of proteins to stabilize films, the adsorbed layer is much stiffer and presents viscoelastic properties (Chen and Dickinson, 1995), which is originated from the protein/protein interaction.

Viscoelastic characteristics of polymer dilutions have been accomplished in the range of relatively low frequencies where viscoelastic properties are mainly influenced by motion than length of polymer chains (Osaki et al., 2001). The linear viscoelastic region presents reversible changes of the structure in the suspension, hence, evaluation within the linear viscoelastic region will determine intrinsic properties of the colloidal system (Li et al., 2005). The elastic response is understood as the deformation capability of the intermolecular interaction to overcome proportional stresses and strains without disrupting the integrity of the network structure, which is only complying within the limits of linear viscoelasticity (Schramm, 2002).

Although the linear viscoelasticity characteristic of polymer melts (at high concentration) has been used to understand intrinsic properties, the application in real fluids to link to distinct molecular structures has been very difficult and less efforts have been done in this matter for polymer solutions and even lesser work for amphiphilic biopolymers. Creep and recovery and oscillatory dynamic tests are the most common test to study the linear response in polymer solutions. In a creep and recovery test, the deformation response is measured over the time when a constant stress is applied until an equilibrium response is achieved. Similarly, oscillatory controlled stress/strain is applied in small amplitude oscillatory frequency sweeps and the response is evaluated (Sunthar, 2010).

The solid-like behavior of polymer solutions has been associated to self-assemble network formation between association of an hydrophobic polymer and a nonionic surfactant (Talwar et al., 2006). Polymeric nanocomposite materials have been shown to

behave as viscoelastic liquid by the evaluation of interrelation between their elastic modulus (G') and viscous modulus (G'') through their relaxation time "λ" spectrum (Utracki, 2004) . The relaxation time "λ" is associated with the large scale motion (or changes) in the structure of the polymers (Chhabra, 2010; Roland, 2008). It is evident that the rheological properties of polymers in diluted or concentrated solution are very sensitive to molecular structure and functionality (Chamberlain and Rao, 2000) and the understanding of intermolecular interactions based on rheological tests will be very helpful for the application of amphiphilic biopolymers as carriers of bioactive compounds for food and pharmaceuticals.

The purpose of this study was to evaluate the self-assembly characteristics of pure or a combination of OSA-modified polysaccharides and whey proteins in aqueous solution. The fluorescent spectroscopy and rheological tests provide critical information about the structure and the type of association presented by the different biopolymers in aqueous solution. Information about the self-assembly association of these biopolymers will be helpful for future design of encapsulating materials in aqueous solution depending on the structure and concentration of pure and a combination of these different biopolymers.

4.3 Materials and methods

4.3.1 Materials

Waxy corn and waxy rice starches (Ingredion, Westchester, IL) were depolymerized with α-amylase-heat stable (Sigma-Aldrich Co., St. Louis, MO) to produce high dextrose equivalent (DE) values (DE= 22 - 24). Depolymerized waxy corn and waxy rice starches as well as phytoglycogen (a highly branched polysaccharide) (Kewpie Corporation, Japan) were modified at different percentage of substitution (approx. 3 and 7%) with Octenyl succinic anhydride (OSA) (Dixie Chemical Co, Houston, TX). Whey protein isolate, whey protein concentrate (80%) and α-Lactalbumin (DAVISCO Foods International, Inc., Eden Prairie, MN) were used without any modifications. Glucose standard, and other reagents and solvents were purchased from Sigma-Aldrich and VWR International (West Chester, PA).

4.3.2 Preparation of OSA-modified polysaccharides

Twenty five grams of waxy starch sample was added into distilled water in a glass beaker with agitation. The reaction condition for optimum preparation of OSA-waxy starch was carried out as follows: starch concentration in water of 31.5%, temperature 34°C, pH 8.6, and reaction time of 18.7 h (Liu et al., 2008). The pH of the mixture was kept constant adding 0.1N NaOH and the reaction was terminated by reducing the pH to 6.5 using 0.1N HCl. To collect the samples, three volumes of ethanol were added to the mixture and the precipitate was centrifuged at 3200 x g for 20 minutes (Allegra 25R centrifuge, Beckman Coulter, Fullerton, CA) and subsequently washed

with ethanol and centrifuged 3 more times. Afterwards, the sample was dried in a vacuum oven (Squared Lab Line Instruments, Melrose Park, IL) at 60°C overnight.

4.3.3 Percentage of modification (%OSA)

Octenyl succinate modification in waxy starches and phytoglycogen was quantified using a method from the Joint FAO/WHO Expert Committee on Food Additives (JECFA, 2011) with some modifications. The sample (0.5g) was acidified with 3 ml of 2.5 M HCL for 30 minutes. Ten ml of pure isopropanol was added, followed centrifugation at 3200 x g for 20 minutes. Subsequently, the precipitate was washed and centrifuged 3 more times or until the test of chloride ions using one drop of 0.1 M $AgNO_3$ on the supernatant showed negative haze formation. Afterwards, 30 ml of distilled water was added to the precipitate and heated in boiling water for 30 min, and then titrated using 0.01 M NaOH. The percentage of OSA modification (%OSA) was calculated by the following equations:

$$A = \frac{(V - V_0) * 0.01}{0.5} \tag{4.1}$$

$$\%\, OSA = \frac{210 * A}{1000} * 100 \tag{4.2}$$

Where A (mmol/g) is the molar amount of octenyl succinate groups in one gram of derivative; 210 is the molecular weight of octenyl succinate group (g/mol); *V* (ml) is the

volume of NaOH solution consumed by the octenyl succinate derivative; V_0 (ml) is the volume of NaOH consumed by the native waxy starches or phytoglycogen; 0.5 is the weight of material in grams and 0.01 is the molar concentration of NaOH (JECFA, 2012).

4.3.4 Enzymatic treatment of waxy starches

Waxy corn and rice starch samples (5 g, dry weight) were mixed with water to a 35% suspension by weight containing 200ppm of $CaCl_2$. The pH of the mixture was adjusted to 5.9 with 0.1N NaOH and α-amylase at 20 U per gram of starch was added into the mixture (Liu et al., 2008). The suspension was heat up on a hot plate at 100°C for 20 minutes and then incubated in a shaking water bath (VWR International, West Chester, PA) set at 65°C and 100 rpm for 360 minutes. The reaction was stopped by reducing the mix pH to 4.0 with 0.5N HCl. Three volumes of ethanol were added to the mixture, followed by centrifugation at 3200 x g for 20 minutes (Allegra 25R centrifuge, Beckman Coulter, Fullerton, CA) and the precipitate solid were dried in a vacuum oven (Squared Lab Line Instruments, Melrose Park, IL) at 60°C overnight. The dextrose equivalent (DE) value was confirmed based on the following equation:

$$DE = \frac{Reducing\ sugar\ content\ (\frac{mg}{g})}{Total\ sugar\ content\ (\frac{mg}{g})} \quad (4.3)$$

4.3.5 Total sugar content

The phenol-sulfuric acid assay method was carried out (Fournier, 2001). This method is very general, and can be applied to many classes of carbohydrates including oligosaccharides where reducing and non-reducing sugars are present. The phenol-sulfuric acid method is based on the absorbance at 490 nm of colored aromatic complex formed between phenol and the carbohydrate. The amount of sugar present was determined by comparison with a calibration curve of D (+) glucose using a spectrophotometer (Thermo Scientific Genesys 10S UV-Vis, Waltham, MA). One hundred mg of sample was diluted in 10 ml of distilled water. One ml of the previous dilution was subsequently diluted in 9 ml of distilled water. A blank was prepared using 50 µl of distilled water. Five hundred µl of 4% phenol was added to 50 µl of later dilution and followed by 2.5 ml 96% sulfuric acid. The mixture was allowed to cool down at room temperature for 15 minutes and its absorbance measured in a spectrophotometer (Thermo Scientific Genesys 10S UV-Vis, Waltham, MA) at 490 nm.

4.3.6 Reducing sugar content

Quantification of reducing sugars was determined by the Somogyi-Nelson method (Fournier, 2001). This method utilizes the reducing properties of certain types of carbohydrates based on the absorbance at 500 nm of a colored complex formed between a copper-oxidized sugar and arsenomolybdate. The amount of reducing sugar present was determined by comparison with a glucose calibration curve using a spectrophotometer (Thermo Scientific Genesys 10S UV-Vis, Waltham, MA). One

hundred mg of sample was diluted in 10 ml of distilled water. One ml of the previous dilution was subsequently diluted in 9 ml of distilled water. A blank was prepared using 50 µl of distilled water. One ml of low-alkalinity copper agent was added to the 50 µl of later dilution and heated in boiling water for 10 min. Then, 1 ml of arsenomolybdate reagent was added with an extra 2900 µl of distilled water and the mixture was allowed to cool down at room temperature for 15 minutes and its absorbance measured in a spectrophotometer (Thermo Scientific Genesys 10S UV-Vis, Waltham, MA) at 500 nm.

4.3.7 Sample preparation

Concentrated biopolymer solutions (184 g/L) were prepared in distilled water, vortexed for at least 30 seconds, stored in at room temperature for 6 hours or until complete dissolution of biopolymer. Afterwards, the solution was filtered with 0.2 µm nylon filters (VWR, West Chester, PA), then re-diluted in distilled water to different biopolymer concentrations (0.18 – 100.0 g/L) and subsequently stored in to 4°C overnight. The following day the samples were let to warm up at room temperature (approx. 23°C) for 1 hour prior to performing the fluorescent and rheological tests at room temperature.

4.3.8 Fluorescent method

The critical micelle concentration (CMC) was determined by preparing a pyrene ethanolic stock solution (5 mM), and subsequently dissolved in a series of aqueous solutions of biopolymer at different concentrations in order to achieve the same, constant

pyrene concentration target of about 2 μM per sample. The pyrene molecule was excited at 337 nm and its emission was read at 373 nm (I_1) and 383 nm (I_3). The intensity ratio of those third and first fluorescent spectrum peak (I_3/I_1) of pyrene has been related with a micelle formation in aqueous solution based on the microenvironment polarity of the pyrene monomers. Micelle type structure formation has been considered at steady state reached by the intensity fluorescent ratio curve of pyrene. The measurements were done at 23 ± 1°C using a Fluorometer Turner™ Model 450 (Thermo Fisher Scientific, Waltham, MA).

4.3.9 Rheological evaluation

All different tests were performed with a Haake RheoStress 6000 Rheometer (Thermo Fisher Scientific, Waltham, MA) using a cone and plate sensor, in which the rotating cone was 60 mm in diameter with an angle of 1°, with a gap of 0.052 mm. About 1 ml of each sample was carefully placed in the plate, and left to rest for 5 min for structure recovery. The temperature was maintained at 23°C with the help of Peltier TC 81 Thermo Haake system (Thermo Fisher Scientific, Waltham, MA) in all the experiments. Analysis was carried out by triplicate on each sample after 1 day of preparation and storage at 4°C as described before. Amplitude sweeps were performed at 1 Hz and 0.1 Hz at 23°C to characterize the linear viscoelastic region (LVR) of diluted samples of proteins as reference biopolymers. Creep and dynamic oscillatory tests of all samples were performed at 0.01 Pa of stress based on the LVR of proteins. The zero shear viscosity (ZSV) was calculated from the creep test (sections 2.6.2 and 2.6.3 in

Chapter II). The storage modulus (G'), loss modulus (G''), and complex viscosity (η*) were calculated from dynamic oscillatory test (section 2.6.4 in Chapter II).

4.3.10 Statistical analysis

All experiments were replicated three times and the results were reported as average. Statistical analysis software (IBM SPSS Statistics, Version 14, IBM Corporation, Armonk, NY) was used to perform Ducan's multiple mean comparison test and analysis of covariance (ANCOVA) in a general linear model adjustment of multiple comparisons with Bonferroni's test to compare relaxation times "λ" slope calculated from dynamic oscillatory test as indication of self-assembly structure by pure or combination of biopolymers (Whey protein isolate, α-lactalbumin, 3% and 7% OSA-modified depolymerized waxy rice starch and phytoglycogen). Significance was predetermined at $P < 0.05$.

4.4 Results and discussion

4.4.1 Fluorescent characterization of biopolymers

The critical concentration of micelle-type structure formation of α-lactalbumin and WPI was around 2.5 g/L and 0.6 g/L , respectively (Figure 4.1 A and B), determined at the inflection point right before the intensity fluorescent ratio curve of pyrene reached a steady state. On the other hand, micelle-type structure formation was not observed on 3 and 7 % of OSA-modified phytoglycogen, DWxRc and DWxCn (Figure 4.2, 4.3, and 4.4); up to a maximum concentration of 100 g/L.

These results indicate that proteins have a better hydrophobic molecular interaction due to their amino acid residues that impart hydrophobic domain in the core of their structure. Thus, less concentration of proteins effectively formed a closed-end structure similar to micelle.

A curve inflection was observed around 10 g/L for OSA-modified depolymerized waxy starches, which could indicate a formation of a structure (Figures 4.2 and 4.3).This curve inflection was more noticeable on 7 % OSA-modified starch (Figure 4.2B and 4.3B). Contrary to the later results, a critical micelle concentration of about 5 g/L was reported for different OSA-modified starches with a minimum surface tension of 40mN/m (Varona et al., 2009). These results confirm the inaccuracy of surface tension measurements in the presence of impurities, as it was observed previously the presence of fatty acid had significant effect on the interfacial behavior of β-lactoglobulin (Clark et al., 1995).

Similarly, OSA-modified phytoglycongen showed a noticeable curve inflection around 20 g/L of carbohydrate concentration (Figure 4.4 A and B) and no differences were observed between both percentages of OSA modification (Figure 4.2, 4.3, and 4.4).

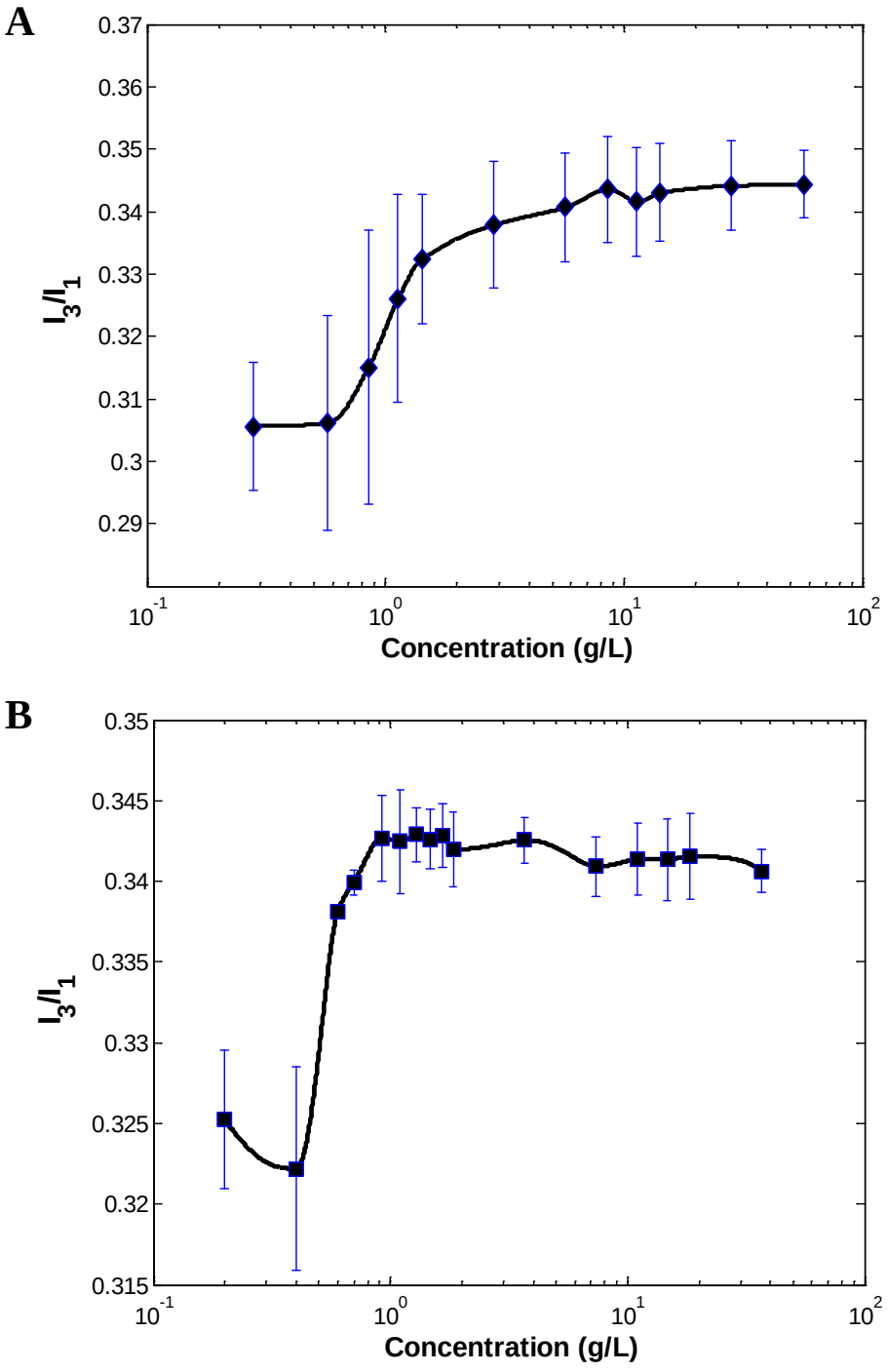

Figure 4.1. Critical Micelle Concentration (CMC) of (A) α- lactalbumin and (B) whey protein isolate by a fluorescent method using 2 μM of pyrene at 23°C. Pyrene excitation at 337 nm and local polarity based on the intensity ratio of emission at I_1 (373 nm) and I_3 (383 nm).

These later results indicate a non-micelle structure formation in the 3 and 7% OSA-modified polysaccharides and the possible formation of other type of structures. Because micelles are a defined spherical structures and the formation only occur on specific balance between the headgroups polarity and hydrophobic characteristic of the no polar components.

It is possible that OSA-modified depolymerized waxy starches aligned in parallel because the quasi-linearity of the depolymerized amylopectin chains forming a comb-like structure without closed-end terminals. The small side hydrocarbon chain of OSA alkenyl esters with approximately 11 carbons (Bai, 2008) compared to it pack molecular volume (hydrodynamic diameter of 15 nm see Chapter III) does not allow the OSA-modified depolymerized waxy starches to pack into micellar structures.

Van der Waals and hydrophobic interactions of the OSA ester groups increase the tendency to approach closely enough to permit association between parallel chains and the higher number of exposed hydroxyl groups imparts hydrophilic properties to the small amylopectin branches (see Chapter III) that keep the branches sufficiently separated to avoid aggregation and subsequent precipitation. Conversely, a higher concentration of such as phytoglycogen particles must be necessary to provide sufficient OSA ester groups and impart van der Waals and hydrophobic attraction forces among particles in order to hold a spontaneous assembly and overcome the steric repulsion of the phytoglycogen particles (hydrodynamic diameter 40 nm see Chapter III), thus forming a cluster-like structure.

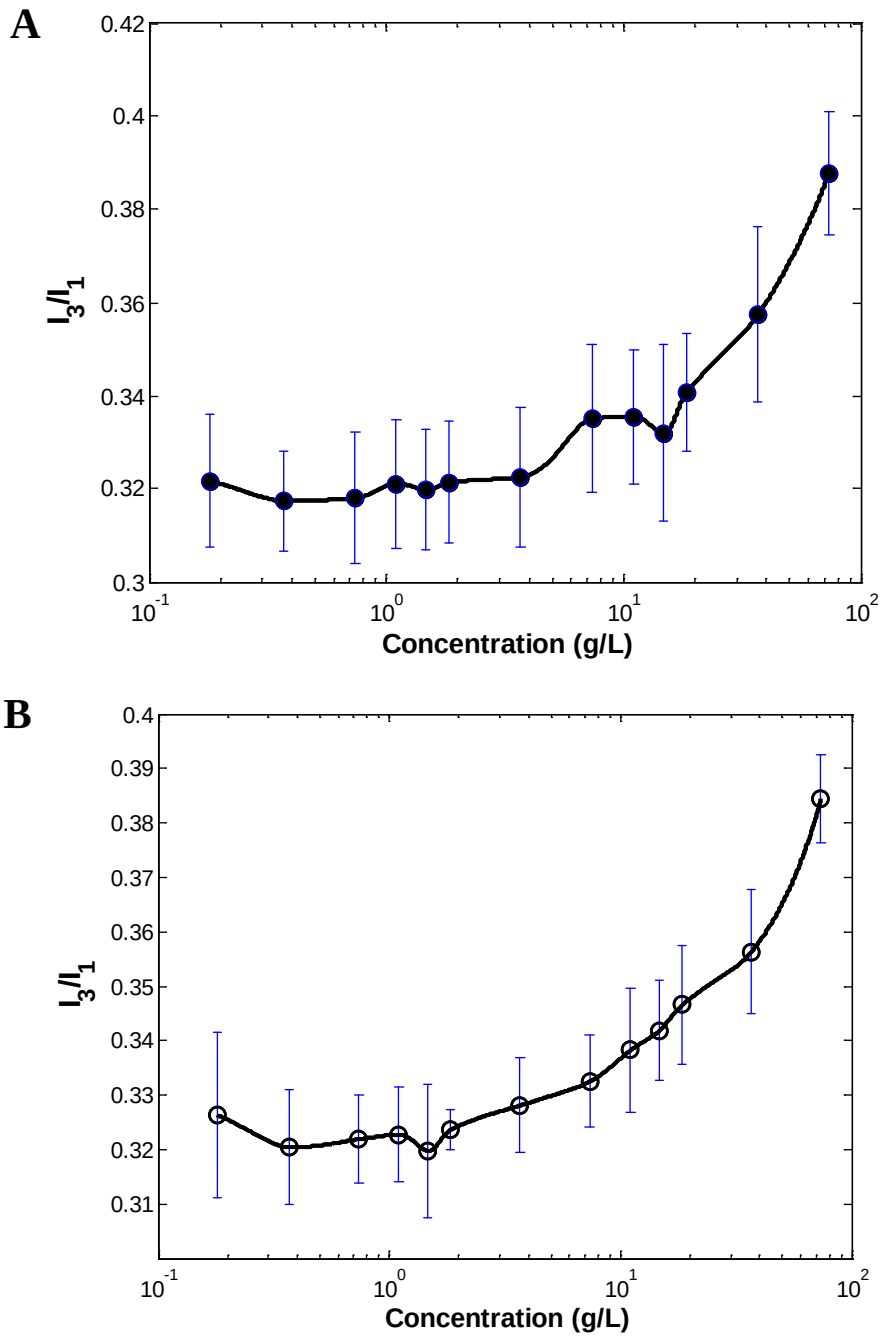

Figure 4.2. Critical Micelle Concentration (CMC) of (A) 3% OSA-modified depolymerized (DE=24) waxy rice starch (DWxRc3) and (B) 7% OSA-modified depolymerized (DE=24) waxy rice starch (DWxRc7) by a fluorescent method using 2 μM of pyrene at 23°C. Pyrene excitation at 337 nm and local polarity based on the intensity ratio of emission at I_1 (373 nm) and I_3 (383 nm).

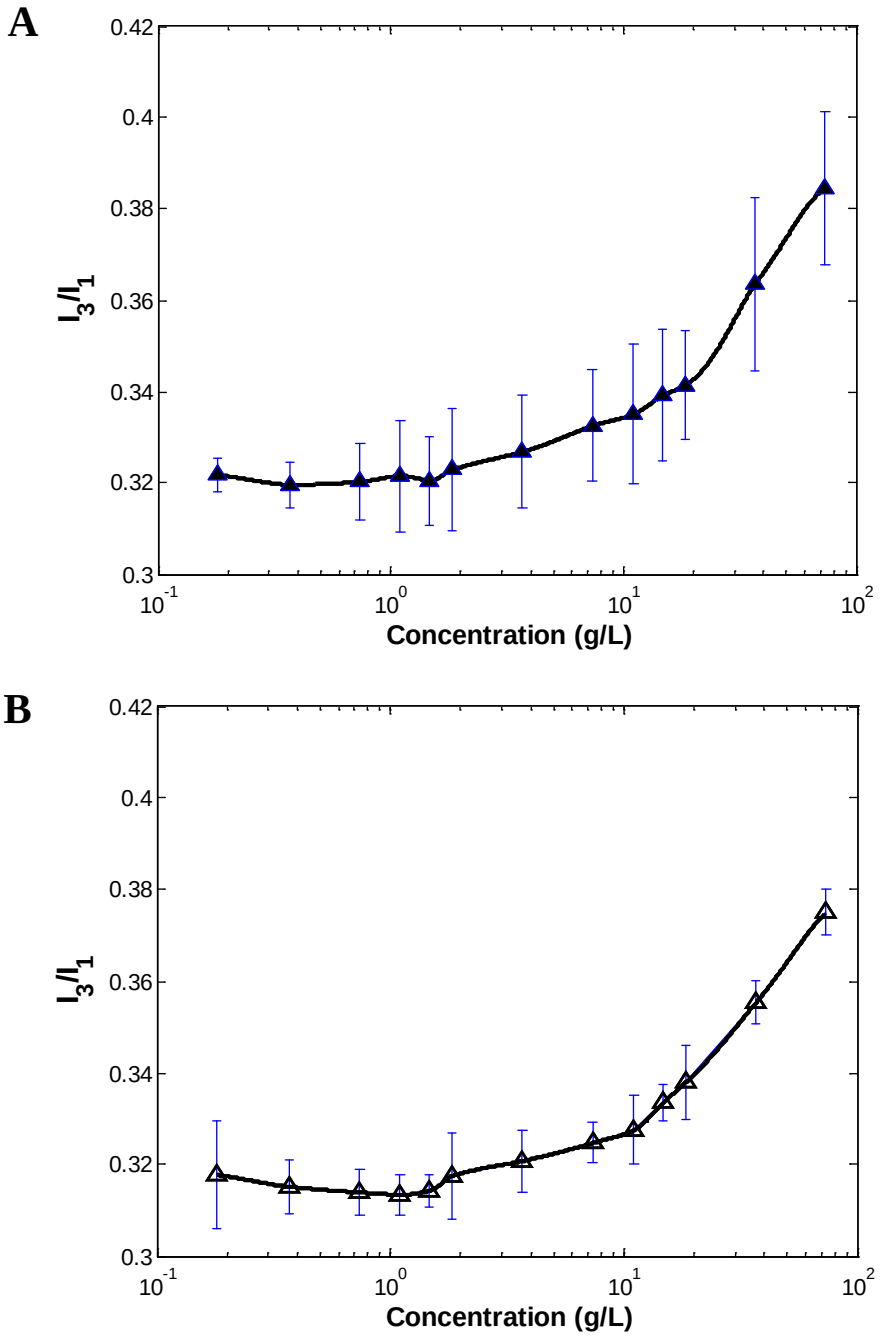

Figure 4.3. Critical Micelle Concentration (CMC) of (A) 3% OSA-modified depolymerized (DE=22) waxy conr starch (DWxCn3) and (B) 7% OSA-modified depolymerized (DE=22) waxy corn starch (DWxCn7) by a fluorescent method using 2 μM of pyrene at 23°C. Pyrene excitation at 337 nm and local polarity based on the intensity ratio of emission at I_1 (373 nm) and I_3 (383 nm).

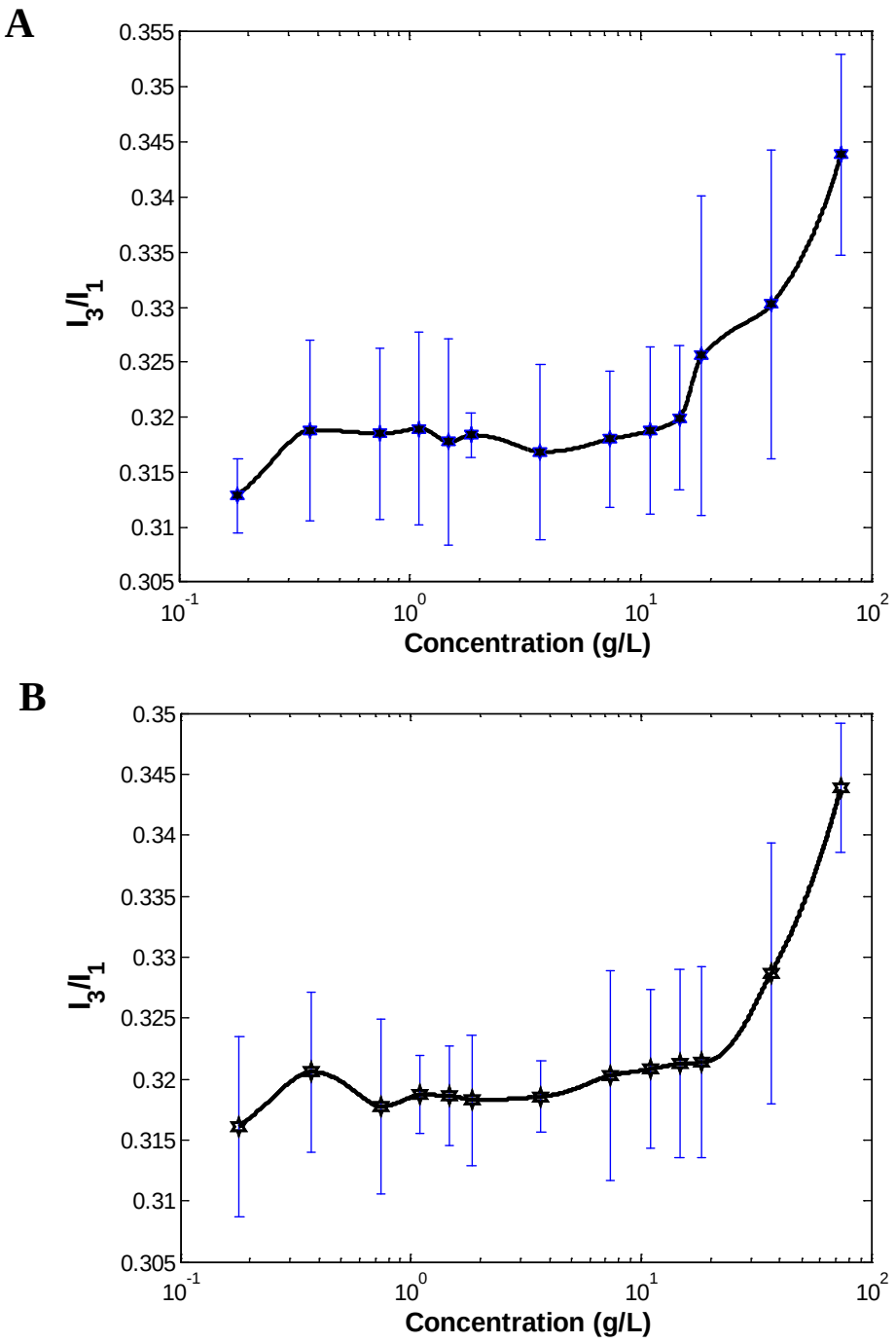

Figure 4.4. Critical Micelle Concentration (CMC) of (A) 3% OSA-modified phytoglycogen (Phytg3) and (B) 7% OSA- phytoglycogen (Phytg7) by a fluorescent method using 2 μM of pyrene at 23°C. Pyrene excitation at 337 nm and local polarity based on the intensity ratio of emission at I_1 (373 nm) and I_3 (383 nm).

4.4.2 Linear viscoelastic region (LVR) of diluted solution of proteins

Linear viscoelasticity of suspensions has been very difficult to measure at high frequency (Li et al., 2005). Solid-like properties have been identified in liquid water at room temperature and at low frequency oscillatory sweep (Noirez and Baroni, 2012). Linear viscoelastic behavior of different concentration (0.18, 1.80, 18.0 g/L) of α-lactalbumin (Figure 4.5) and whey protein isolate (Figure 4.6) are shown at two different frequencies (1.0 Hz and 0.1 Hz). The linear viscoelastic region (LVR) of α-lactalbumin and whey protein isolate was determined in all different dilution concentrations (0.18, 1.8 and 18.0 g/L) when the oscillatory test was performed at 0.1 Hz. Unlike whey protein isolate, which presents similar linear viscoelasticity for all different concentrations, 18.0 g/L of α-lactalbumin had twice higher values of the elastic modulus G', than the lower concentrations (0.18 and 1.8 g/L).

A sharp decline on the elastic modulus was found for both proteins around 0.02 Pa of stress for all different concentrations. It is unquestionable that the inherent characteristic of the colloidal system changes at this value of stress and a second viscoelastic region occurs after 0.05 Pa. The second linear viscoelastic region at higher stress values is related to the viscoelastic characteristics of the dispersed broken structure on the diluted media (e.g. water).

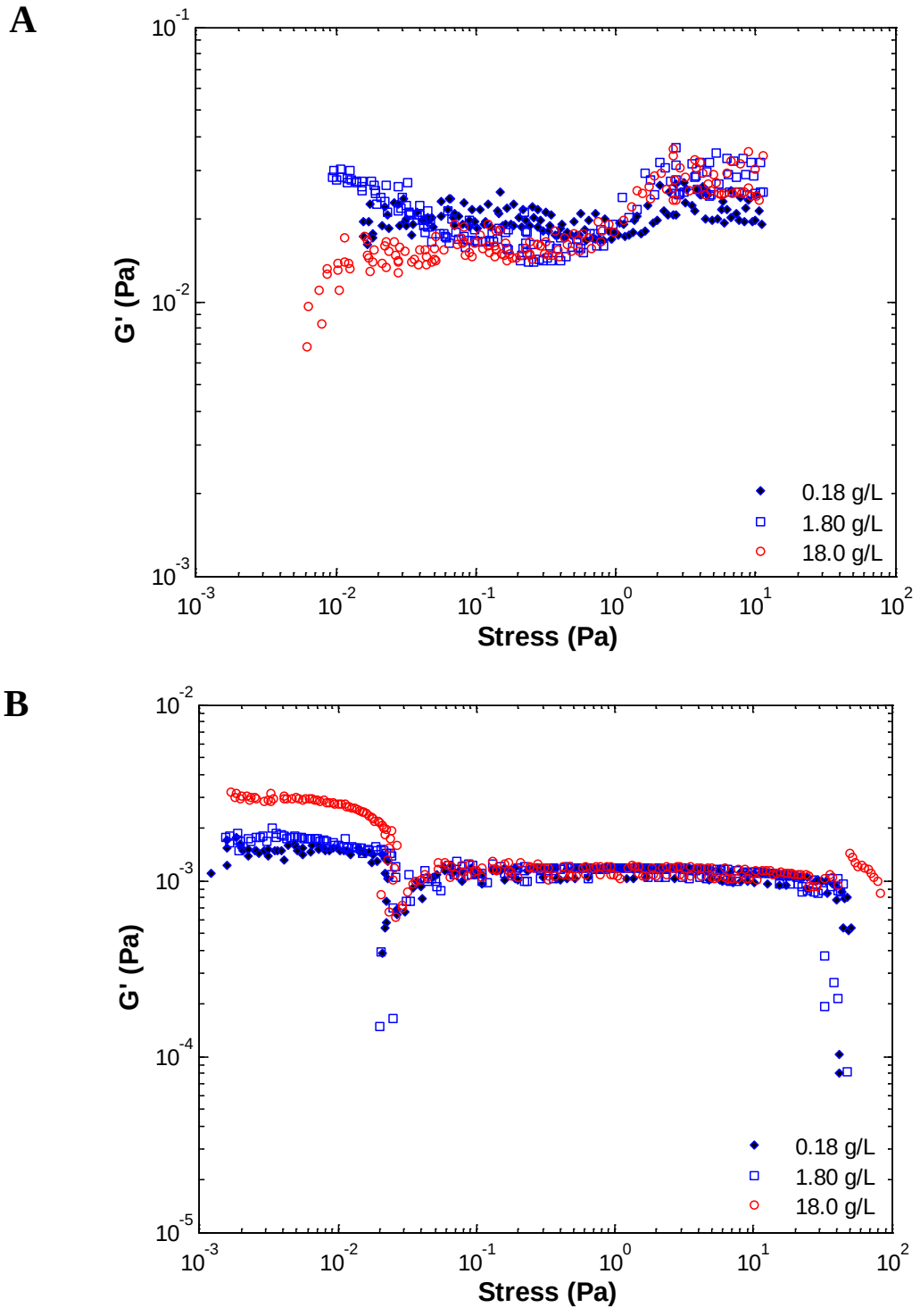

Figure 4.5. Linear viscoelastic region (LVR) of α-lactalbumin and whey protein isolate at (A) 1.0Hz and (B) 0.1 Hz and 23°C.

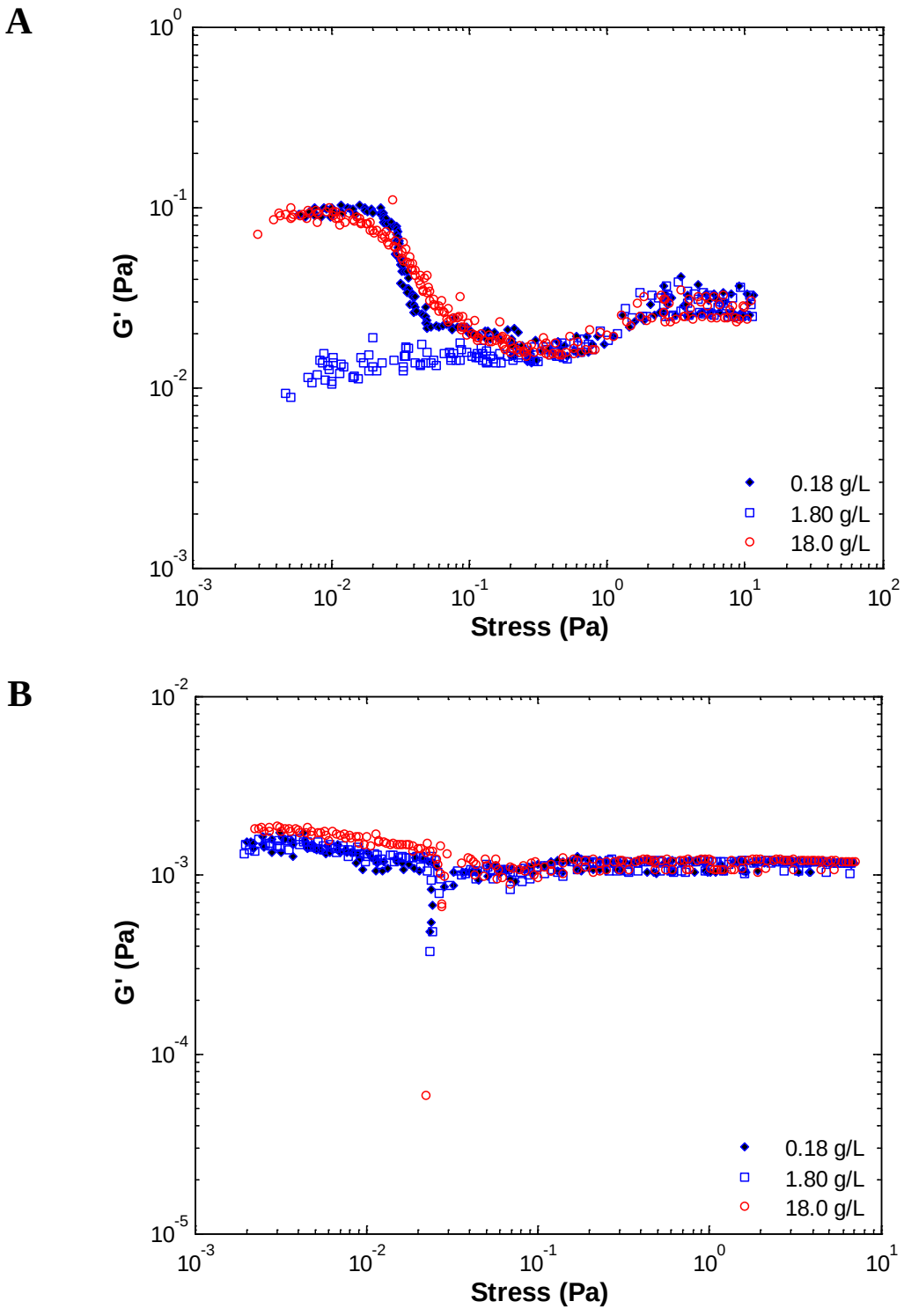

Figure 4.6. Linear viscoelastic region (LVR) of α-lactalbumin and whey protein isolate at (A) 1.0 Hz and (B) 0.1 Hz and 23°C.

The determination of the linear viscoelastic region brought the possibility to perform rheological evaluation of the biopolymer solutions to characterize and identify their intrinsic properties based on their elastic response. This type of analysis will help elucidate the deformation capability of the intermolecular interactions of the biopolymers to overcome proportional stresses and strains without disrupting the integrity of their structure.

4.4.3 Zero shear viscosity (ZSV) of diluted biopolymers by creep test analysis

Results from the creep test showed that the diluted biopolymer solutions did not present Newtonian behavior at very low shear rate (0.1 - 0.5 s^{-1}). Instead, the solutions showed pseudoplastic-like behavior at all levels of dilutions showing higher viscosity values at lower shear rates as it is observed for α-lactalbumin (Figure 4.7 A) and whey protein isolate (Figure 4.8 A). Therefore, the ZSV was estimated using the set of data before the first inflection point at 0.5 seconds observed on the compliance curves (Figures 4.7B and 4.8B) under constant stress of 0.01 Pa at 23°C. The ZSV was calculated using equation 2.6 (see Chapter II):

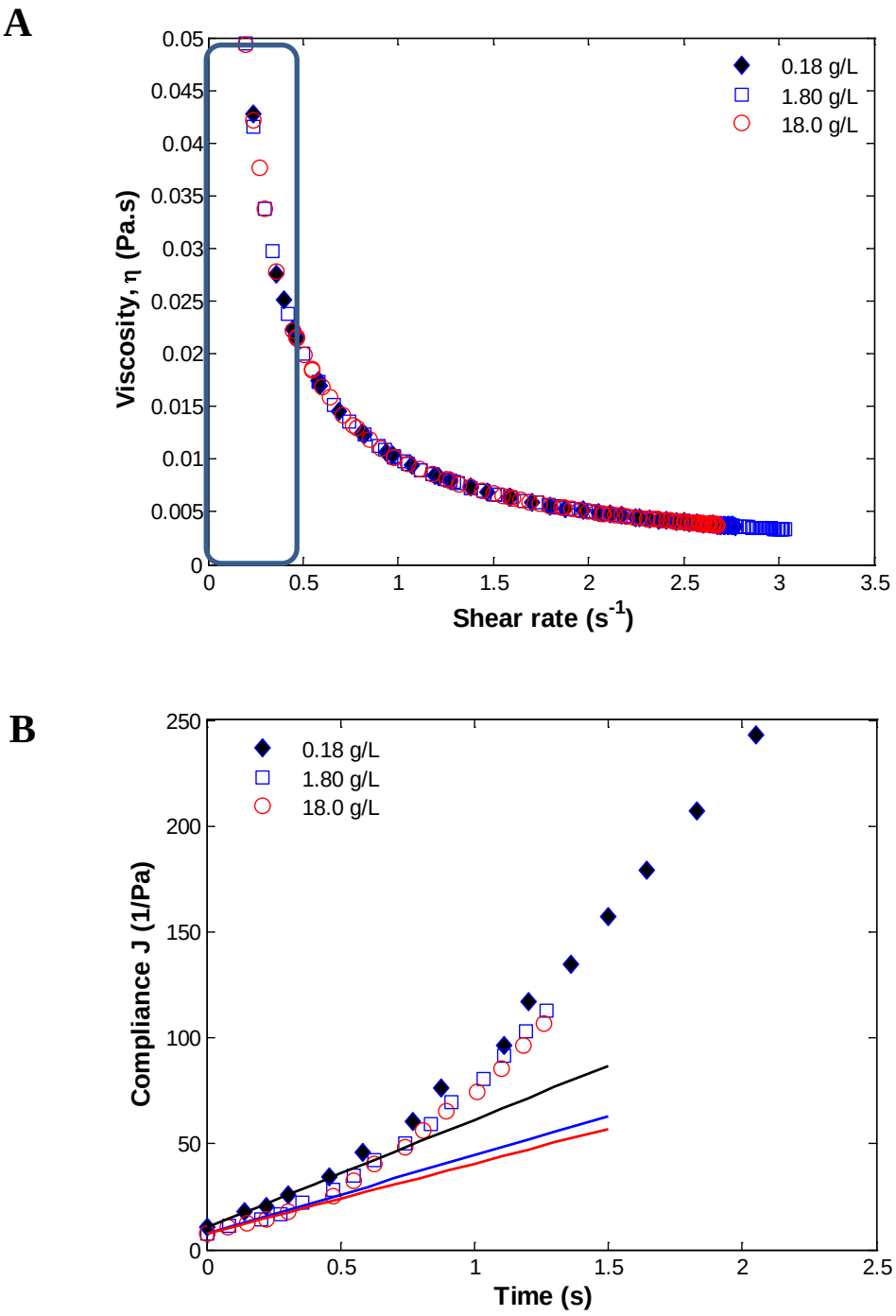

Figure 4.7. Zero Shear Viscosity of α-lactalbumin solutions measured by creep test at 0.01Pa and 23°C. (A) Viscosity values influenced by the shear rate. (B) Compliance curve as function of time application of constant stress (0.01 Pa).

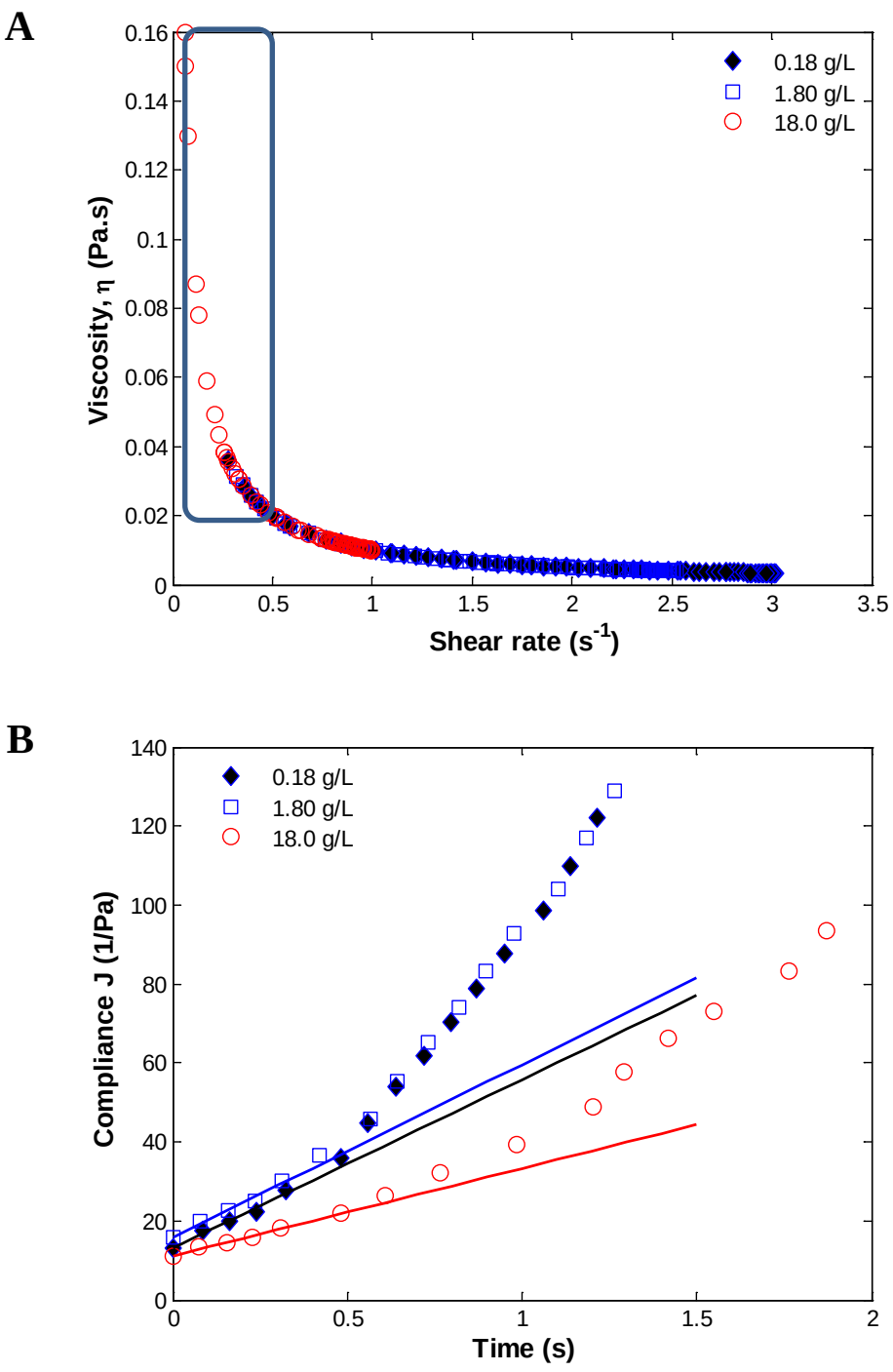

Figure 4.8. Zero Shear Viscosity of whey protein isolate solutions measured by creep test at 0.01Pa and 23°C. (A) Viscosity values influenced by the shear rate. (B) Compliance curve as function of time application of constant stress (0.01 Pa).

The elastic properties of biopolymer solutions were difficult to characterize by the creep test. The characterization of ZSV would be possible at a very small range of shear rates between 0.001 s^{-1} and 0.01 s^{-1} , as it is observed in most polymer melts (high polymer concentrations) (Schramm, 2002); however, higher values of shear rate, over 0.1 s^{-1} were observed at the initiation of creep test at 0.01 Pa and 23°C for all concentrations of biopolymer solutions. Consequently, the determination of ZSV of the biopolymer solutions was limited up to the inflexion point of the compliance curve around 0.5 seconds (Figures 4.7B and 4.8B). This characteristic behavior in all biopolymer solutions could be related to the disruption of the network in self-assembly of amphiphilic molecules.

The pseudoplastic-like behavior displayed by all biopolymer solutions at the initial application of constant stress (0.01Pa) was a consequence of the fast increment on deformation and subsequent disruption of the self-assembled structure. The self-assembled structure breaks because the hydrophobic junctions are strained beyond their mechanical limits and individual molecules start to disentangle and moving apart with respect to each other allowing an irreversible shear thinning flow (Schramm, 2002). The values of ZSV, calculated applying equation 2.6 (see Chapter II), for serial dilutions of α-lactalbumin, whey protein isolate, 3% OSA-modified depolymerized waxy rice (DWxRc3), 7% OSA-modified depolymerized waxy rice (DWxRc7), 3% OSA-modified phytoglycogen (Phytg3), and 7% OSA-modified phytoglycogen (Phytg7) are shown in Figures 4.9A, 4.9B, 4.10A, 4.10B, 4.11A and 4.11B; respectively.

Independent of the type of biopolymer, all curves present low, rise, high and decreasing values of the average ZSV as the biopolymer concentration increases. Different patterns were observed between α-lactalbumin (Figure 4.9A) and whey protein isolate (Figure 4.9B). Although a high average ZSV value of 0.036Pa.s for 0.7 g/L of whey protein isolate is close to the value of 0.6 g/L found as its CMC determined by the fluorescent spectroscopy, inconsistent results were observed for α-lactalbumin, which showed a low ZSV value of 0.027Pa.s at its corresponding CMC of 2.5 g/L.

In general, different curve patterns were observed among all biopolymers evaluated; however, a similar pattern was observed between depolymerized waxy rice starch at different percentages of OSA-modification (Figures 4.10A and B). Different percentages of OSA-modified phytoglycogen also showed a distinct curve pattern (Figures 4.11A and B). Unlike the other biopolymers, OSA-modified phytoglycogen showed high ZSV values at low biopolymer concentration (0.18 g/L).

Even though the creep test was carried out at a low constant stress of 0.01 Pa, which is in the range of the linear viscoelasticity regions for both α-lactoalbumin (Figure 4.5B) and whey protein isolate (Figure 4.6B), a rapid decrement of the viscosity increased the variability of ZSV among sample repetitions, which makes this method problematic to determine precise structure formation associated with the rising of ZSV, as it was previously described on the observation of ZSV values as a function of nonionic surfactant (NPe) concentration in combination with comb-like hydrophobic polymers (Talwar et al., 2006).

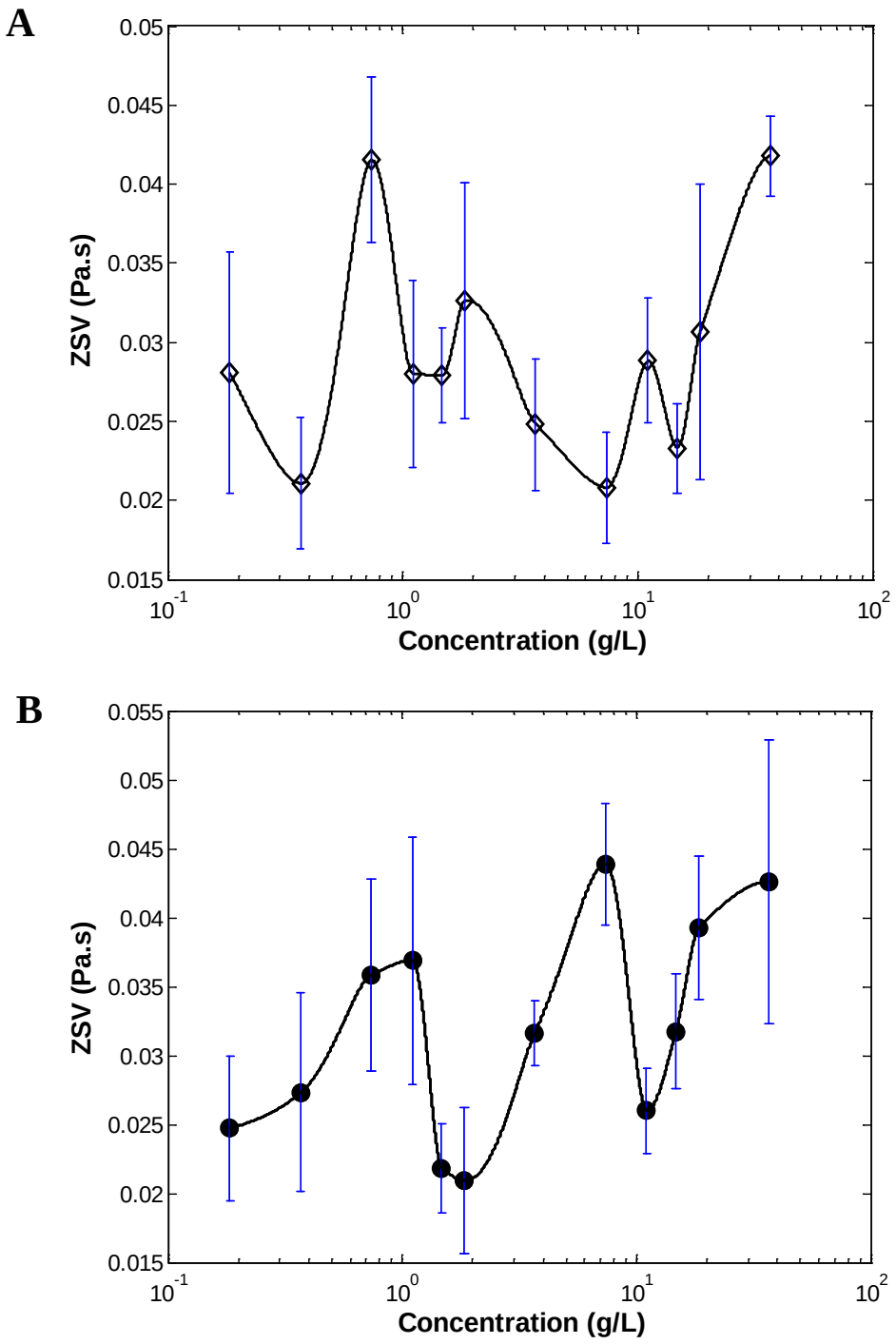

Figure 4.9. Zero-shear-viscosity (ZSV) for serial dilutions of (A) α-lactalbumin and (B) whey protein, calculated from creep test at 0.01Pa and 23°C.

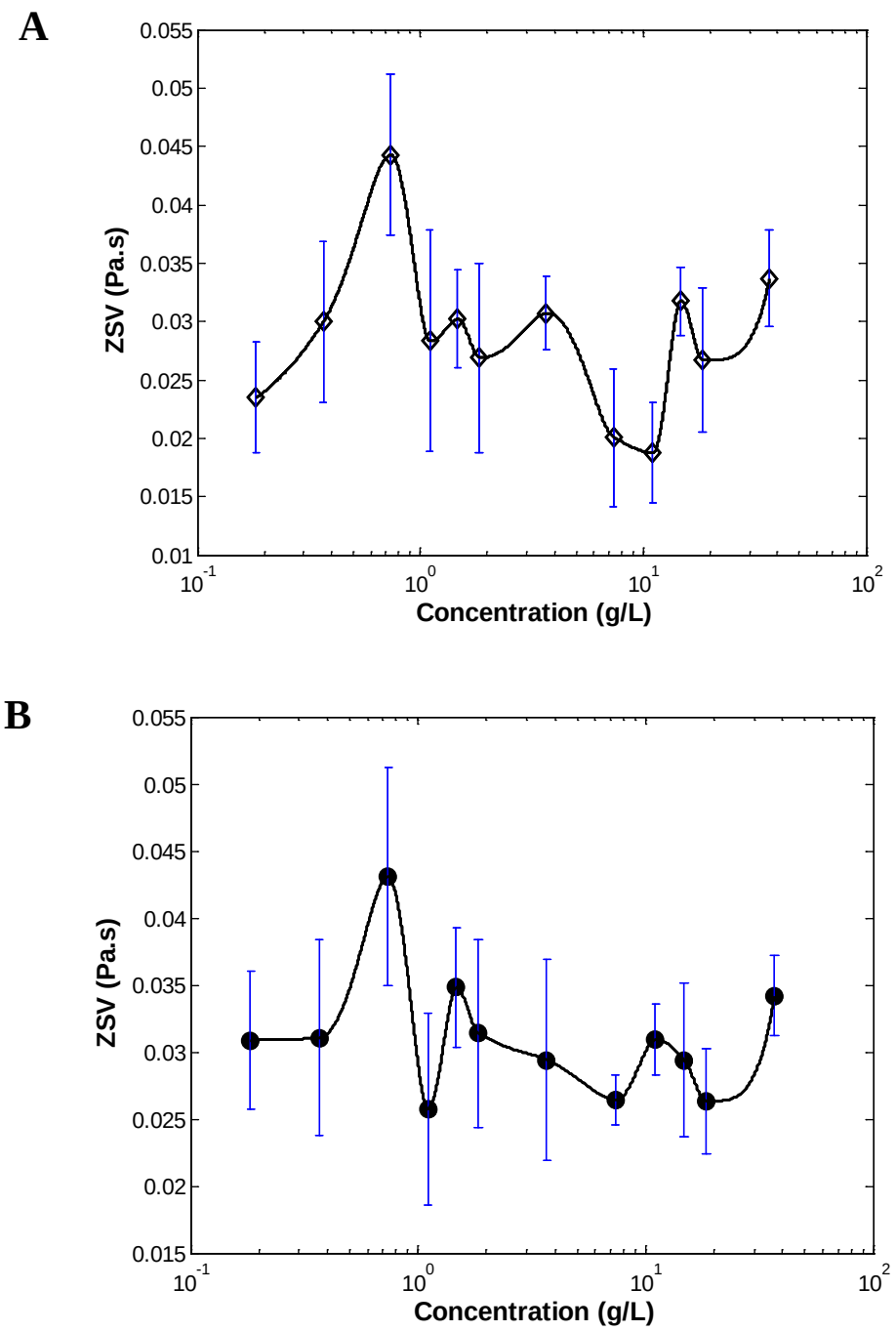

Figure 4.10. Zero-shear-viscosity (ZSV) for serial dilutions of (A) 3% OSA-modified depolymerized waxy rice (DWxRc3) and (B) 7% OSA-modified depolymerized waxy rice (DWxRc7), calculated from creep test at 0.01Pa and 23°C.

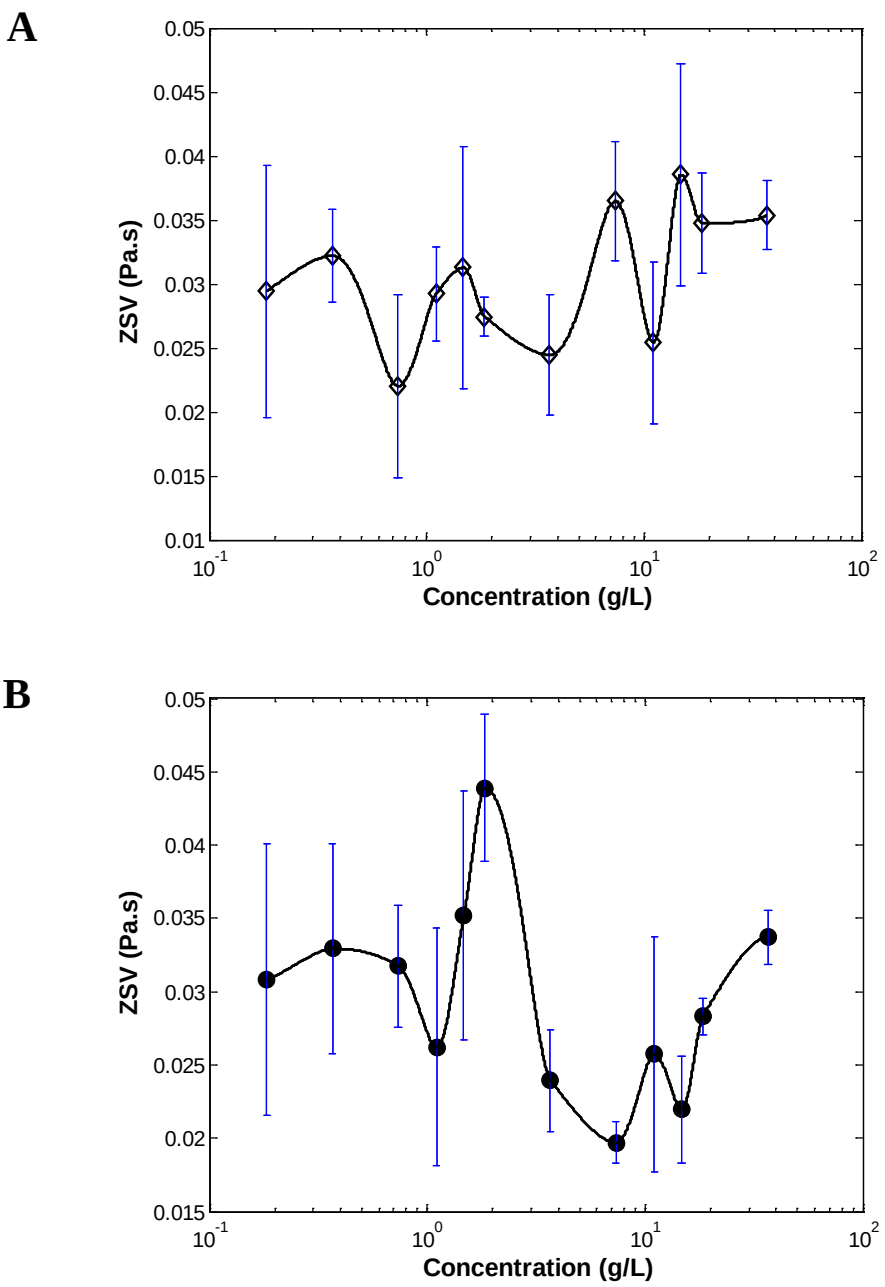

Figure 4.11. Zero-shear-viscosity (ZSV) for serial dilutions of (A) 3% OSA-modified phytoglycogen (Phytg3) and (B) 7% OSA-modified phytoglycogen (Phytg7), calculated from creep test at 0.01Pa and 23°C.

4.4.4 Oscillatory sweep test

The oscillatory frequency sweep test produces much lesser deformation on the fluid substances and the results were subsequently evaluated and analyzed at different concentrations of the biopolymers previously tested.

Oscillatory frequency sweep results for different solutions (0.18, 1.80, and 18.0 g/L) of α-lactalbumin (α-L), whey protein isolate WPI, 3% OSA-modified depolymerized waxy rice (DWxRc3), 7% OSA-modified depolymerized waxy rice (DWxRc7), 3% OSA-modified phytoglycogen (Phytg3), and 7% OSA-modified phytoglycogen (Phytg7) are shown in Figures 4.12 to 4.17, respectively. Elastic-type behavior was observed on certain concentrations of dilute amphiphilic biopolymers at 0.01Pa of stress and low frequency sweeps between 0.01 and 1 Hz (Figures 4.12A, 4.13A, 4.15A, 4.16A and 4.17A).

In general, dilute solutions of hydrocolloids show viscous (G'') moduli larger than elastic (G') moduli over the entire frequency range but approach each other at higher frequencies (Steffe, 1996). For concentrated solutions G'' and G' curves intersect at the middle of the frequency range indicating a clear tendency for more solid-like behavior at higher frequencies, which could be assumed as the formation of an entangled network system. For instance, the gels have significantly higher G'with the modulus practically constant throughout the frequency range (Chamberlain and Rao, 2000; Steffe, 1996).

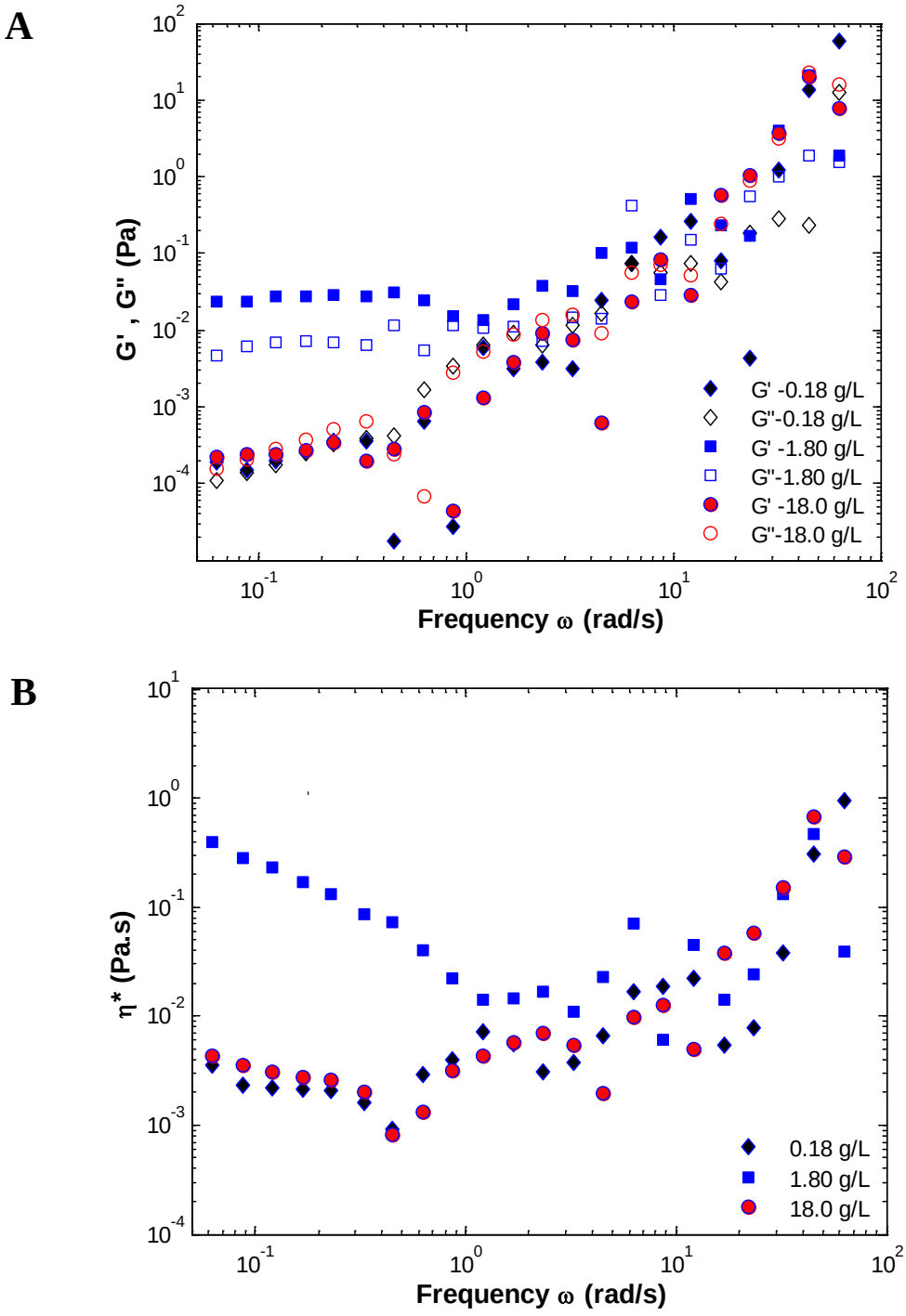

Figure 4.12. Elastic modulus (G'), viscous modulus (G") (A) and complex viscosity (η*) curves (B) for different concentrations of α-lactalbumin solutions. Oscillatory frequency sweep test was performed at 0.01 Pa and 23°C.

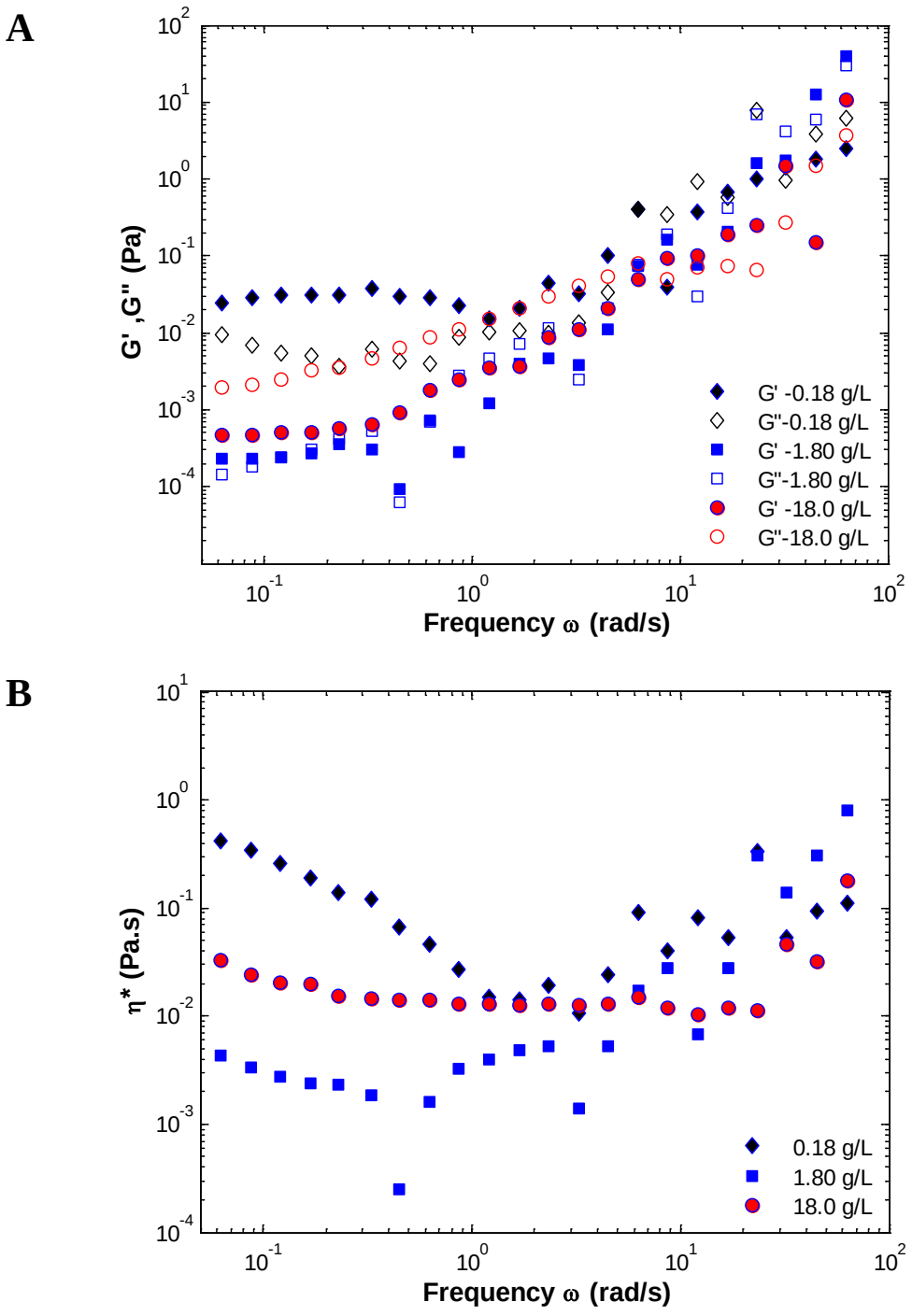

Figure 4.13. Elastic modulus (G'), viscous modulus (G") (A) and complex viscosity (η*) curves (B) for different concentrations of whey protein isolate solutions. Oscillatory frequency sweep test was performed at 0.01 Pa and 23°C.

Unlike hydrocolloids that always show greater dynamic response magnitudes of viscous (G") than elastic (G') modulus at all different concentrations evaluated (Chamberlain and Rao, 2000), the amphiphilic molecules such as biopolymers studied in this work had greater elastic (G') than viscous (G") modulus as a function of concentration, frequency and the type of biopolymer evaluated.

Lower dilute concentrations of WPI (0.18g/L) (Figure 4.13A) showed more solid-like behavior (G' > G') than α-lactalbumin (1.8 g/L) (Figure 4.12A). This result correlates very well with that found for protein concentration for micelle-type structure formation observed by the fluorescent test (Figure 4.1). The concentration of WPI necessary to form a micelle was approximately five times less (0.6 g/L) than that for α-lactalbumin. The higher elastic modulus at low frequencies (< 1.0 rad/s) correspond to a solid-like behavior that might be associated with entanglement formation by hydrophobic association of the biopolymer at the specific protein concentration, although the micelle-type structure formation was observed to develop at higher protein concentrations (Figure 4.1). For WPI, liquid-like behavior (G" > G') was observed at higher biopolymer concentrations (1.8 and 18.0 g/L) and this behavior was more noticeable at 18.0 g/L (Figure 4.13A). For α-lactalbumin, both moduli (G' and G") overlapped at 0.18 and 18.0 g/L concentrations, suggesting there is no direct effect on the viscoelastic behavior of the material as the amount of protein increases (Figure 4.12A). Similarly, associative networks in self-assemble hydrophobic polymer/nonionic surfactants were reported to present not a direct relationship with the increase in surfactant concentration (Talwar et al., 2006).

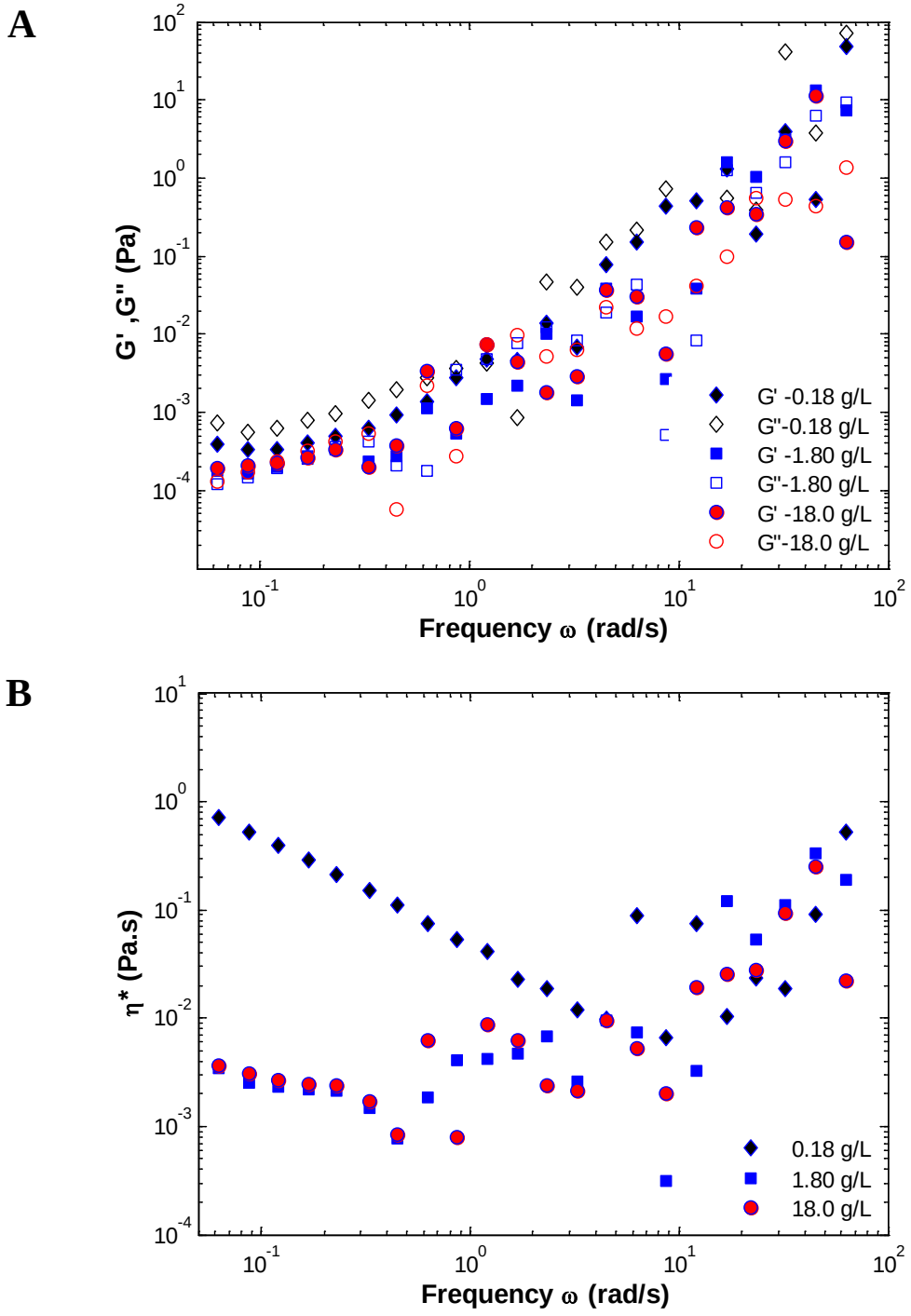

Figure 4.14. Elastic modulus (G'), viscous modulus (G") (A) and complex viscosity (η*) curves (B) for different concentrations of 3% OSA-modified depolymerized waxy rice (DWxRc3) solutions. Oscillatory frequency sweep test was performed at 0.01 Pa and 23°C.

The frequency dependency of the complex viscosity, η*, which describes the resistance to dynamic shear, is shown in Figures 4.12B, 4.13B, 4.14B, 4.15B, 4.16B and 4.17B for of α-L, WPI, DWxRc3, DWxRc7, Phytg3, and Phytg7, respectively. The trend at different concentrations of proteins has similar characteristics with the elastic (G') modulus at the same concentration and type of protein (Figure 4.12A and 4.13A). An interesting observation is the linear region pattern in the range of 0.06 to 0.6 rad/sec for all the protein concentration levels. The highest η* values coincide with the highest elastic modulus for each type of protein (Figure 4.12B and 4.13B).

Similar trends were observed on polymer melts and concentrated solutions of high molecular weight polymers (Schramm, 2002).

The oscillatory frequency sweep tests on DWxRc3 (Figure 4.14A) and DWxRc7 (Figure 14.15A) only showed higher G' at 1.8 g/L of 7% of OSA modification. This result is similar to that found on α-lactalbumin (Figure 4.12A). The solid-like behavior of the biopolymer at this concentration could be associated to self-assemble network formation that has been reported in hydrophobic polymer/nonionic surfactant association (Talwar et al., 2006). It is also possible that the higher percentage of OSA modification on DWxRc7 induced polymer hydrophobic self- association as it was also observed in proteins, although no indication of micelle formation was observed on the fluorescent tests (Figure 4.2B).

Similarly to proteins, liquid-like behavior was observed without any direct correlation with the biopolymer concentration and both moduli (G' and G") overlap each other (Figures 4.14A and 4.15A).

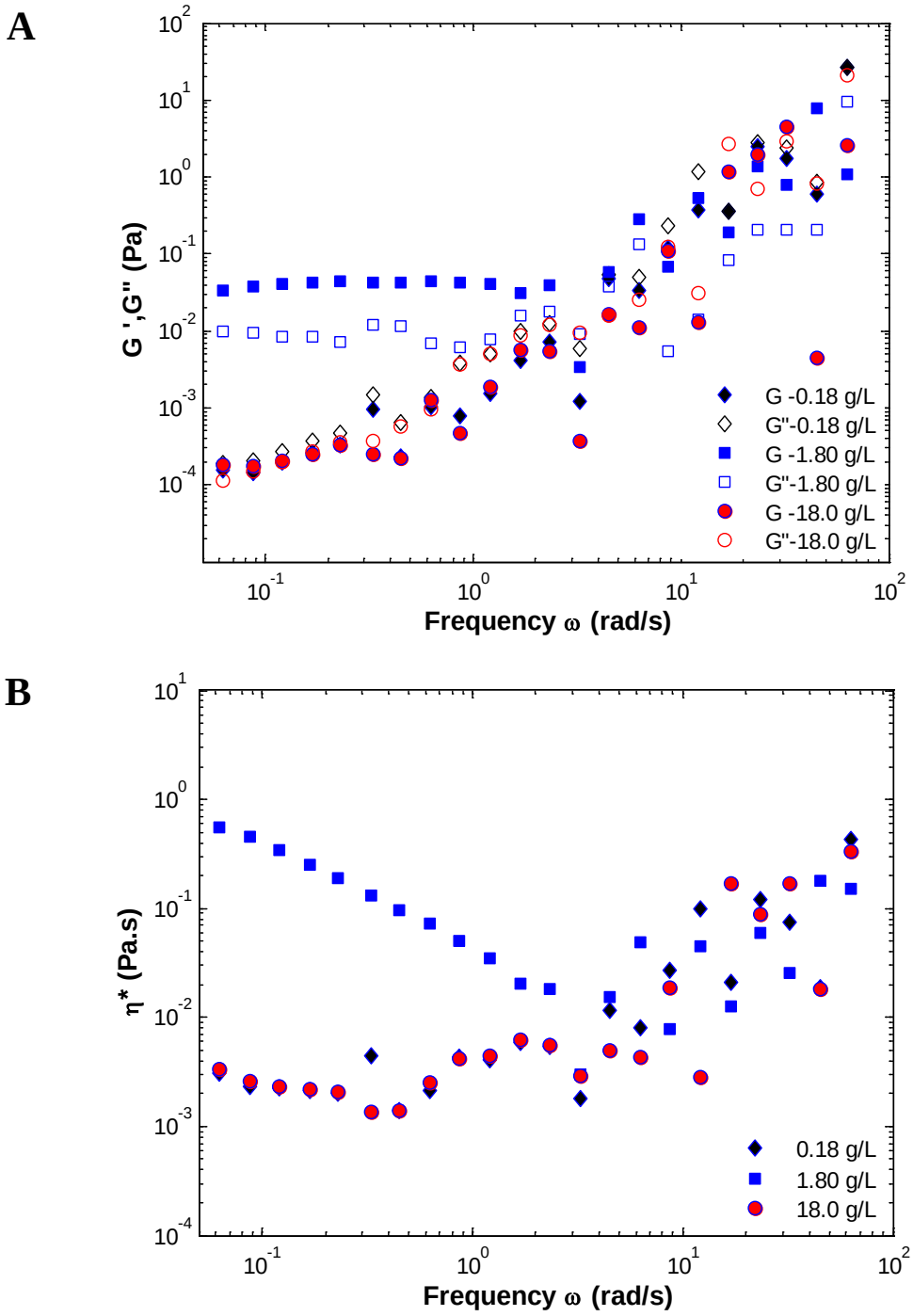

Figure 4.15. Elastic modulus (G'), viscous modulus (G") (A) and complex viscosity (η*) curves (B) for different concentrations of 7% OSA-modified depolymerized waxy rice (DWxRc7) solutions. Oscillatory frequency sweep test was performed at 0.01 Pa and 23°C.

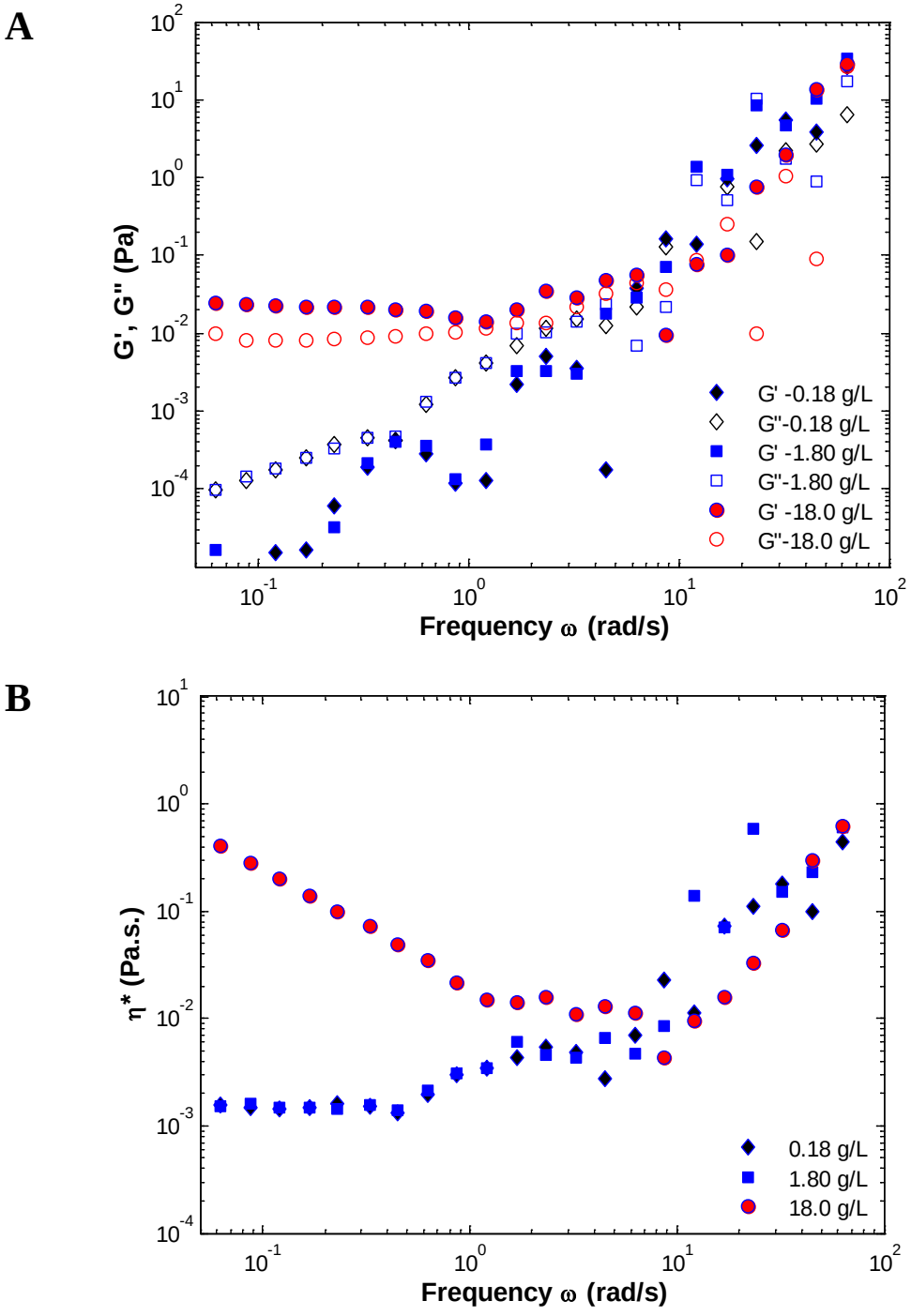

Figure 4.16. Elastic modulus (G'), viscous modulus (G") (A) and complex viscosity (η*) curves (B) for different concentrations of 3% OSA-modified phytoglycogen (Phytg3) solutions. Oscillatory frequency sweep test was performed at 0.01 Pa and 23°C.

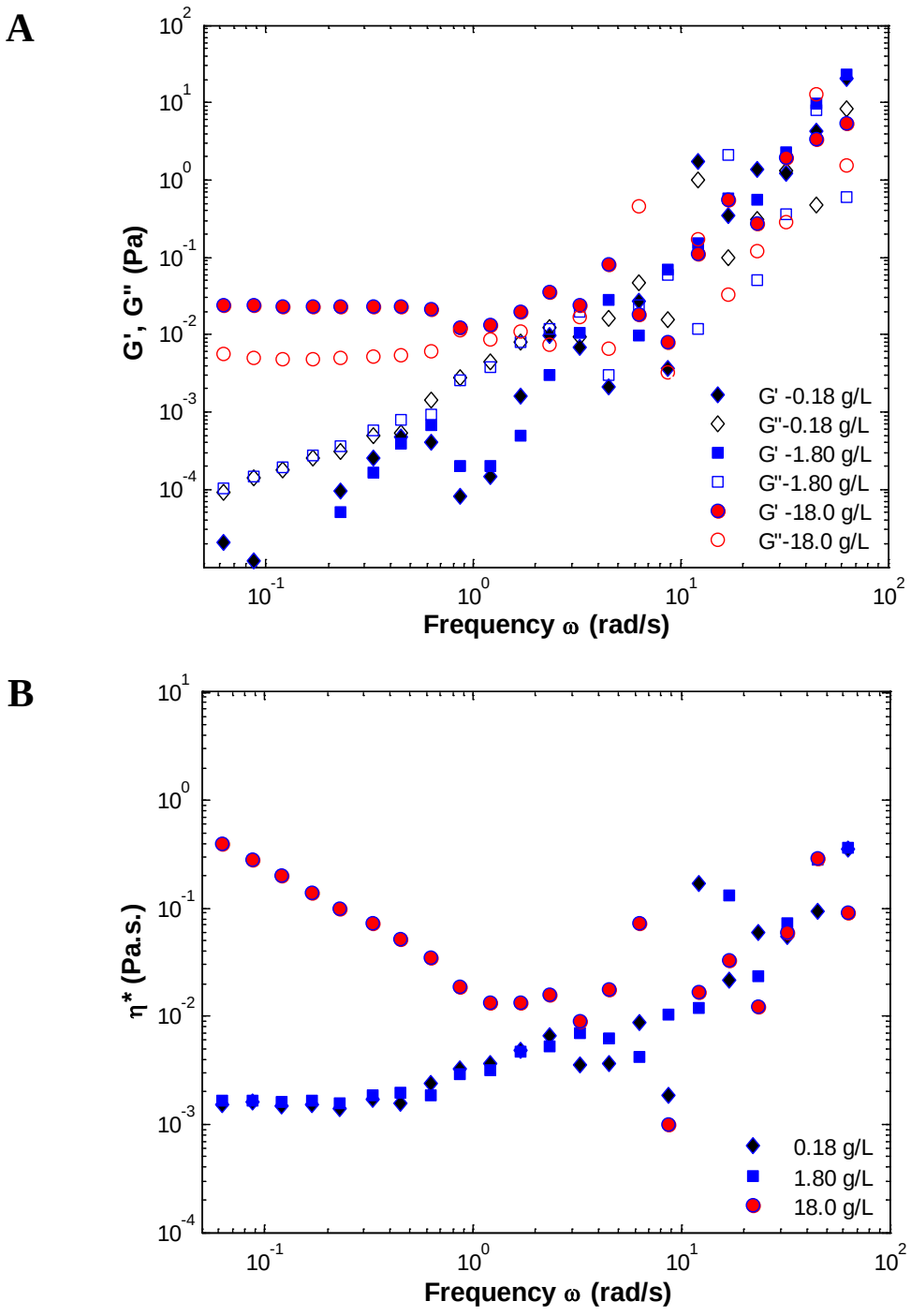

Figure 4.17. Elastic modulus (G'), viscous modulus (G") (A) and complex viscosity (η*) curves (B) for different concentrations of 7% OSA-modified phytoglycogen (Phytg7) solutions. Oscillatory frequency sweep test was performed at 0.01 Pa and 23°C.

The frequency dependence of the complex viscosity, η*, shown in Figures 4.14B and 4.15B for all different concentrations of DWxRc was similar compared to that observed for α-L. Moreover, the complex viscosity behavior of different concentrations of DWxRc7 showed a similar pattern to that of α-lactalbumin where solid-like behavior was observed at a concentration of 1.8 g/L. Similarly, the linear trend of the complex viscosity was related to the biopolymer concentration and it was more influence in this case by the percentage of OSA modification. This result suggests that higher percentage of OSA modification increases the self-assembly capability for DWxRc.

Solid-like behavior of OSA-modified phytoglycogen characterized by oscillatory frequency sweep response was only observed at 18.0 g/L of polymer concentration at both degrees of OSA modification (3 and 7%). Similar liquid-like behavior was observed for both lower polymer concentrations of 0.18 and 1.8 g/L (Figures 4.16A and 4.17A). Thus, self-association of OSA-modified phytoglycogen seems to be influenced by biopolymer concentration and an overlap of both moduli (G', G") was observed on high frequency as it was observed on proteins and OSA-modified DWxRc.

The frequency dependence of the complex viscosity showed a similar pattern for both percentage of OSA modification. Similarly to the elastic modulus, the complex viscosity was higher at the higher concentration evaluated (18.0 g/L) (Figure 4.16B and 4.17B).

The different types of biopolymers evaluated in this study presented different effects on their behavior as a function of biopolymer concentration. Unlike OSA-modified phytoglycogen, biopolymer concentration of proteins and OSA-modified

DWxRc did not influence their solid-like behavior. The biopolymer's capability to self-assemble is primary influenced by their biopolymer structure and secondary by the percentage of OSA modification.

To better understand the possible mechanism influencing the solid-like and liquid-like behavior of biopolymer solutions, a relationship of the elastic (G') and viscous (G") moduli as a function of the angular frequency was analyzed in this work. According to Maxwell's fluid element dynamic analysis, the elastic and viscous moduli could be written as a function of angular frequency ω (rad/s) and relaxation time λ (s/rad) according to equations 2.12 to 2.19 in section 2.6.4 (Chapter II). Similar interrelations between G' and G'' have been found through the relaxation spectrum for incompressible, linear viscoelastic liquids (Utracki, 2004) when testing polymeric nanocomposite materials.

The relaxation time "λ" is the time associated with large scale motion (or changes) in the structure of the polymers (Chhabra, 2010; Roland, 2008).The values of λ seem to be sensitive to the frequency and polymer concentration (Figures 4.18, 4.19, and 4.20). The values of λ decreased as the frequency increased up to a critical frequency value (CFV) where the λ values changed from a linear decreasing trend (slope) to a more scattered distribution. An early study on combinations of polyamide-6 and polymeric nanocomposites suggested structural changes at the critical frequency, which was associated with apparent break of the disks-like (or platelet) structure that occurred at higher frequencies (Utracki and Lyngaae-Jørgensen, 2002). Moreover, similar λ slopes have been suggested as indication of similar structure (Utracki et al., 2010).

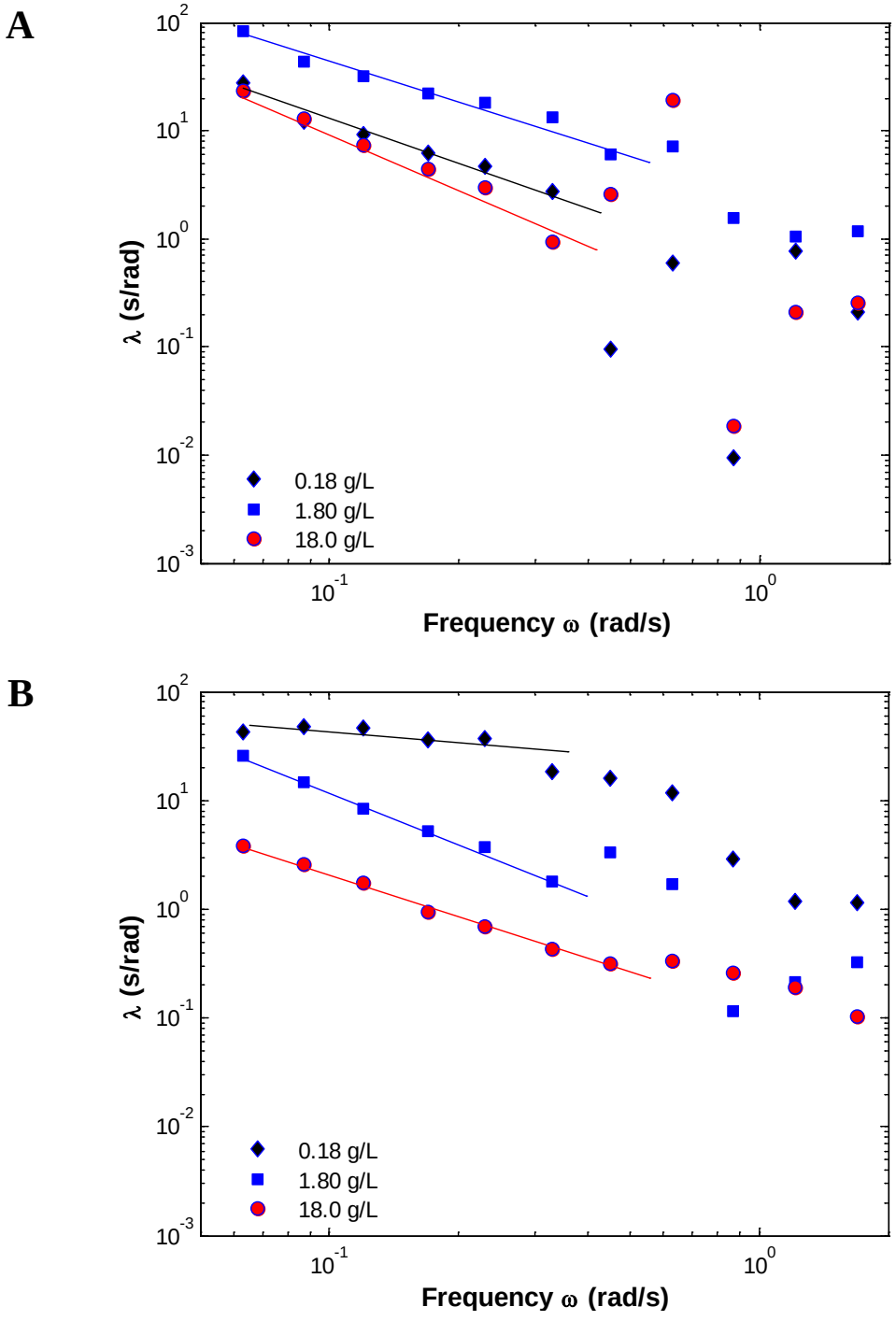

Figure 4.18. Relaxation time (λ) curves for different concentrations of (A) α-lactalbumin and (B) whey protein isolate (WPI) evaluated by oscillatory frequency sweep test at 0.01 Pa and 23°C.

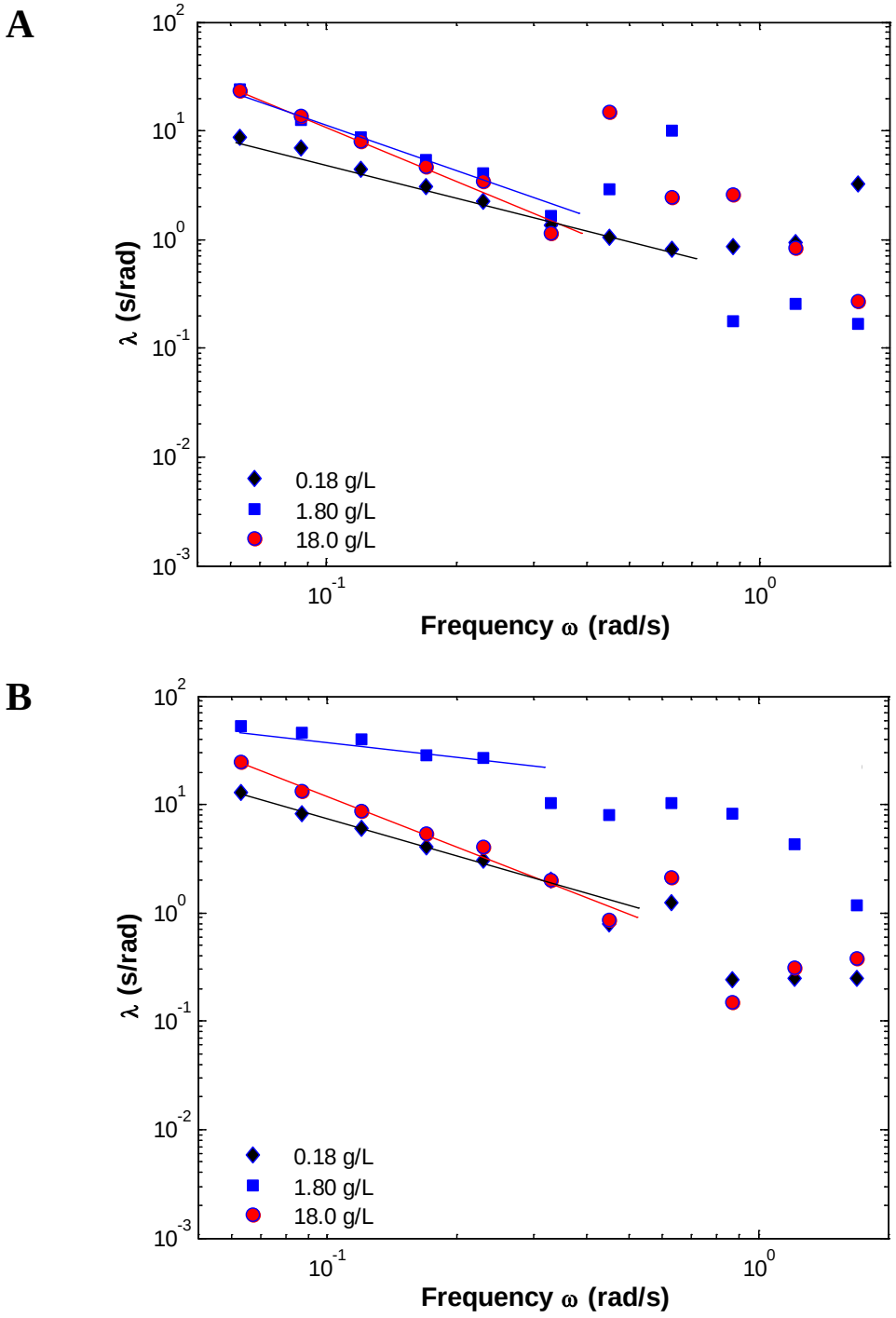

Figure 4.19. Relaxation time (λ) curves for different concentrations of (A) 3% OSA-modified depolymerized waxy rice (DWxRc3) and (B) 7% OSA-modified depolymerized waxy rice (DWxRc7) evaluated by oscillatory frequency sweep test at 0.01 Pa and 23°C.

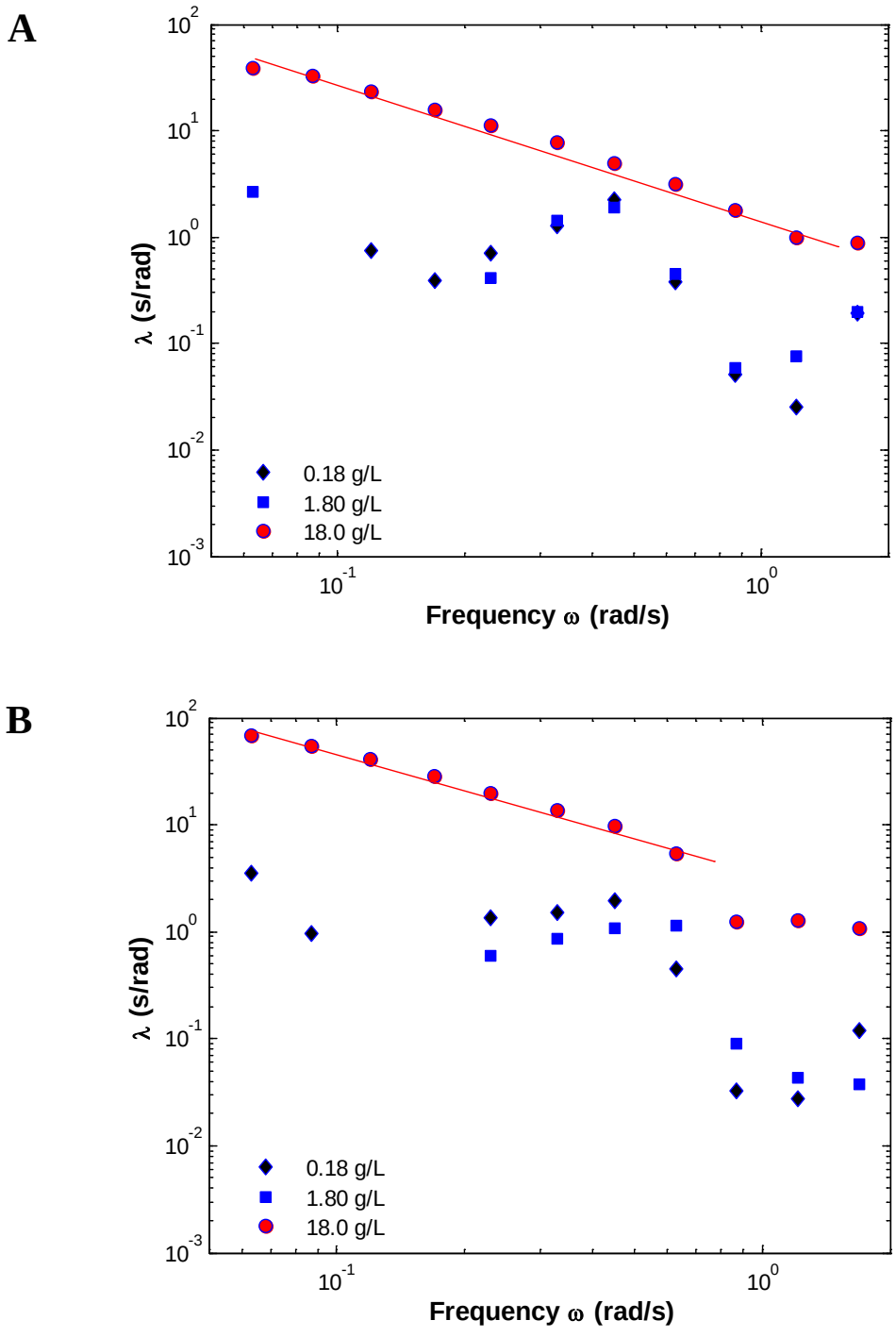

Figure 4.20. Relaxation time (λ) curves for different concentrations (A) 3% OSA-modified phytoglycogen (Phytg3) and (B) 7% OSA-modified phytoglycogen (Phytg7) evaluated by oscillatory frequency sweep test at 0.01 Pa and 23°C.

Proteins, DWxRc3 and DWxRc7 showed a defined slope at all different polymer concentration. Contrarily, dilutions of OSA-modified phytoglycogen only showed a defined slope at the highest concentration evaluated (18.0 g/L) which is in agreement with the solid-like behavior observed in the dynamic test (Figures 4.16A and 4.17A). An interesting observation is that the higher values of λ are related to the solid-like behavior previously observed by the changes in dynamic moduli (G' and G") (Figures 4.12A - 4.17A).

Self-assembling structures produce viscoelastic behavior as observed by oscillatory shear (Pätzold and Dawson, 1996). It is possible to associate the solid-like dynamic behavior with structures that present difficult rotational movement. For example, rods and ellipsoids (e.g. platelets, and disks) have been easy to differentiate based on their rotational motility (Goldsmith and Mason, 1962), which have been related to their geometric aspect ratio. The ratio of the largest to the smallest dimension seems to be more realistic to define different structures (Utracki et al., 2010). Therefore, the aspect ratio for a rod could be defined as r=length/diameter >> 1, for sheet-type structure r=length/thickness >> 1, for disk or platelets as r=diameter/thickness > 1, and spheroids r= ~1. In consequence, the solid-like behavior observed by the dynamic response of solutions of 0.18 g/L WPI, 1.8 g/L α-lactalbumin, 7% OSA-modified WxRc, and 3% and 7% OSA-modified phytoglycogen was influenced by the low rotational motility offered by these types of structures. For instance, β-lactoglobulin, the main constituent of WPI, has been observed to exist mainly as noncovalently associated dimer structures at room temperature in the pH range of 2.0 - 3.7 and 5.2 - 9.0 (Verheul et al., 1999); therefore,

the dimer structure must present a motility similar to a hinge-like structure with the geometric aspect ratio r = length/thickness >> 1. Likewise, a geometric aspect ratio structure much bigger that 1 must be assembled for the other biopolymer concentrations with solid-like behavior.

The critical frequency for proteins and OSA substituted DWxRc was between 0.23 and 0.63 rad/s (Table 4.1) depending on polymer type and concentration. However, the critical frequency for OSA-modified phytoglycogen at 18.0 g/L was 0.63 and 1.21 rad/s for 7% and 3% OSA-modified phytoglycogen, respectively (Table 4.1). These results are in agreement with the fluorescent test results and the dynamic oscillatory tests, where higher concentration of phytoglycogen particles must be necessary to provide sufficient OSA ester groups and impart van der Waals, and hydrophobic attraction among particles in order to hold a spontaneous assembly and overcome the steric repulsion of the bigger phytoglycogen particles (approx. 40 nm); therefore, it is possible that the higher the critical frequency, the bigger size of the structure. In consequence, 3% OSA-modified might form the biggest size structure.

According to the analysis of covariance in a general linear model, adjustment of multiple comparisons with Bonferroni test was used to compare relaxation time (λ) slopes among different concentrations of biopolymers calculated from the frequency sweep test (Table 4.1). The frequency sweep test was considered as covariance because this variable is not directly tested but it was observed to have a direct influence on the dependent variable, the relaxation time "λ" (Figures 4.18, 4.19, and 4.20).

Table 4.1. Relaxation time (λ) slope and critical frequency value (CFV) for different concentrations of biopolymers evaluated by oscillatory frequency sweep test at 0.01 Pa and 23°C.

Polymer type	**λ Slope**	**CFV (rad/s)**	**R^2**
α-L			
0.18 g/L	-1.295 ± 0.501[ab]	0.33	0.955
1.80 g/L	-1.132 ± 0..408[ab]	0.63	0.961
18.0 g/L	-1.602 ± 0.187[a]	0.33	0.996
WPI			
0.18 g/L	-0.1577 ± 0.321[c]	0.23	0.935
1.80 g/L	-1.503 ± 0.229[a]	0.33	0.993
18.0 g/L	-1.363 ± 0.199[a]	0.45	0.993
DWxRc3			
0.18 g/L	-1.080 ± 0.172[ab]	0.63	0.992
1.80 g/L	-1.353 ± 0.284[a]	0.33	0.987
18.0 g/L	-1.499 ± 0.219[a]	0.33	0.993
DWxRc7			
0.18 g/L	-1.091 ± 0.122[ab]	0.33	0.996
1.80 g/L	-0.5727 ± 0.175[bc]	0.23	0.972
18.0 g/L	-1.376 ± 0.275[a]	0.45	0.988
Phytg3			
18.0g/L	-0.9840 ± 0.219[ab]	1.21	0.985
Phytg7			
18.0g/L	-0.9637 ± 0.180[ab]	0.63	0.989

Values represent mean ± standard deviation of three replicates per set of data.
Means values with same letter are not significantly different ($P > 0.05$)

The biopolymer concentration was evaluated as independent variable and considered as fixed factor for the covariance analysis. In general, with the exception of 0.18 g/L WPI and 1.8 g/L DWxRc7, there were no significant differences ($P > 0.05$) among all slopes of α-lactalbumin, DWxRc3, 18.0 g/L Phytg3 and Phytg7 (Table 4.1), which suggest the formation of a similar structure among these different concentrations of biopolymers. The latest assumption is based on previous studies that indicate the connection between symmetrical structure geometry of anisotropic structures and rheological characteristics, which is influenced by the characteristic period of structure rotational motility (Goldsmith and Mason, 1962). Hence, similar structure geometry would present similar rotational motility, therefore similar relaxation time slope value.

4.4.5 Relaxation time curve slopes of diluted combination of biopolymer solutions

A direct effect on the reduction of λ as a result of the increment in frequency was only observed in a combination of 18.0 g/L of DWxRc7 and 3.6 g/L of α-lactalbumin, showing a defined slope with a CFV of 0.5 rad/s (Figure 4.21B). The other combinations of 3.6 g/L α-lactalbumin and OSA-modified polysaccharides showed scattered λ values at all frequencies (Figures 4.21A, 4.22A, and 4.22B) . These results indicate that no self-association occurs in those combinations.

Unlike the interaction between α-lactalbumin (Figures 4.21A, 4.22A, and 4.22B) and OSA-modified polysaccharides, WPI presented hydrophobic interactions with all different OSA-modified polysaccharides at the levels of concentration evaluated in this study (Figures 4.23A, 4.23B, 4.24A, and 4.24B).

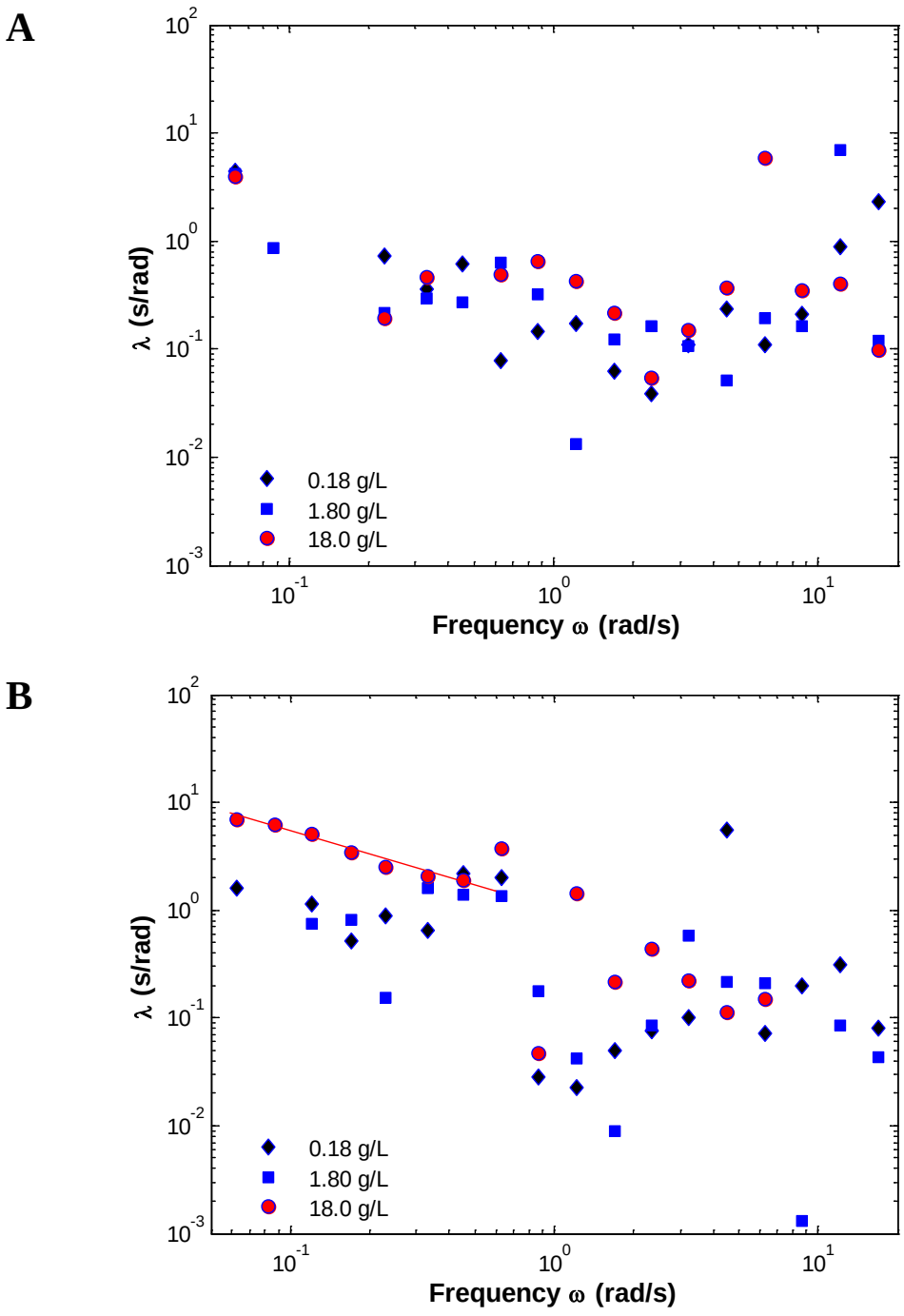

Figure 4.21. Comparison of hydrophobic interaction of 3.6 g/L α-lactalbumin with different concentrations of (A) 3% OSA-modified depolymerized waxy rice (DWxRc3) and (B) 7% OSA-modified depolymerized waxy rice (DWxRc7) by relaxation time (λ) values at 0.01Pa and 23°C of different aqueous concentrations.

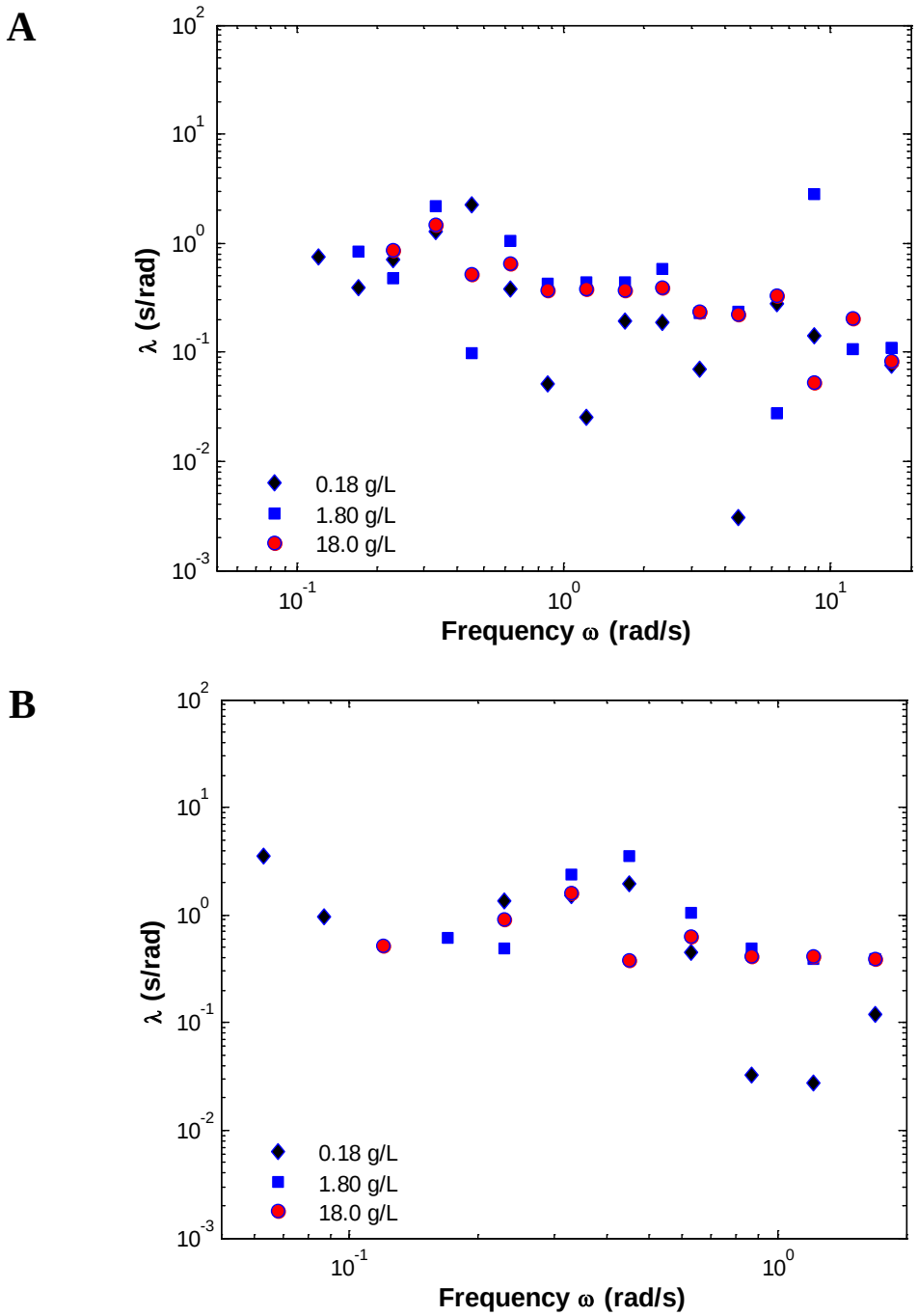

Figure 4.22. Comparison of hydrophobic interaction of 3.6 g/L α-lactalbumin with different concentrations of (A) 3% OSA-modified phytoglycogen (Phytg3) and (B) 7% OSA-modified phytoglycogen (Phytg7) by relaxation time (λ) values at 0.01Pa and 23°C of different aqueous concentrations.

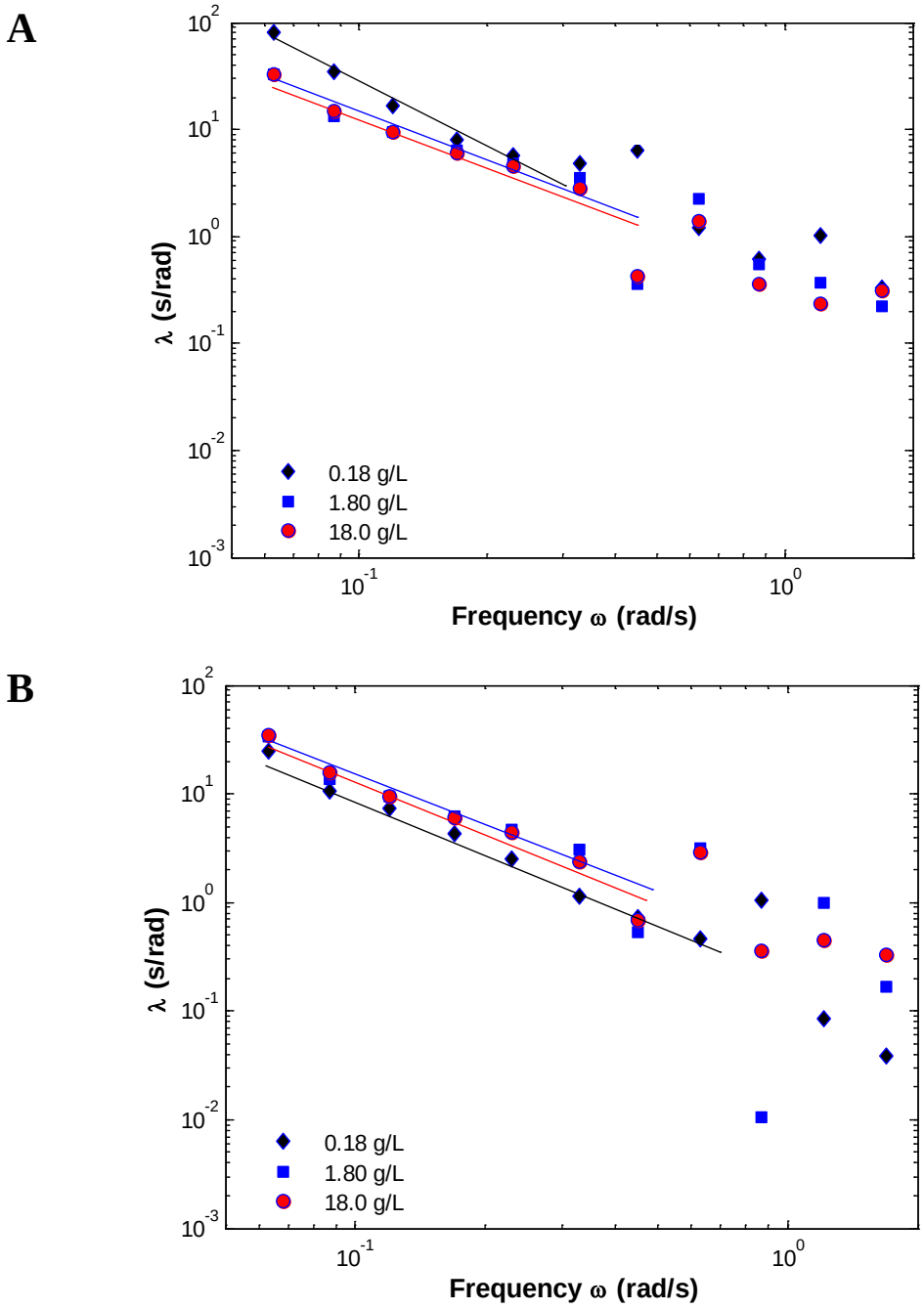

Figure 4.23. Comparison of hydrophobic interaction of 3.6 g/L whey protein isolate with different concentrations of (A) 3% OSA-modified depolymerized waxy rice (DWxRc3) and (B) 7% OSA-modified depolymerized waxy rice (DWxRc7) by relaxation time (λ) values at 0.01Pa and 23°C of different aqueous concentrations.

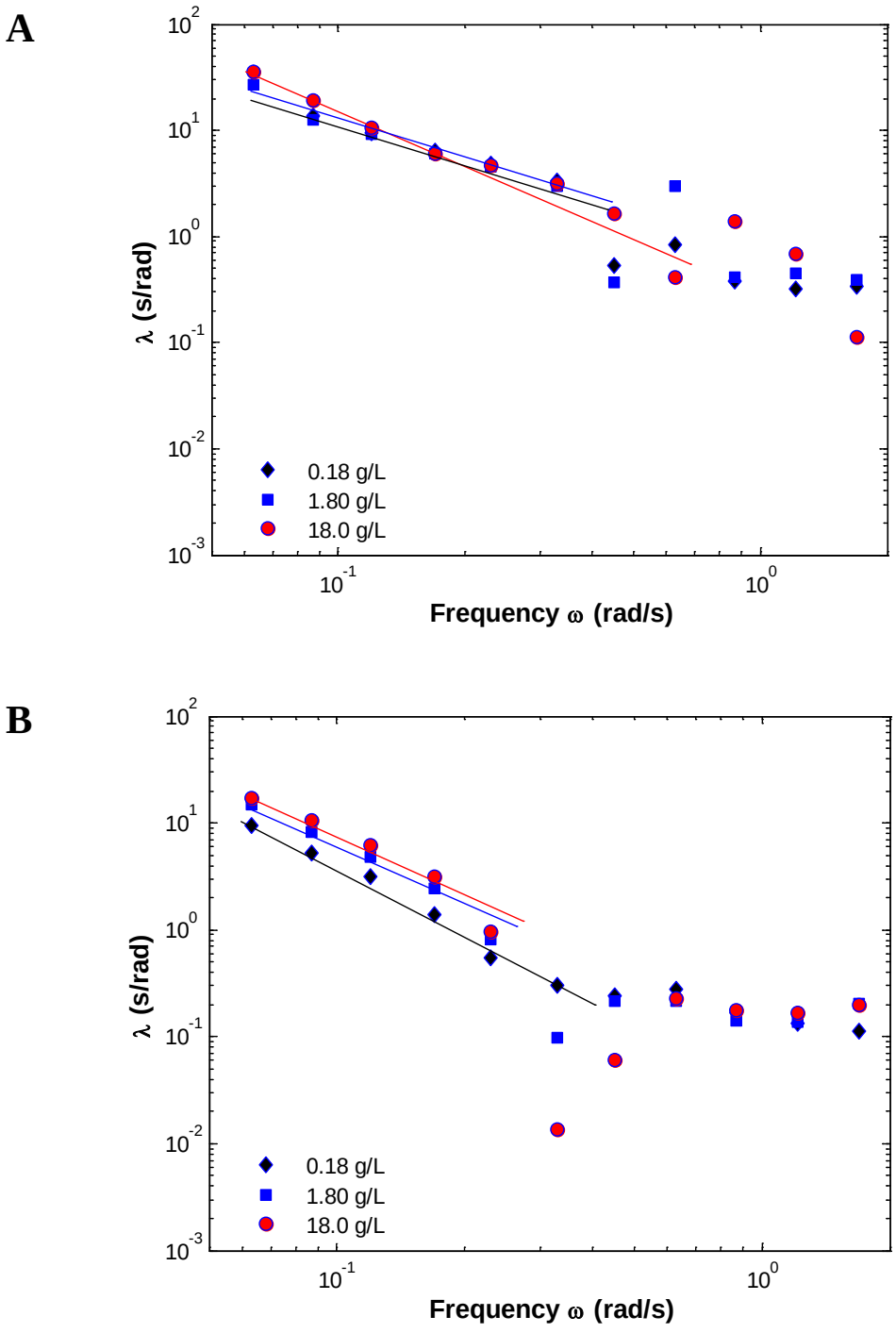

Figure 4.24. Comparison of hydrophobic interaction of 3.6 g/L whey protein isolate with different concentrations of (A) 3% OSA-modified phytoglycogen (Phytg3) and (B) 7% OSA-modified phytoglycogen (Phytg7) by relaxation time (λ) values at 0.01Pa and 23°C of different aqueous concentrations.

A defined λ slope was observed for all combinations of 3.6 g/L WPI at different concentrations (0.18, 1.8, and 18.0 g/L) of OSA-modified polysaccharides. A low CFV of 0.33 rad/s was obtained for the combination of WPI and the different concentrations of DWxRc3. However, higher critical frequency values at 0.63 rad/s and 0.45 rad/s were obtained in combination with 0.18 g/L DWxRc7 and Phytg7, respectively (Figures 4.23B and 4.24B). This result indicates that larger hydrophobic interactions of WPI occur with higher level of OSA modification at lower polysaccharide concentration. On the other hand, a high critical frequency value of 0.45 rad/s was obtained for the combination of WPI with the higher concentration of Phytg3 (Figures 4.24A). These results indicate that WPI needs more molecules to form association when the OSA modification is lower.

A degree of competition in the self-association of WPI with higher OSA-modified polysaccharides could be producing smaller structures as the concentrations of OSA-modified polysaccharides increase. It seems that the type of protein and polysaccharide structure have a strong influence in their molecular interactions.

The high affinity of WPI with the different OSA-modified polysaccharides seems to be influenced by the CMC of these proteins. For instance, the concentration of WPI (3.6 g/L) used in combination with the different OSA-modified polysaccharides is 6 times higher than the CMC (0.6 g/L) found previously. On the other hand, the concentration of α-lactalbumin (3.6 g/L) used in combination with the different OSA-modified polysaccharides is close to the CMC (2.5 g/L) found previously.

Table 4.2. Relaxation time (λ) slope and critical frequency value (CFV) for different biopolymers combinations, evaluated by oscillatory frequency sweep test at 0.01 Pa and 23°C.

Polymer Type	**λ Slope**	**CFV (rad/s)**	**R^2**
α-L 3.6 g/L +			
DWxRc7-18.4 g/L	-0.7087 ± 0.158[c]	0.45	0.973
WPI 3.6 g/L +			
DWxRc3-0.184 g/L	-2.394 ± 0.337[a]	0.33	0.996
DWxRc3-1.84 g/L	-1.88 ± 0.639[ab]	0.33	0.964
DWxRc3-18.4 g/L	-1.863 ± 0.495[ab]	0.33	0.979
WPI 3.6 g/L +			
DWxRc7-0.184 g/L	-1.963 ± 0.371[a]	0.63	0.988
DWxRc7-1.84 g/L	-1.942 ± 0.589[a]	0.33	0.972
DWxRc7-18.4 g/L	-1.923 ± 0.375[a]	0.33	0.988
WPI 3.6 g/L +			
Phytg3-0.184 g/L	-1.955 ± 0.725[a]	0.33	0.961
Phytg3-1.84 g/L	-1.584 ± 0.483[ab]	0.33	0.969
Phytg3-18.4 g/L	-1.767 ± 0.209[ab]	0.45	0.995
WPI 3.6 g/L +			
Phytg7-0.184 g/L	-1.871 ± 0.189[a]	0.45	0.997
Phytg7-1.84 g/L	-1.826 ± 0.218[a]	0.23	0.997
Phytg7-18.4 g/L	-1.694 ± 0.312[ab]	0.23	0.992

Values represent mean ± standard deviation of three replicates per set of data.
Means values with same letter are not significantly different ($P > 0.05$)

Although previous work from Jones and Brass (1991) indicated that interactions mediated by ionic and hydrophobic forces usually occur at concentrations below the CMC of the small amphiphilic surfactants (Jones and Brass, 1991), additional nonspecific interactions seem to be needed for α-lactalbumin (approx. 5nm) to interact with bigger amphiphilic molecules like OSA-modified polysaccharides (15 - 50 nm).

The hydrophilic characteristic of the polysaccharides is attributed to the polarity of hydroxyl groups (-OH) which impart its hydrophilicity forming hydrogen bonds with water (Wurzburg, 1972); therefore, different polysaccharides such as carboxymethylcellulose, pectins and OSA-modified phytoglycogen showed ionic characteristic within a wide range of acidic pH (Hernández-Marín et al., 2013; Jones et al., 2010b; Scheffler et al., 2010b). The presence of unfavorable repulsive interactions between α-lactalbumin and most of the OSA-modified polysaccharides evaluated, suggest a high probability of ionic repulsive forces and mutual exclusion (steric effects) of each amphiphilic biopolymer in the solution.

Table 4.2 presents the results of the analysis of covariance in a general linear model comparing the relaxation time (λ) slopes among all the combinations of 3.6 g/L concentration of α-lactalbumin or WPI with different concentrations of OSA-modified polysaccharides influenced by an increment in the oscillatory frequency.

According to the analysis of covariance, the λ slope of the combination of 3.6 g/L of α-lactalbumin with 18.0 g/L DWxRc7 showed significant difference ($P < 0.05$) compared to the combination of 3.6 g/L WPI with the different concentrations (0.18, 1.8, and 18.0 g/L) of OSA-modified polysaccharides. No significant differences ($P > 0.05$)

were observed among the λ slopes from combinations of 3.6 g/L of WPI and the different concentrations (0.18, 1.8, and 18.0 g/L) of polysaccharides, independently of the percentage of OSA modification, which suggests the formation of similar structures in all these different combinations of OSA-modified polysaccharide and WPI. However the structure size, indicated by the critical frequency, seems to be influenced by the percentage of OSA modification. These results suggest that the type of protein has strong influenced in the intermolecular associations with OSA-modified polysaccharides, and the percentage of OSA modification in polysaccharides influence to a certain extent on the amount of molecules interacting with the proteins (e.g. WPI); consequently, more molecules of lower percentage of OSA-modified polysaccharides is needed to self-assemble with protein molecules, forming bigger size structures

4.5 Conclusions

Fluorescent spectroscopic techniques yielded a critical value of concentration for micelle-type structure formation of α-lactalbumin and WPI to be at around 2.5 g/L and 0.6 g/L, respectively. Micelle-type structure formation was not observed on 3% and 7 % of OSA-modified phytoglycogen, DWxRc and DWxCn. However, a curve inflection point occured around 1.0 g/L for the OSA-modified polysaccharides, which indicates the formation of a different type of structure. Thus, the bulk volume of OSA-modified polysaccharides associated with their short length of OSA hydrocarbon chains does not allow the OSA-modified polysaccharides to self-assemble into a micelle-type structure.

α-lactalbumin and whey protein isolate suspensions showed a distinct linear viscoelastic region (LVR) at all dilution concentrations tested (0.18, 1.8 and 18.0 g/L) when the oscillatory stress sweep test was performed at 0.1 Hz and 23°C. Hence, intrinsic properties of amphiphilic structures formed by biopolymers were evaluated since no changes occured in the elastic (G') and viscous (G") characteristics of the biopolymer system within the LVR.

The creep test at constant stress of 0.01 Pa and 23°C yielded relatively high values of shear rate for all protein concentrations evaluated in this study. All samples showed pseudoplastic-like flow behavior at a minimum shear rate of 0.2 s^{-1}; hence, the elastic properties of the solutions were difficult to characterize by this method. Furthermore, the variability on the ZSV values at each biopolymer concentration makes it unreliable to characterize structure formation associated with the increase in ZSV values.

Unlike OSA-modified phytoglycogen, which showed solid-like behavior (G' > G") only at higher concentrations, both proteins and OSA-modified depolymerized waxy rice starch did not show concentration dependent G' and G" values; however, the moduli changed with the type of biopolymer at a certain concentration. In the case of proteins, WPI (0.18g/L) showed solid-like behavior at lower dilute concentrations than α-lactalbumin (1.8 g/L). This result is in agreement with that determined by the fluorescent test on protein concentration for micelle-type structure formation. The solid-like behavior might be associated to hydrophobic association of the biopolymer at these

specific concentrations, although a micelle-type structure formed at higher protein concentration.

The influence of percentage of OSA modification on the self-assembly network formation seems to depend on the structure type of polysaccharide. The complex viscosity curves (η*) showed a linear trend for all different proteins and OSA-modified polysaccharides. These results correlate with the values of the elastic modulus (G') at each level of biopolymer concentration.

The relationship of the elastic (G') and viscous (G") moduli with of the frequency, called relaxation time "λ", was very sensitive to the value of frequency and polymer concentration. The values of λ decreased linearly with increasing frequency up to a critical frequency value (CFV) where the trend of λ values suddenly changed to a more scattered distribution, which could present the breaking point of the stucture. Higher values of λ are closely related to the solid-like behavior observed by the dynamic elastic (G') modulus response. Proteins and OSA-modified DWxRc showed defined slope at all concentrations. On the other hand, dilutions of OSA-modified phytoglycogen only showed a defined slope at the highest concentration evaluated (18.0 g/L) which is in agreement with the solid-like behavior described by the G' values. The solid-like dynamic response of certain concentrations of the biopolymer must be influenced by the low rotational motility of the assembled structure, which can be related to its geometry.

The CFV observed on the change of slope tendency for proteins and OSA substituted DWxRc did not depend on polymer concentration. However, the CFV of OSA-modified phytoglycogen at 0.18 g/L was influenced by the percentage of OSA

modification. With the exception of WPI (0.18 g/L) and DWxRc7 (1.8 g/L), all other λ slopes were not significantly different ($P > 0.05$), which sugests the formation of a similar structure with identical geometriy among the different levels of concentration of the biopolymers.

α-lactalbumin (3.6 g/L) showed structure formation only in combination with 18.0 g/L DWxRc7 presenting a high CFV at 0.45 rad/s. The scattered distribution observed indicates that no self-association is present when in combination with the other OSA-modified polysaccharides. On the other hand, WPI (3.6 g/L) presented self-assemble interactions with all different OSA-modified polysaccharides at the different concentrations evaluated in this study (0.18, 1.8, and 18.0 g/L), independently of the percentage of OSA modification and concentration of polysaccharide. The higher CFV was observed in combination of WPI with the lowest concentration (0.18 g/L) of 7% OSA-modified polysaccharides. It seems that both the type of protein and polysaccharide structure such as size and number of OSA hydrocarbon chains have a strong influence in their molecular interactions. The structure size, indicated by the CFV, seems to be influenced by the percentage of OSA modification in polysaccharides. The rheological analysis for intermolecular interactions between biopolymers provides a better understanding of their properties and structure formation for practical applications as natural carriers of bioactive compounds. Further studies should be performed with the help of microscopy visualization to associate the type of structure geometry with the relaxation time or other rheological parameters.

CHAPTER V

EVALUATION OF ENTRAPMENT EFFICIENCY, RHEOLOGY AND MICROSTRUCTURE FORMATION OF ELECTROSTATICALLY PRECIPITATED PROTEINS IN COMBINATION WITH OSA-MODIFIED POLYSACCHARIDES

5.1 Overview

Electrostatic precipitation of protein alone or in combination with OSA-modified polysaccharides is a feasible method to entrap volatile and thermolabile compounds. Absorbance measurements were in agreement with OSA-modified polysaccharides interaction-adsorption by electrostatically precipitated proteins, which in turn were congruent with the entrapment efficiency based on the amount of precipitated protein. The dynamic oscillatory test at 0.01Pa, 23°C and neutral pH (~7.0) should be complemented by an additional analysis of the relaxation time "λ"value, which is the time associated with large scale motion (or changes) in the structure of polymers. The dynamic oscillatory response (solid-like or liquid-like) of proteins alone or in combination with OSA-modified polysaccharides has been related to the rotational capability of structures. Structures with high geometric aspect ratio are more difficult for rotational displacement compared to those with a small ratio. The linear decrements of relaxation time "λ"values (slope) have been associated as an indicator of structure formation. Similar characteristic λ slopes values suggest similar structural shape, while the critical frequency, which point out the change of λ slope value, indicates the structure's size. Transmission electron microscope (TEM) visualization of

electrostatically precipitated proteins alone or in combination with OSA-modified polysaccharides corroborated in some way the λ slope values and the critical frequency with the shape and size of the assembled structure. The effectiveness of this method enhances the possibility to evaluate the geometry of electrostatically precipitated particles by quantifying their rheological dynamic behavior of self-assembled structures in aqueous solution.

5.2 Introduction

Currently, food technologists have a great number of options from different natural polymers as good alternatives with similar performance to synthetic ones. Consumer concerns of the use of synthetic materials have also increased the interest in the utilization of natural polymers. Proteins and polysaccharides are natural food materials, are considered GRAS (generally recognized as safe), widely available, and relatively inexpensive (Livney, 2008). Whey proteins alone or in combination with polysaccharides has been extensively investigated for delivering of hydrophobic bioactive compounds(Ganzevles et al., 2006; Jones et al., 2010a; Livney, 2010; Recio et al., 2008; Sekhon, 2010).

β-Lactoglobulin (BLG) comprises more than 50% of the whey proteins, therefore influencing their assembly behavior (Hansted et al., 2011).The monomeric unit of BLG consists of 162 amino acid residues and has a molecular mass of about 18.3 kDa with a capability to bind and transport small hydrophobic molecules (e.g. fatty acids and retinol) in the beta barrel calix (Verheul et al., 1999). The secondary structures are

formed by folding up into 8-stranded antiparallel β–barrel structures, distinctive feature of lipocalins proteins, with an additional 3-turn lone α–helix located on the surface of the molecule (Kontopidis et al., 2004).

α-lactalbumin along with glycomacropeptides are the next most abundant proteins (approximately 20% each) constituent of the whey proteins. The monomeric unit of α-lactoalbumin is composed of 123 amino acid, 4 tryptophan residues, 4 disulfide bridges, and has a molecular weight of 14.18 kDa (Engel et al., 2002). In a native state α-lactalbumin consists of a large α-helical domain composed of 3 major α-helices and 2 short helical structure and a second small domain β-sheet composed of series of loops, where tree-stranded antiparallel β-pleated sheet are connected by calcium binding and a short helical structure connected by hydrogen bonds (Permyakov and Berliner, 2000).

Similarly, polysaccharides such as starch and phytoglycogen have been hydrophobically modified by reaction with octenyl succinate anhydride (OSA) to become strongly surface active (Prochaska et al., 2007; Scheffler et al., 2010a; Wang et al., 2011) and have been successfully handled to impart functional application as rheology modifiers, emulsion stabilizers, surface modifiers, encapsulation matrix for nanoparticles, and drug delivery vehicles (Gurruchaga et al., 2009; Krstonošić et al., 2011; Liu et al., 2008; Scheffler et al., 2010b)**.**

Surface active molecules such as proteins and OSA-modified polysaccharides possess self-assemble capability mediated by hydrophobic (e.g. weaker van der Waals forces) and hydrophilic interactions (e.g. hydrogen bonding and electrostatic interactions

of ionic forces) (Israelachvili, 2010), which make them to be called amphiphilic molecules.

The capability of proteins to aggregate at certain conditions of temperature, pH, ionic strength or enzymatically induced by microbial transglutaminase (Jones et al., 2010a; Majhi et al., 2006; Shpigelman et al.; Tang et al., 2006) make this biopolymer as suitable material to prepare and isolate nanoparticles for drug delivery systems. For example, denatured components (via pressure, heat, pH, etc.) of native β-lactoglobulin, which is about 3.6 nm in length, can reassemble to form larger structures, like fibrils or aggregates (Sekhon, 2010). Similarly, self-assembled nanotubes of about 20 nm outer diameter have been reported to form from combination of calcium and partially hydrolyzed α –lactalbumin by serine protease. This structure have a good capability to serve as a carrier for nanoencapsulation of nutrients, supplements, and pharmaceuticals (Ipsen and Otte, 2007).

Among all the different techniques to encapsulate bioactive compounds by proteins aggregation, only electrostatic precipitation of protein is a reversible process and do not involve significant change on the protein native structure (Majhi et al., 2006). The advantages of this electrostatic precipitation method are its relative low cost, can be carried out with simple equipment in batch or continuous process, the aggregate is often stable for long term storage (Harrison et al., 2003) and can be performed at cold or room temperature, which make it a feasible method to entrap volatile and thermolabile compounds.

Visible spectrophotometric measurements such as absorbance and transmittance has been useful to evaluate the solution turbidity as indication of proteins aggregation induced by enzymatic or heat treatment as well as solubility reduction at a pH called isoelectric point (pI). The net charge of the protein influences its solubility in the medium, therefore, proteins precipitate when the net charges of the protein become zero at pI (Shaw et al., 2001). α-Lactalbumin showed a pI value of pH 4.2 (Nylander et al., 2008), while whey protein showed a pI value of ~4.6 (Wu et al., 2013). Similar pI value of ~4.6 has been also reported for β-lactoglobulin (Jones et al., 2010a; Jones et al., 2010b; Majhi et al., 2006).

The information obtained from spectrophotometric measurements is helpful to evaluate the interaction-adsorption that defines protein aggregation in combination with other amphiphilic biopolymers. However, how those intermolecular interaction influence the type of structure assembled is been difficult to connect. On the other hand, rheological methods have demonstrated to be related to type of assembled structure. Self-assembling structures produce a viscoelastic behavior observed by oscillatory shear (Pätzold and Dawson, 1996). Structures with apparent different geometric (aspect ratio) such as prolate and oblate ellipsoids have been predicted to present the same period of rotational motility based on rheological characterization (Utracki et al., 2010). Rods and ellipsoids (e.g. platelets, and disks) have been easy to difference based on the rotational motility (Goldsmith and Mason, 1962). The geometry aspect ratio for anisotropic particles defined by Utraki et al. (Utracki et al., 2010) as the ratio of the larges to the

smallest dimension, was assumed in this work. The ratio of the largest to the smallest dimension seems more realistic parameter to define different structures.

Low oscillatory frequency sweep tests have been adequate to measure viscoelasticity behavior of proteins aggregation induced by transglutaminase (Tang et al., 2006) as well as self-associative interaction between proteins or in combination with OSA-modified polysaccharides in diluted solutions (Chapter IV). Polymeric nanocomposites materials have been also shown to behave as viscoelastic liquid by the evaluation of interrelation between their elastic (G') and viscous (G'') moduli through their relaxation spectrum (Utracki, 2004) . The relaxation time "λ" is associated with the large scale motion (or changes) in the structure of the polymers (Chhabra, 2010; Roland, 2008). It is therefore evident that the rheological properties are very sensitive to molecular structure and functionality (Chamberlain and Rao, 2000).

The linear viscoelastic region (LVR) presents reversible changes of the structure in the suspension, hence, evaluation within the linear viscoelastic region will determine intrinsic properties of the colloidal system (Li et al., 2005). The LVR for different whey proteins in aqueous solutions was obtained at 23°C and an oscillatory frequency of 0.01Hz (Chapter IV).

The understanding of intermolecular interactions based on rheological tests will help to engineer amphiphilic biopolymers as a carrier of bioactive compounds for food and other applications. The purpose of the present study was to evaluate the application of visible spectroscopy and rheological oscillatory tests to understand the entrapment capability of a hydrophobic compound (e.g. trans-cinnamaldehyde) and the structure-

type formation by the self-assemble characteristic in aqueous solution of pure whey proteins or in combination with OSA-modified polysaccharides for future design of encapsulation materials.

5.3 Materials and methods

5.3.1 Materials

Waxy corn and waxy rice starches (Ingredion, Westchester, IL) were depolymerized with α-amylase-heat stable (Sigma-Aldrich Co., St. Louis, MO) to produce high dextrose equivalent (DE) values (DE= 22 - 24). Depolymerized waxy corn and waxy rice starches as well as phytoglycogen (a highly branched polysaccharide) (Kewpie Corporation, Japan) were modified at different percentage of substitution (approx. 3 and 7%) with Octenyl succinic anhydride (OSA) (Dixie Chemical Co, Houston, TX). Whey protein isolate, whey protein concentrate (80%) and α-Lactalbumin (DAVISCO Foods International, Inc., Eden Prairie, MN) were used without any modifications. Glucose standard, and other reagents and solvents were purchased from Sigma-Aldrich and VWR International (West Chester, PA).

5.3.2 Preparation of OSA-modified waxy rice starch

Twenty five grams of waxy starch sample was added into distilled water in a glass beaker with agitation. The reaction condition for optimum preparation of OSA-waxy starch was carried out as follows: starch concentration in water of 31.5%, temperature 34°C, pH 8.6, and reaction time of 18.7 h (Liu et al., 2008). The pH of the

mixture was kept constant adding 0.1N NaOH and the reaction was terminated by reducing the pH to 6.5 using 0.1N HCl. To collect the samples, three volumes of ethanol were added to the mixture and the precipitated material was centrifuged at 3200 x g for 20 minutes (Allegra 25R centrifuge, Beckman Coulter, Fullerton, CA) and subsequently washed with ethanol and centrifuged 3 more times. Afterwards, the sample was dried in a vacuum oven (Squared Lab Line Instruments, Melrose Park, IL) at 60°C overnight.

5.3.3 Percentage of modification (%OSA)

Octenyl succinate modification in waxy starches and phytoglycogen was quantified using a method from the Joint FAO/WHO Expert Committee on Food Additives (JECFA, 2011) with some modifications. The sample (0.5g) was acidified with 3 ml of 2.5 M HCL for 30 minutes. Ten ml of pure isopropanol was added, followed centrifugation at 3200 x g for 20 minutes. Subsequently, the precipitate was washed and centrifuged 3 more times or until the test of chloride ions using one drop of 0.1 M $AgNO_3$ on the supernatant showed negative haze formation. Afterwards, 30 ml of distilled water was added to the precipitate and heated in boiling water for 30 min, and then titrated using 0.01 M NaOH. The percentage of OSA modification (%OSA) was calculated by the following equations:

$$A = \frac{(V - V_0) * 0.01}{0.5} \quad (5.1)$$

$$\% \, OSA \; = \; \frac{210 * A}{1000} * 100 \qquad (5.2)$$

Where A (mmol/g) is the molar amount of octenyl succinate groups in one gram of derivative; 210 is the molecular weight of octenyl succinate group (g/mol); *V* (ml) is the volume of NaOH solution consumed by the octenyl succinate derivative; V_0 (ml) is the volume of NaOH consumed by the native waxy starches or phytoglycogen; 0.5 is the weight of material in grams and 0.01 is the molar concentration of NaOH (JECFA, 2012).

5.3.4 Enzymatic treatment of waxy starches

Waxy corn and rice starch samples (5 g, dry weight) were mixed with water to a 35% suspension by weight containing 200ppm of $CaCl_2$. The pH of the mixture was adjusted to 5.9 with 0.1N NaOH and α-amylase at 20 U per gram of starch was added into the mixture (Liu et al., 2008). The suspension was heat up on a hot plate at 100°C for 20 minutes and then incubated in a shaking water bath (VWR International, West Chester, PA) set at 65°C and 100 rpm for 360 minutes. The reaction was stopped by reducing the mix pH to 4.0 with 0.5N HCl. Three volumes of ethanol were added to the mixture, followed by centrifugation at 3200 x g for 20 minutes (Allegra 25R centrifuge, Beckman Coulter, Fullerton, CA)and the precipitate solid were dried in a vacuum oven (Squared Lab Line Instruments, Melrose Park, IL) at 60°C overnight. The dextrose equivalent (DE) value was confirmed based on the following equation:

$$DE = \frac{Reducing\ sugar\ content\ (\frac{mg}{g})}{Total\ sugar\ content\ (\frac{mg}{g})} \quad (5.3)$$

5.3.5 Total sugar content (TS)

The phenol-sulfuric acid assay method was carried out (Fournier, 2001). This method is very general, and can be applied to many classes of carbohydrates including oligosaccharides where reducing and non-reducing sugars are present. The phenol-sulfuric acid method is based on the absorbance at 490 nm of colored aromatic complex formed between phenol and the carbohydrate. The amount of sugar present was determined by comparison with a calibration curve of D (+) glucose using a spectrophotometer (Thermo Scientific Genesys 10S UV-Vis, Waltham, MA). One hundred mg of sample was diluted in 10 ml of distilled water. One ml of the previous dilution was subsequently diluted in 9 ml of distilled water. A blank was prepared using 50 µl of distilled water. Five hundred µl of 4% phenol was added to 50 µl of later dilution and followed by 2.5 ml 96% sulfuric acid. The mixture was allowed to cool down at room temperature for 15 minutes and its absorbance measured in a spectrophotometer (Thermo Scientific Genesys 10S UV-Vis, Waltham, MA) at 490 nm.

5.3.6 Reducing sugar content

Quantification of reducing sugars was determined by the Somogyi-Nelson method (Fournier, 2001). This method utilizes the reducing properties of certain types of

carbohydrates based on the absorbance at 500 nm of a colored complex formed between a copper-oxidized sugar and arsenomolybdate. The amount of reducing sugar present was determined by comparison with a glucose calibration curve using a spectrophotometer (Thermo Scientific Genesys 10S UV-Vis, Waltham, MA). One hundred mg of sample was diluted in 10 ml of distilled water. One ml of the previous dilution was subsequently diluted in 9 ml of distilled water. A blank was prepared using 50 µl of distilled water. One ml of low-alkalinity copper agent was added to the 50 µl of later dilution and heated in boiling water for 10 min. Then, 1 ml of arsenomolybdate reagent was added with an extra 2900 µl of distilled water and the mixture was allowed to cool down at room temperature for 15 minutes and its absorbance measured in a spectrophotometer (Thermo Scientific Genesys 10S UV-Vis, Waltham, MA) at 500 nm.

5.3.7 Absorbance as indicator of particle formation

Insoluble complexes were effectively monitored through absorbance (Abs) measurements. The biopolymer combinations were mixed for 30 seconds by a vortex mixer (VWR International, West Chester, PA, USA).and let to stand for 1 h at room temperature. The solutions were subsequently agitated by a vortex mixer right before the absorbance of the mixture was measured at 600 nm with a spectrophotometer (Shimadzu UV-1601, Columbia, MA) in a 1 cm path length quartz cuvette. The maximum sorption at different pH was considered as indication of maximum complexes formation. The pH value was measured with an Orion 811 pH meter equipped with a Beckman refillable combination pH electrode and calibrated with pH 7 and pH 4 buffers.

5.3.8 Polysaccharides adsorption by protein precipitation

The adsorption of OSA-modified polysaccharides (PSC) at different ratios of polysaccharide and protein (0.01 - 10) was evaluated based on the total amount of sugar adsorbed in the protein precipitated (ppt.). Total amount of sugar was quantified using the phenol-sulfuric acid assay method (Fournier, 2001). Fifty µl of supernatant was taken before and after the protein electrostatically precipitated at pH of approximately 4.5 and the amount of PSC adsorbed was calculated as follows:

$$\frac{PSC}{Protein} = \frac{(\Delta\, TS\ in\ supernatant\ before\ and\ \ after\ ppt.(mg))}{Total\ weight\ of\ protein\ (mg)} \tag{5.4}$$

5.3.9 Bradford protein assay

The assay is based in observation that the maximum absorbance for an acidic solution of Coomassie Billiant Blue G-250 shifts from 465 to 595nm when binding to protein occurs (Bradford, 1976). Both the hydrophobic and ionic interaction stabilize the anionic form of the dye, causing a visible color change. The amount of protein present was determined by comparison with a calibration curve of Albumin. Ten mg of sample was diluted in 10 ml of distilled water. Equal volume of 1 M of NaOH was added to all samples and standards and vortex. Five ml of dye reagent (acidic solution of Coomassie Billiant Blue G-250) was added and incubated at room temperature for 5 minutes and the

absorbance was measured at 595 nm by using a spectrophotometer (Shimadzu UV-1601, Columbia, MA).

5.3.10 Particle synthesis

Particles were obtained by acid precipitation of complexes structure formed between different weight ratios (1:0, 1:1, 1:2, and 1:3) of proteins and OSA-modified polysaccharides to achieve a biopolymer total amount of 184 g/L in aqueous solution. *Trans*-cinnamaldehyde 99% (TCNN) (Sigma-Aldrich Co., St. Louis, MO) was selected as a model hydrophobic bioactive compound, due to its use as highly effective antimicrobial (Gomes et al., 2011). First, an emulsion of TCNN (1.32 mg/L, 10 μM) in water was prepared by addition of protein alone or in combination with octanyl succinate modified polysaccharides. The mixture was vortexed for 30 seconds and left to rest at 4°C overnight. After 16 hours the particle was precipitated by addition of citrate buffer (1 M) at pH 4.0 to achieve the isoelectric point of the proteins involved in the particle complex (approx. pH 4.5). After 30 minutes the solution was centrifuge (Allegra 25R centrifuge, Beckman Coulter, Fullerton, CA) at 4°C for 20 minutes and the liquid supernatant was separated for further quantification of non-entrapped trans-cinnalmadehyde content. After centrifugation, the precipitate was kept at –20 ◦C overnight and then lyophilized at –50 ◦C and 1.45 × 10−4 psi vacuum for 12 h in a Labconco Freeze Dry- 5 unit (Labconco, Kansas City, MO). Afterwards, the particles were stored at -20°C.

5.3.11 Entrapment efficiency

The entrapment capability of TCNN by the complex structure formed between different weight ratios (1:0, 1:1, 1:2, and 1:3) of proteins and OSA- modified polysaccharides was evaluated by measuring the remaining TCNN on the supernatant ($TCNN_{suptt}$) after centrifugation of biopolymeric complexes electrostatically precipitated at 23°C. The total amount of precipitated biopolymers was calculated based on the amount of β-lactoglobuline (MW=18.4 kDa) to evaluate an entrapment of equal molar ratio compared to TCNN (10 mM). A control TCNN solution (1.32 mg/L, 10 mM) was prepared with the absence of biopolymers ($TCNN_{control}$). To quantify the amount of TCNN, a 100 µl-sample of was diluted 20 times in Acetonitrile and the solution was passed through 0.2 μm nylon membrane syringe filters (VWR Intl., West Chester, Pa.,U.S.A.) to remove all biopolymer complexes precipitated on the Acetronile. The filtered solution was then measured spectrophotometrically (Shimadzu UV-1601 spectrophotometer, Columbia, MA) at 280 nm in a 1 cm path length quartz cuvette and the amount of TCNN was calculated from a standard curve. The entrapment efficiency (EE%) was calculated as,

$$EE\% = \frac{(TCNN\ control - TCNN\ suptt)}{TCNN\ Control} * 100 \qquad (5.5)$$

5.3.12 Rheological test

All different tests were performed with a Haake RheoStress 6000 Rheometer (Thermo Fisher Scientific, Waltham, MA) using a cone-plate sensor, in which the rotating cone was 60 mm in diameter and angle of 1° with a gap of 0.052 mm. About 1 ml of each sample was carefully placed in the plate, and left to rest for 5 min for structure recovery and the temperature was maintained at 23°C with the help of TC-81 Peltier system (Thermo Fisher Scientific, Waltham, MA) in all the experiments. Analysis was carried out by triplicate on each sample after 1 day of prepared and stored at 4°C. Dynamic frequency sweeps were performed at 0.01 Pa of stress, which was characterized within the linear viscoelastic region (LVR) of protein solutions (Chapter IV). The possibility of self-assembly structures of pure α-lactalbumin or WPI and in combinations with OSA-modified polysaccharides (total biopolymer concentration 180 g/L), was evaluated by the relationship of the elastic (G') and viscous (G") moduli in function of the angular frequency, which represents the relaxation time "λ" associated with large scale motion (or changes) in the structure of the polymers

5.3.13 Particle morphology

Aqueous suspensions of electrostatically precipitated biopolymers were examined using a FEI Morgagni Transmission Electron Microscope (TEM) (FEI Company, Hillsboro, OR) at the School of Veterinary Medicine and Biomedical Sciences of Texas A&M University (College Station, TX). Aqueous suspensions of particles were placed on 300 mesh copper grids and stained with a 2% (w/v) uranyl

acetate aqueous stain (Electron Microscopy Sciences, Hatfield, PA) to provide contrast under magnification. Excess liquid on the mesh was removed with filter paper and the grid was allowed to dry before viewing under 50,000-100,000 times magnification. Observations were performed at 80 kV.

5.3.14 Particle size measurement

The sample of electrostatically precipitated biopolymers was dissolved in distilled water at a concentration of 10 mg/ml and vortexed for 30 seconds. Next, the particle size was measured at room temperature using a Particle Size Analyzer (Delsa™ Nano C, Beckman Coulter, Pasadena, CA). This machine uses photon correlation spectroscopy (PCS), which determines particle size based on the dynamic properties of particles moving in a solvent. The hydrodynamic diameter was calculated based on the rate of fluctuations in laser light intensity scattered by equivalent spherical particles as they diffuse through the solvent.

5.3.15 Statistical analysis

All experiments were replicated at two or three times, and the results were reported as average. Statistical analysis software (IBM SPSS Statistics, Version 14, IBM Corporation, Armonk, NY) was used to perform analysis of Covariance (ANCOVA) in a general linear model, adjustment of multiple comparison with Bonferroni's test to compare relaxation times "λ" slope calculated from dynamic oscillatory test as indication of self-assembly structure by pure or combination of biopolymers (Whey

protein isolate, α-lactalbumin, 3% and 7% OSA-modified depolymerized waxy corn starch, waxy rice starch and phytoglycogen). Oscillatory frequency sweep was considered as covariance because this variable is not directly tested but has been observed to have a direct influence on the dependent variable that is the relaxation time, λ. The relaxation time (λ) slopes of different biopolymers alone or in combination was evaluated as independent variable and considered as fixed factor for the covariance analyses. Mean comparison analysis was also performed with Duncan test to compared differences on the entrapment efficiency among samples with a $P < 0.05$ being considered to be a significant difference between means.

5.4 Results and discussion

5.4.1 Electrostatically precipitation protein

The solubility of α-lactalbumin and whey protein isolate (WPI) at different pH values is shown in Figures 5.1 and 5.2. The minimum solubility of different concentrations of α-lactalbumin (1.4 and 2.8 g/L) (Figure 5.1B) and WPI (3.6 and 7.2 g/L) (Figure 5.2A) was similar for each protein evaluated, and the minimum solubility pH range was independent of the concentration. A whitish haze was observed as a visual indicator of protein precipitation (Figure 5.1A). The maximum values of absorbance read were in a narrow range of pH, which indicated the minimum solubility (maximum precipitation) of proteins. α-lactalbumin showed precipitation at pH range between 3.8 and 5.4 (Figure 5.1A). The absorbance values at 600 nm confirmed a minimum solubility (maximum precipitation) at pH range from 4.0 to 4.8 (Figure 5.1B). Isoelectric

point at pH value of 4.2 was previously reported for α-lactalbumin (Nylander et al., 2008).

The precipitation of WPI was observed at the pH range between 4.0 and 5.8 (Figure 5.2A). Whitish haze formation was also observed in WPI precipitation as indicator of protein precipitation (Figure 5.2A). The absorbance values at 600 nm confirmed a minimum solubility (maximum precipitation) at pH range from 4.2 to 5.2 (Figure 5.2B). Similar pI value at pH ~4.6 has been reported for whey protein (Wu et al., 2013), which coincided with the pI reported for β-lactoglobulin (Jones et al., 2010a; Jones et al., 2010b; Majhi et al., 2006). β-Lactoglobulin is a major constituent of the whey protein (about 58 %), hence dominate the assembly behavior of whey proteins proteins (Hansted et al., 2011). According to these results the pH value of 4.5 was selected for electrostatic precipitation of α-lactalbumin and WPI.

Based on the absorbance values, α-lactalbumin seemed to yield higher precipitate at lesser amount of protein compared to WPI. A protein content of α-lactalbumin and WPI evaluated using Bradford protein assay showed that α-lactalbumin contained as much as twice the percentage of protein as WPI (Table 5.1); however, the amount of protein precipitated by solution of α-lactalbumin was almost three times the amount of precipitated WPI.

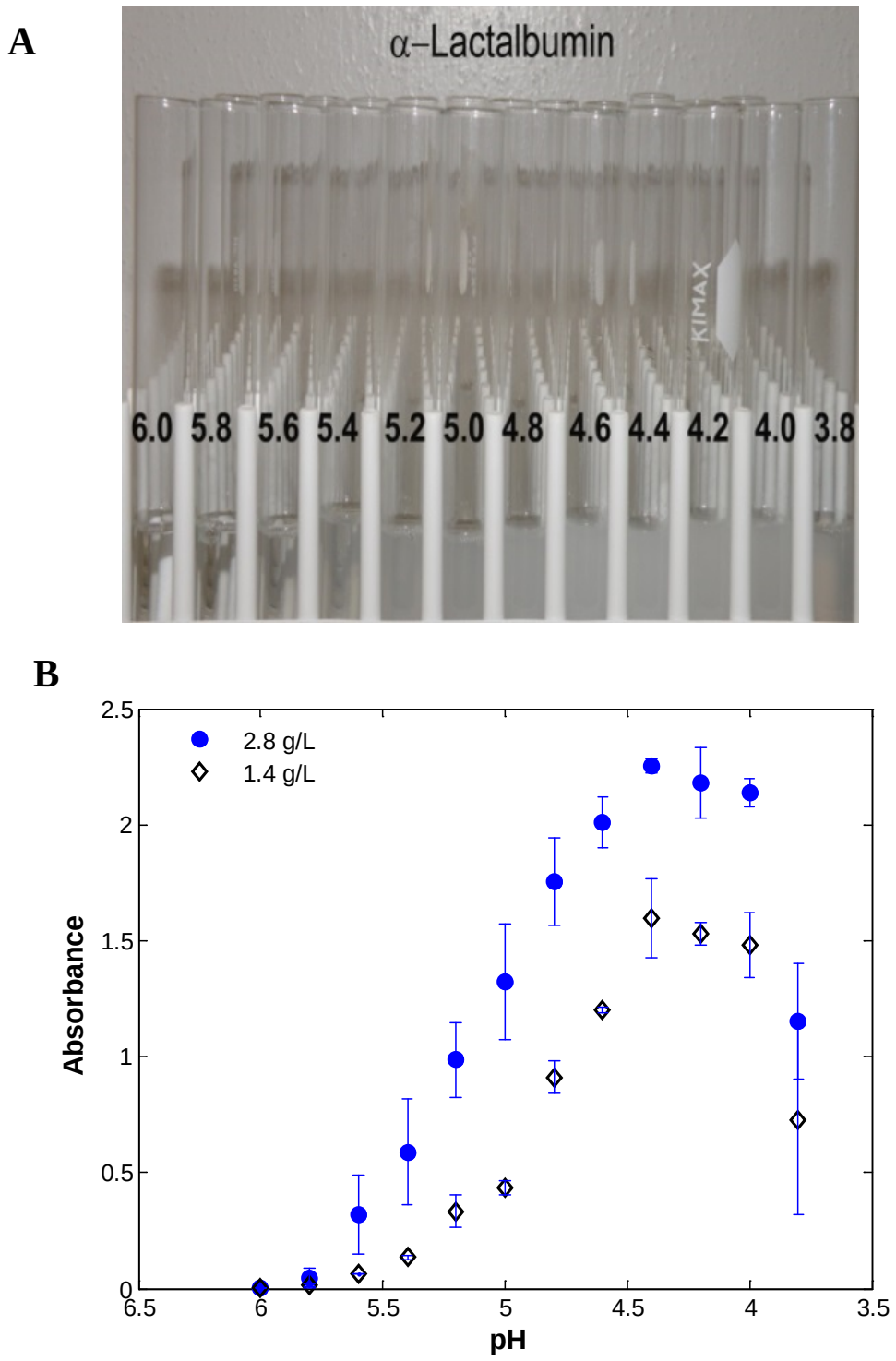

Figure 5.1. Visual observation (A) and absorbance values at 600 nnm (B) for different concentrations of α-lactalbumin precipitation at different pH values measured at 23°C.

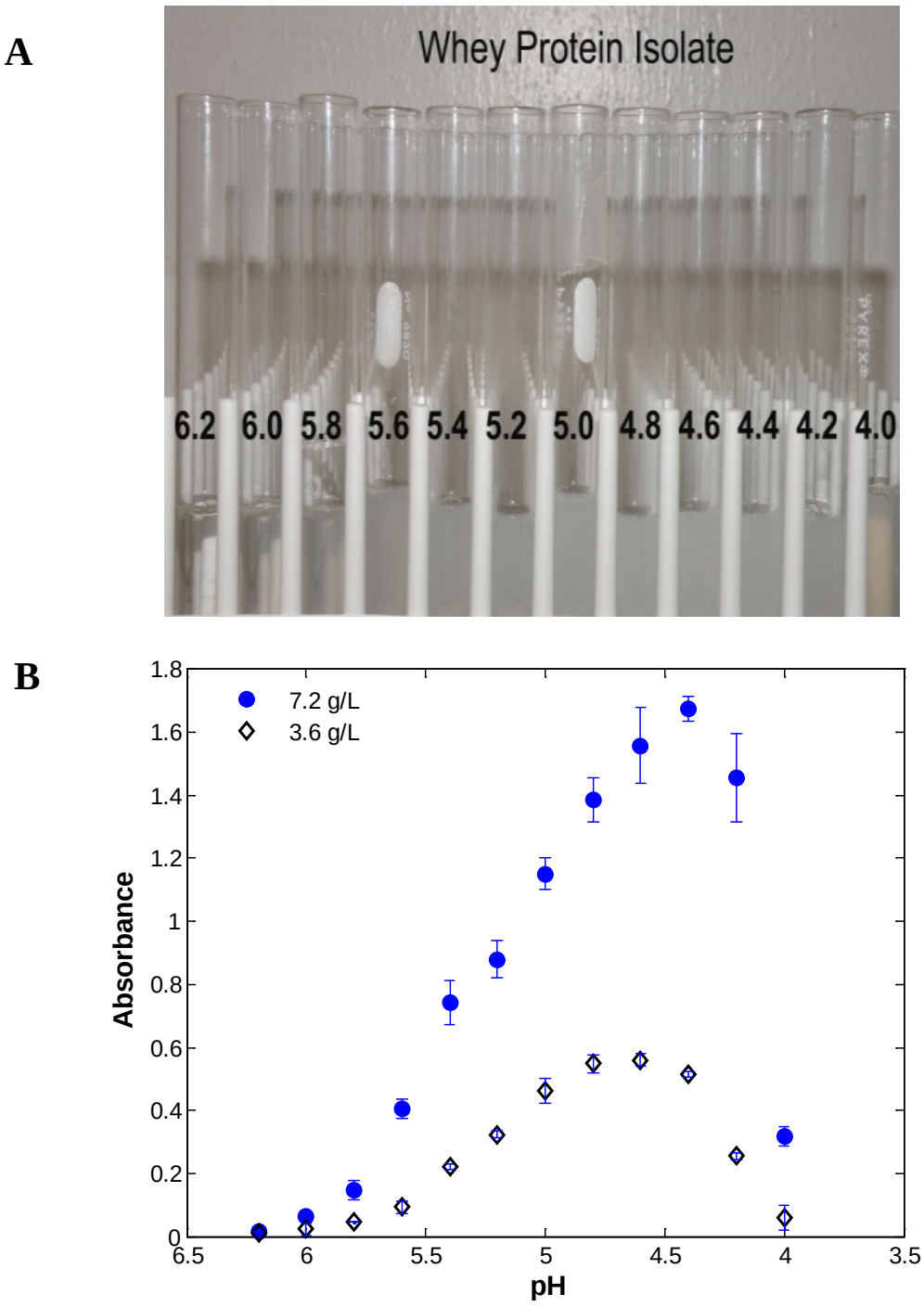

Figure 5.2. Visual observation (A) and absorbance values at 600 nnm (B) for different concentrations of whey protein isolate (WPI) precipitation at different pH values measured at 23°C.

Table 5.1. Protein concentration and amount of precipitated protein after electrostatic aggregation at pH 4.5 of 184 g/L.

Protein type	Protein concentration mg/ml[A]	Weight of precipitated protein (g)[B]
α-L	85.18 ± 0.05[a]	1.67 ± 0.050[a]
WPI	42.98 ± 0.02[b]	0.63 ± 0.051[b]

Values represent mean of three replicates per sample.
Means values with same letter are not significantly different (P > 0.05)
[A] Protein concentration was quantified by Bradford protein assay (Bradford, 1976).
[B] Precipitate weight was measured after centrifugation at 3200 x g for 20 minutes.

These results indicate that other proteins present in the WPI such as glycomacropeptides, the third most abundant protein (approximately 20%), have a different isoelectric point (pI) and probably did not precipitate at pH 4.5. Certainly, the pI of glycomacropeptides evaluated by sodium dodecyl sulfate polyacrylamide gel electrophoresis (SDS-PAGE) test has been reported with a pH value of 3.6 (Rojas and Torres, 2013).

The difference in the amount of precipitate at pH 4.5 from equal amount (184 g/L) of α-lactalbumin and WPI concentration is shown on Figure 5.3. This observation confirmed that the amount of α-lactalbumin precipitated is significant bigger than the amount of WPI precipitated.

A

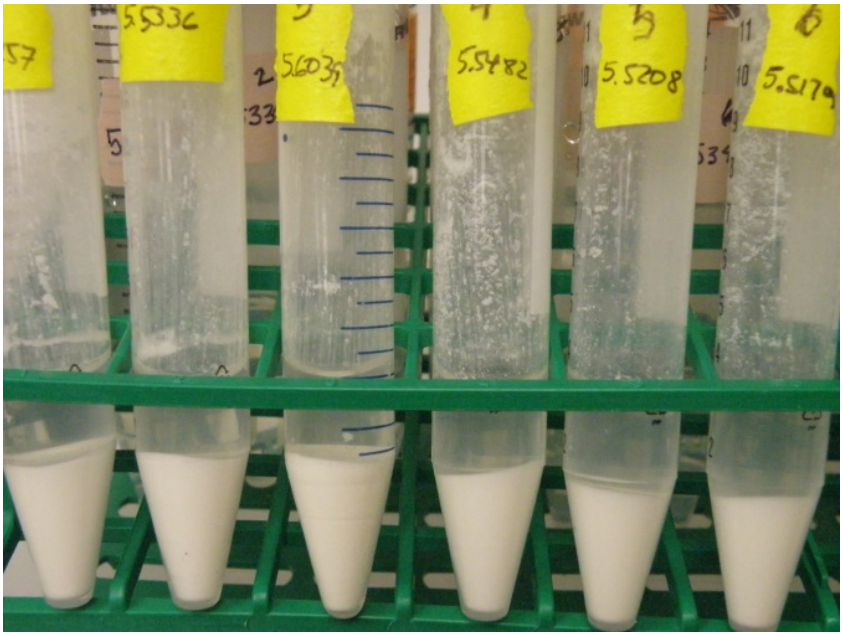

B

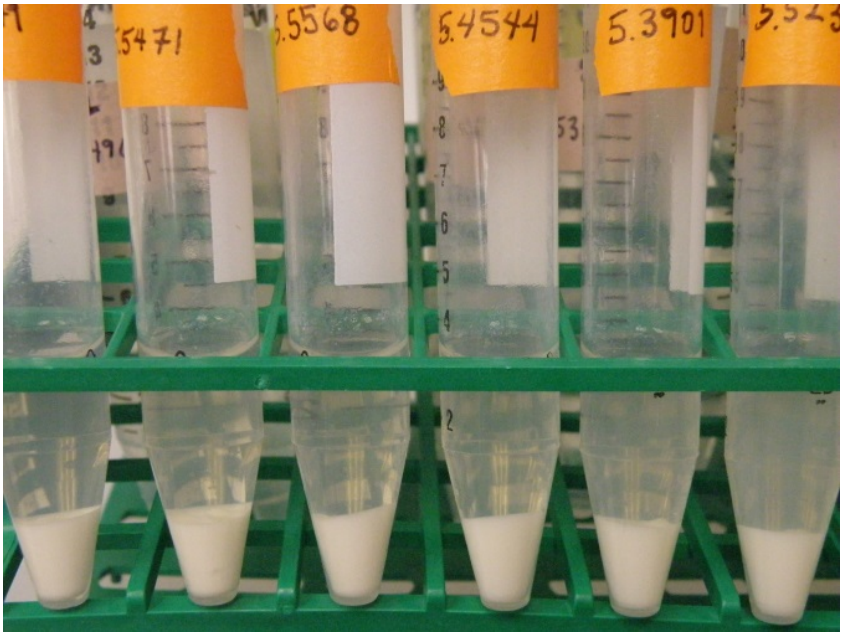

Figure 5.3. Electrostatic precipitation at pH 4.5 of 184 g/L of (A) α-lactalbumin and (B) whey protein isolate.

The addition of different OSA-modified polysaccharides into protein solution did not interfere or change the pH range of precipitation for α-lactalbumin or WPI, (Figure 5.4). However, it is interesting to note that the absorbance seemed to increase for the combination of the different OSA-modified polysaccharides with proteins compared to the protein alone. This result was more noticeable on WPI combinations than in α-lactalbumin.

The high affinity of WPI with the different OSA-modified polysaccharides seems to be influenced by the critical micelle concentration (CMC) of these proteins. The concentration of WPI (3.6 g/L) used in combination with the different OSA-modified polysaccharides is 6 times higher to the CMC (0.6 g/L) found previously (Chapter IV). Similarly, the concentration of α-lactalbumin (1.4 g/L) used in combination with the different OSA-modified polysaccharides (Figure 5.4A), except for the 3% OSA-modified DWxRc, showed at most 30% increased absorbance, though not as much as the increment observed with WPI (Figure 5.4B) that was at most 300%. The concentration of α-lactalbumin was almost half lower than the CMC (2.5 g/L) found previously (Chapter IV).

The interactions mediated by ionic and hydrophobic forces usually occur at concentration below the CMC of the small amphiphilic surfactants (Jones and Brass, 1991), and nonspecific interaction could also occur close to the CMC of the amphiphilic molecules as they become associated (Nylander et al., 2008), which indicate that better interaction between α-lactalbumin and OSA-modified polysaccharides would be at a combination with at least 2.5 g/L of α-lactalbumin.

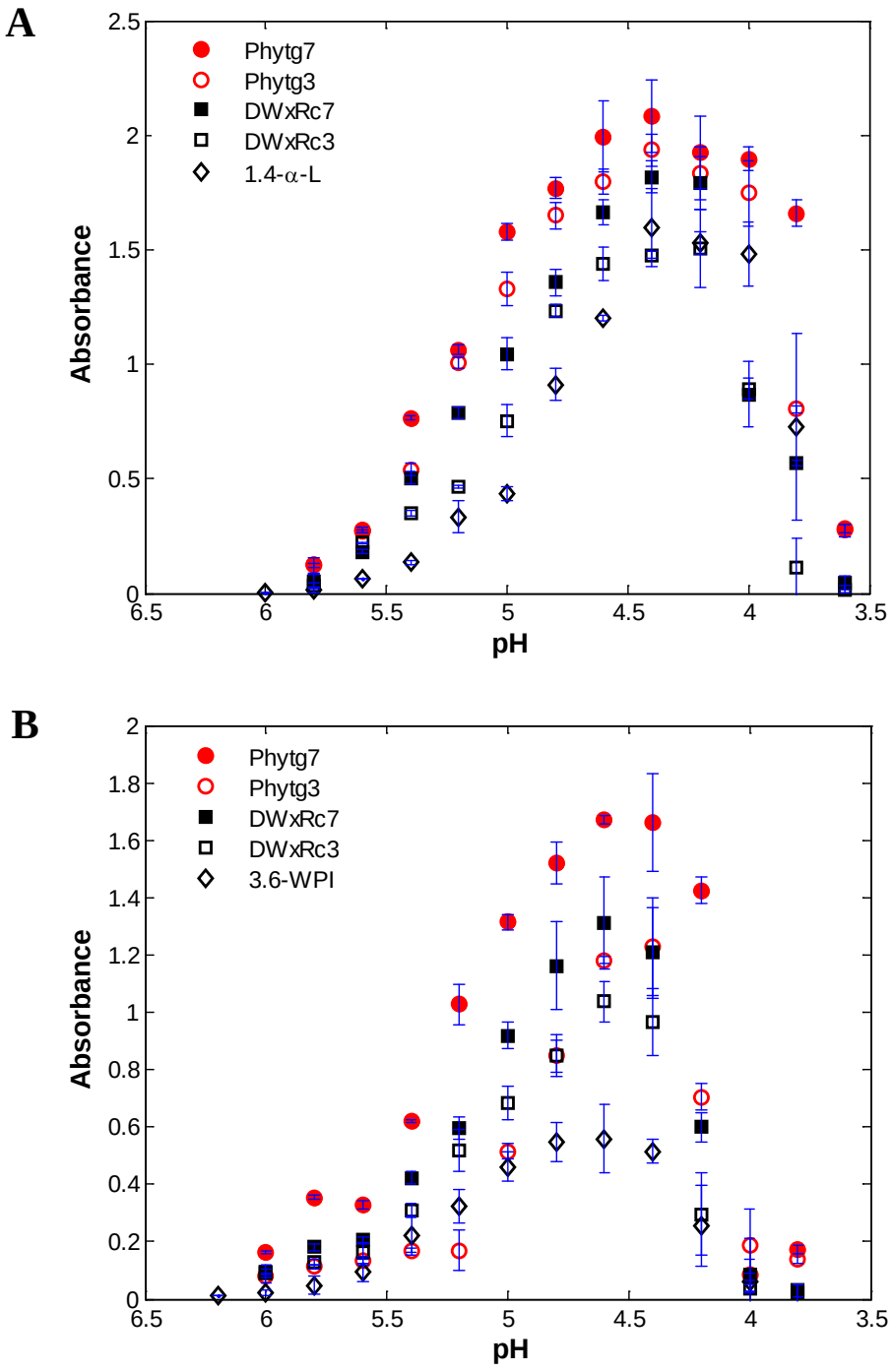

Figure 5.4. Effect of pH on absorbance at 23°C for combination of 3.6 g/L of depolymerized waxy corn and phytoglycogen at different percentages of OSA modification with (A) 1.4 g/L of α-lactalbumin and (B) 3.6 g/L of whey protein isolate.

Higher absorbance at pH of precipitation occurred for the combination of both types of protein, α-lactalbumin and WPI, with 7% of OSA-modified polysaccharide compared to the 3% of OSA-modified polysaccharide. These results suggest a higher interaction of higher percentage of OSA-modified polysaccharides and both types of proteins. Additionally, OSA-modified phytoglycogen seem to provide higher interaction in combination with both types of proteins compared to DWxRc with the same percentage of OSA modification.

According to the absorbance values in Figure 5.4, precipitation increases when protein is combined with the different OSA-modified polysaccharides compared to protein alone. Based on these results, the interaction of proteins and OSA-modified polysaccharides was investigated using different amounts of α-lactalbumin and WPI on concentrations over the CMC observed previously.

5.4.2 Interaction of protein and OSA-modified polysaccharides in aqueous solution

At this time, the concentration of protein used was over the CMC of both proteins (Chapter IV). The adsorption of OSA-modified polysaccharides (PSC) at different ratios of polysaccharide/protein (0.01 - 10) is shown in Figure 5.5. Contrary to previous work (Chapter IV) that showed no interaction at neutral pH (~7.0) for the combination ratios of 0.05, 0.5, and 5.0 between OSA-modified polysaccharide and α-lactalbumin (3.6 g/L), significant binding adsorption was observed at pH of 4.5 over an equal concentration of α-lactalbumin and the distinct OSA-modified polysaccharides (Figure 5.5A).

A good affinity binding occurs at acid pH 4.5 between α-lactalbumin or WPI and OSA-modified polysaccharides over a higher ratio of 1:1 polysaccharide/protein (Figure 5.5). This high affinity of α-lactalbumin and WPI with the different OSA-modified polysaccharides seems to be more effective in higher percentage of OSA modification as it was observed previously with the absorbance values (Figure 5.4A). Similar total sugar adsorption was observed for both proteins at each combination. At the highest combination of OSA-modified polysaccharides and proteins (10/1), OSA-modified phytoglycogen showed more adsorption (~6 mg/mg protein) than OSA-modified DWxRC (~3 mg/mg protein) though at the combination of 1/1 the total sugar adsorption was more influenced by the percentage of OSA modification than by the type of polysaccharide.

Proteins interact with OSA-modified polysaccharides in very similar way as small ionic surfactants molecules. The type of interaction between proteins and OSA-modified polysaccharides seems to depend on the concentration of the OSA-modified polysaccharide. At low surfactant to protein ratios, the interaction stabilized the protein structure as it was observed against thermally unfolding β-lactoglobulin in combination with SDS (Hegg, 1980); however, at high surfactant to protein ratios, the interaction were observed to produce unfolding of β-lactoglobulin in 1:10 combination with SDS (Waninge et al., 1998). This is a particular characteristic of proteins structures with low content of α–helix in their native form, such as β-lactoglobulin that present a lone α–helix located on the surface of the molecule (Kontopidis et al., 2004) In this regard, β-lactoglobulin, the most abundant protein in the WPI, seems to become unfolded at higher

ratio of 1:1 OSA-modified polysaccharides/protein, exposing more hydrophobic domains, which in combination with the reduction of the electrostatic repulsion due to a pH close to the β-lactoglobulin pI (~5.2),an increment in the biding of more OSA-modified polysaccharides occurs. The β-lactoglobulin seems to continue open up its structure upon interaction with higher concentration of OSA-modified polysaccharides.

However, not all proteins will become unfolded upon interaction with high concentration of ionic surfactants. A reverse phenomena has been observed for proteins with high α–helix content (Mattice et al., 1976) like α-lactalbumin, which consists of a large α-helical domain composed of 3 major α-helices and 2 short helical structures (Permyakov and Berliner, 2000). The folding and unfolding stage of α-lactalbumin has been identified to occur under certain conditions of pH and temperature via an intermediate stage called molten globular state (Dickinson and Matsumura, 1994; Engel et al., 2002), which is somewhere between the native and complete unfolded state, characterized by a retention of secondary structure, but a modified tertiary structure (Kataoka et al., 1997).

At molten globular state, the protein is more expanded and exposed more hydrophobic domain (Nylander et al., 2008). α-lactalbumin has been found to be more surface active in conditions that exits as molten globular state(Engel et al., 2002), which was enhanced as pH was reduce to a point that displacement of Ca^{2+} from binding loops between secondary structures occurs (Permyakov and Berliner, 2000).

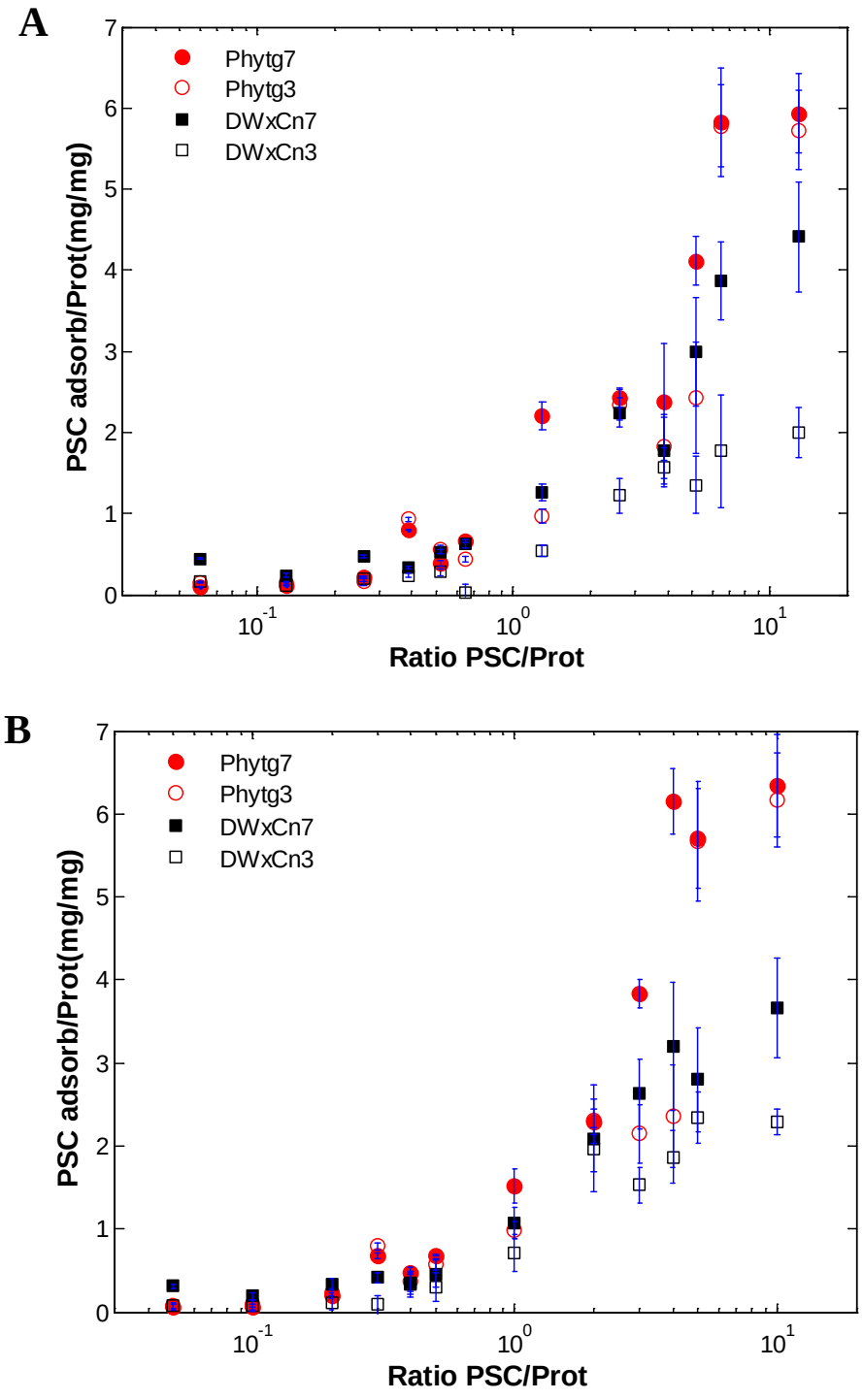

Figure 5.5. OSA-modified polysaccharide (PSC) adsorption after precipitation of (A) 2.8 g/L α-lactalbumin and (B) 3.6 g/L WPI at pH 4.5 and 23°C for different concentration ratios of PSC and protein.

The α-lactalbumin still retains a globular shape in its molten globule state, but is simply swollen from the native state. At low pH, α-lactalbumin undergo conformational transition forming molten globule intermediates (Kuwajima, 1989). Therefore, it is supposed that α-lactalbumin at the precipitation pH of 4.5 presents a molten globular state exposing more hydrophobic domain, which in combination with the reduction of the electrostatic repulsion due to a pH close to its pI (~4.2) and the increment of OSA-modified polysaccharides/protein ratio, more binding of polysaccharides occurred during the precipitation process (Figure 5.5A).

5.4.3 Entrapment efficiency of different combinations of protein/OSA-modified polysaccharides

The entrapment efficiency of 10 mM of trans-cinnamaldehyde (TCNN) by different combination ratios (1:0, 1:1, 1:3, and 1:10) of α-lactalbumin or WPI with 3% and 7% of OSA-modified DWxRc and phytoglycogen is presented in Table 5.2.

According to the weight ratio of proteins/OSA-modified polysaccharide, α-lactalbumin alone showed the highest average entrapment efficient (EE%) value (50.33 $\pm$ 6.07%) compared to its combination with all other OSA-modified polysaccharides, as well as compared to WPI alone or in combination with OSA-modified polysaccharides. The maximum average entrapment efficiency was for α-lactalbumin alone (50.33% $\pm$ 6.07). No significant differences in EE% ($P > 0.05$) were observed among pure α-lactalbumin compared to its combination ratio 1:1 with all other OSA-modified polysaccharides.

Table 5.2. Average entrapment efficiency percentage (EE%) of 10mM trans-cinnamaldehyde for different combination ratios (1:0, 1:1, 1:3, 1:10) of α-lactalbumin and whey protein isolate with OSA-modified depolymerized-waxy rice and phytoglycogen at 23°C. Total mixture concentration of 184 g/L in aqueous solutions.

Polymer Mixture	**Average (EE%) ± Stdev**	**mgTCNN/g protein[A]**
α-Lactalbumin	50.33 ± 6.07^{a}	7.29 ± 0.88^{j}
α-L + DWxRc3 1:1	39.49 ± 4.09^{abc}	11.44 ± 1.19^{ij}
α-L + DWxRc3 1:3	29.91 ± 3.30^{bcdefg}	17.33 ± 1.91^{hij}
α-L + DWxRc3 1:10	21.54 ± 2.78^{efghi}	34.66 ± 4.47^{de}
α-L + DWxRc7 1:1	33.84 ± 4.129^{bcedf}	9.80 ± 1.19^{ij}
α-L + DWxRc7 1: 3	28.05 ± 5.95^{bcedfgh}	16.23 ± 3.45^{hij}
α-L + DWxRc7 1:10	16.70 ± 4.22^{ghi}	26.87 ± 6.79^{efg}
α-L + Phytg3 1:1	41.08 ± 3.60^{ab}	11.90 ± 1.04^{ij}
α-L + Phytg3 1: 3	35.08 ± 4.37^{bced}	20.32 ± 2.54^{fghij}
α-L + Phytg3 1:10	29.42 ± 2.56^{bcdefg}	47.34 ± 4.12^{c}
α-L + Phytg7 1:1	36.68 ± 5.87^{abcd}	10.62 ± 1.70^{ij}
α-L + Phytg7 1: 3	35.97 ± 4.43^{bcd}	20.84 ± 2.57^{efg}
α-L + Phytg7 1:10	32.71 ± 5.22^{bcdef}	52.64 ± 8.40^{c}
WPI	38.70 ± 4.19^{abc}	11.11 ± 1.20^{ij}
WPI + DWxRc3 1:1	29.60 ± 3.95^{bcdef}	16.99 ± 2.84^{hij}
WPI + DWxRc3 1: 3	28.45 ± 3.90^{bcdefgh}	32.66 ± 4.48^{de}
WPI + DWxRc3 1:10	15.40 ± 5.95^{hi}	49.11 ± 18.98^{c}
WPI + DWxRc7 1:1	28.48 ± 3.94^{bcedfgh}	16.35 ± 2.27^{hij}
WPI + DWxRc7 1: 3	23.16 ± 4.22^{defghi}	26.59 ± 4.85^{efg}
WPI + DWxRc7 1:10	13.36 ± 4.99^{i}	42.61 ± 15.91^{cd}
WPI + Phytg3 1:1	27.85 ± 3.39^{bcedfgh}	15.99 ± 1.946^{hij}
WPI + Phytg3 1: 3	27.17 ± 2.22^{cdefgh}	31.19 ± 2.549^{defg}
WPI + Phytg3 1:10	21.06 ± 3.86^{fghi}	67.16 ± 12.31^{b}
WPI + Phytg7 1:1	33.43 ± 4.56^{bcedf}	19.19 ± 2.618^{ghij}
WPI + Phytg7 1: 3	32.41 ± 3.59^{cdefghi}	30.28 ± 3.63^{efg}
WPI + Phytg7 1:10	26.39 ± 3.16^{bcdef}	103.36 ± 11.45^{a}

Values represent mean ± standard deviation of three replicates per sample.
Means values with same letter are not significant different ($P < 0.05$)
[A] Protein concentration was quantified by Bradford protein assay

Lesser entrapment efficiency was found as the ratio of OSA-modified polysaccharide/protein increased. This result suggests that EE% of hydrophobic compounds such as TCNN is mainly influenced by the proportion of protein employed in the biopolymers combination.

Similar results were observed in the combinations of WPI with all different OSA-modified polysaccharides (Table 5.2). The maximum EE% was determined for WPI alone (38.70% $\pm$ 4.19) significantly different to its combination ratio of 1:1 and 1:3 with all other OSA-modified polysaccharides. Lesser EE% was observed as the ratio of OSA-modified polysaccharide/protein increased, which corroborates that the EE% is basically influenced by the amount of precipitated protein, even if more OSA-modified polysaccharide is adsorbed, as observed in Figure 5.5.

According to the percentage of protein and amount of precipitant shown on Table 5.1, the maximum entrapment of TCNN (103 $\pm$ 11.45 mgTCNN/g protein) was at the highest ratio (10/1) 7% OSA-modified phytoglycogen/ WPI, which was consistent with the maximum total sugar adsorbed by the electrostatic precipitation of WPI showed in Figure 5.5B.

The affinity of α-lactalbumin or WPI with the different OSA-modified polysaccharides seems to increase steadily as the ratio OSA-modified polysaccharide/protein increased, which proved to be more effective to entrap TCNN compared to lower combination ratios of 1:1 and 1:3. This result was consistent for the combination of either protein with all OSA-modified polysaccharides. Significant differences ($P < 0.05$) among the entrapment of TCNN (mgTCNN/g protein) by either α-

lactalbumin or WPI with the different OSA-modified polysaccharides were found at the combination ratio of 1:10 compared to the lower combination ratios, while no differences ($P > 0.05$) were observed for combination ratios of 1:1 and 1:3, regardless of the type of protein.

As explained above, high concentration of OSA-modified polysaccharide may unfold the β-lactoglobulin, the most abundant protein of WPI, due to an increment on the electrostatic repulsion and exposition of more hydrophobic domains would bind additional OSA-modified polysaccharides, therefore more TCNN. Additionally, the reduction of the electrostatic repulsion due to a pH close to the β-lactoglobulin pI (~5.2), affect even more the binding of more OSA-modified polysaccharides and hence TCNN. Similarly, the lower pH may cause α-lactalbumin to undergo conformational transition forming into a molten globule state, therefore exposing more hydrophobic domain, this in combination with the reduction of the electrostatic repulsion due to a pH close to its pI (~4.2), causes increase in binding more OSA-modified polysaccharides and more TCNN entraps during the precipitation process.

5.4.4 Relaxation time slopes of solution combinations of biopolymers at ratio 1:1

The relaxation time "λ"values were calculated according to equations 2.12 to 2.19 in section 2.6.4 (Chapter II). Previous work (Chapter IV) indicated that self-association of diluted amphiphilic molecules has been associated with a linear decrement of λ values (slope) as the effect of increment in the frequency oscillatory sweep, up to a critical frequency value (CFV) where the λ values change to a different slope (Figure

5.6). In previous works, changes in λ slope value at a CFV have been related to structure change for combinations between polyamide-6 and polymeric nanocomposites (Utracki et al., 2010) and similar slopes have been considered to present similar structures.

Linear decrement of λ values as the effect of increment in frequency was observed for all solutions of pure protein or in combination with OSA-modified polysaccharides. This result points out to the formation of some type of structure for all combinations of protein with OSA-modified polysaccharides.

Smaller critical frequency values were obtained for combinations of α-lactalbumin or WPI with DWxRc at both percentages of OSA modification (3 and 7%). However, pure proteins and in combination with 3% or 7% of OSA-modified phytoglycogen showed two distinct slopes with the one observed at medium frequency (0.31-6.2 rad/s) having higher CFV. Higher CFVs have been related to bigger size structures (Chapter IV).

These results are in agreement with previous work (Chapter IV), where higher concentration of OSA-modified phytoglycogen (18.0 g/L) is necessary to provide sufficient OSA ester groups and impart van der Waals, and hydrophobic attraction among particles in order to hold a spontaneous assembly and overcome the steric repulsion of the bigger phytoglycogen particles (approx. 40 nm); therefore, the higher the CFV (~32.5 rad/s), the bigger the size structure.

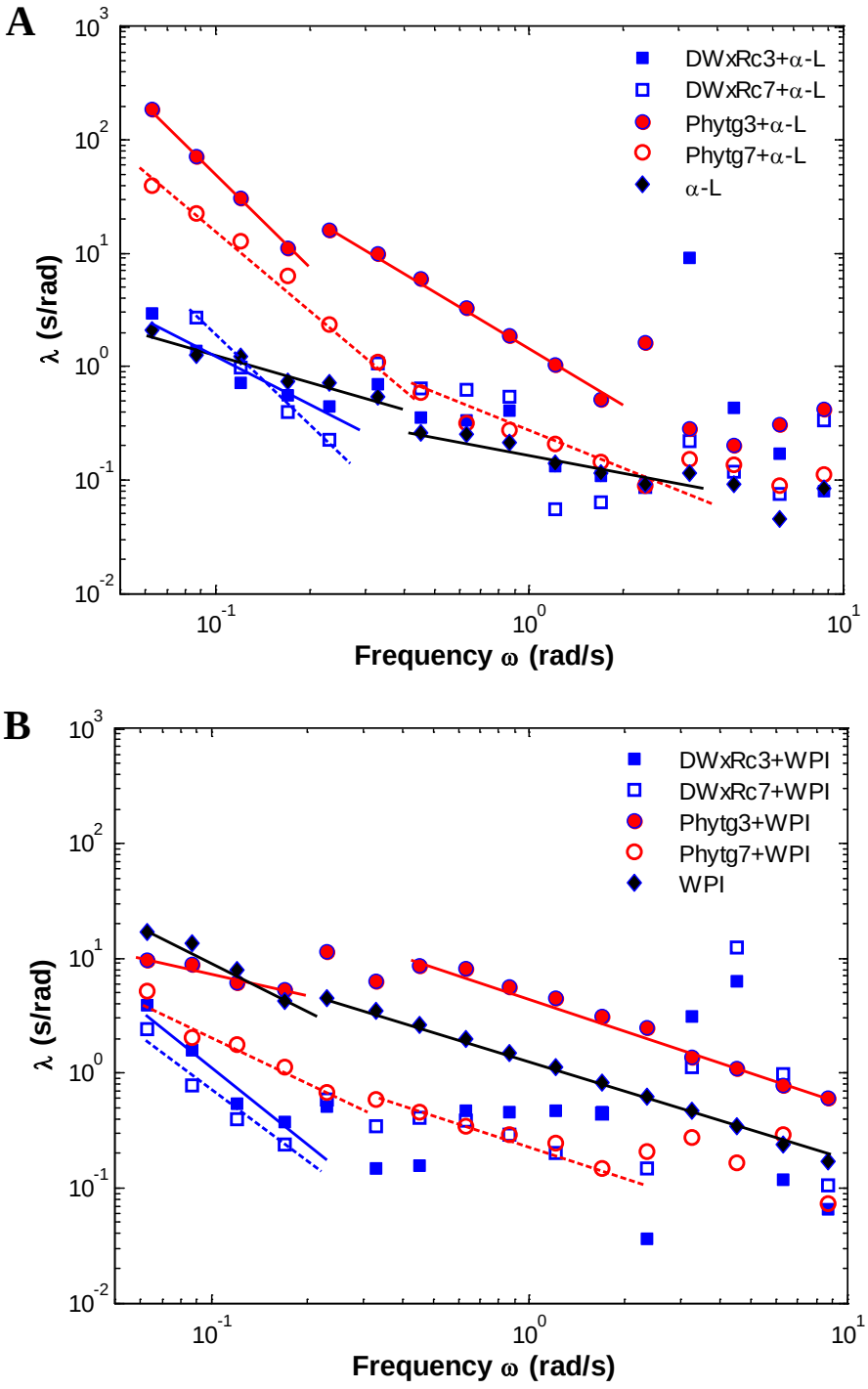

Figure 5.6. Relaxation time (λ) curves for different combination of biopolymers at 1:1 weight ratio with a total concentration of 184 g/L in aqueous solutions, evaluated by oscillatory sweep test at 0.01 Pa and 23°C.

The higher λ values observed on Figure 5.6 also relate to a solid-like dynamic response (Figure 5.6A). On previous work (Chapter IV), solid-like dynamic behavior was associated to structures that present difficult rotational movement, which present a high geometric aspect ratio. This behavior was only showed for the combination between α-lactalbumin and both types of OSA-modified phytoglycogen

Table 5.3 presents the results of the analysis of covariance in a general linear model comparing relaxation time (λ) slopes among solutions of α-lactalbumin or WPI alone and in combination (1:1) with OSA-modified polysaccharides influenced by an increment in the oscillatory frequency. The two distinct slopes observed in solutions of proteins alone or in combination with 3% or 7% of OSA-modified phytoglycogen were evaluated separately.

The two distinct λ slopes at low frequency (0.06- 0.3 rad/s) and medium frequency (0.31-6.2 rad/s) range observed in solutions of α-lactalbumin alone or in combination with 3% or 7% of OSA-modified phytoglycogen were separately evaluated.

According to the analysis of covariance, the two type of structures formed by α-lactalbumin alone are not significantly different ($P > 0.05$), as well as with some structures formed in combination with 3% OSA-modified WxRc and 3% or 7% OSA-modified phytoglycogen.

Table 5.3. Relaxation time (λ) slope and critical frequency value (CFV) for α-lactalbumin and WPI alone or in combinations (1:0, 1:1, 1:3, and 1:10) with different OSA-modified polysaccharides, evaluated with oscillatory sweep test at 0.01Pa and 23°C. Total biopolymers concentration in aqueous solution 180 g/L.

Polymer Mixture	**λ Slope**	**CFV (rad/s)**	**R^2**
α-L (low freq.)	-0.906 ± 0.265^{bc}	0.33	0.957
α-L (medium freq.)	-0.647 ± 0.221^{c}	2.34	0.913
α-L + DWxRc3	-1.627 ± 0.758^{b}	0.23	0.888
α-L + DWxRc7	-2.245 ± 0.576^{a}	0.23	0.955
α-L + Phytg3 (low freq.)	-3.174 ± 0.278^{a}	0.17	0.961
α-L + Phytg3 (medium freq.)	-1.643 ± 0.513^{b}	1.69	0.996
α-L + Phytg7 (low freq.)	-2.088 ± 0.585^{ab}	0.63	0.996
α-L + Phytg7 (medium freq.)	-2.176 ± 0.6036^{ab}	2.34	0.964
WPI (low freq.)	-1.894 ± 1.04^{b}	0.17	0.997
WPI (medium freq.)	-0.808 ± 0.06^{c}	23.4	0.998
WPI + DWxRc3	-2.324 ± 0.69^{ab}	0.17	0.997
WPI + DWxRc7	-2.362 ± 0.99^{ab}	0.17	0.992
WPI + Phytg3 (low freq.)	-1.461 ± 0.60^{b}	0.17	0.919
WPI + Phytg3 (medium freq.)	-0.852 ± 0.30^{c}	32.5	0.969
WPI + Phytg7 (low freq.)	-1.42 ± 1.45^{b}	1.69	0.929
WPI + Phytg7 (medium freq.)	-0.68 ± 0.17^{c}	12.1	0.988

Values represent mean ± standard deviation of three replicates per set of data.
Means values with same letter are not significantly different ($P > 0.05$)

The two λ slopes observed at low frequency (-2.088 ± 0.585) and medium frequency (-2.176 ± 0.6036) range in combination of α-lactalbumin and 7% OSA-modified phytoglycogen were not significantly different (P > 0.050). However, significant difference were found in combinations of α-lactalbumin and DWxRc7 (-2.245 ± 0.576), and some structure was formed with DWxRc3 (-1.627 ± 0.758) and Phytg3 (-1.643 ± 0.513). It is possible that two distinct structures are formed in these combinations of biopolymers.

The two distinct λ slopes observed at low frequency (0.06- 0.3 rad/s) and medium frequency (0.31-6.2 rad/s) range in solutions of WPI alone or in combination with 3% or 7% of OSA-modified phytoglycogen were evaluated independently. According to the analysis of covariance, a significant difference (P < 0.05) was observed between the two λ slopes observed for WPI alone and in combination with 3% and 7% OSA-modified phytoglycogen. Therefore, two distinct structures are possibly formed in these systems. On the other hand, no significant differences (P > 0.05) were found between the structures formed by WPI alone (-1.894 ± 1.04) compared to those formed in combination with DWxRc3 (-2.324 ± 0.69), DWxRc7 (-2.362 ± 0.99) Phytg3 (-1.461 ± 0.60), and Phytg7 (-1.42 ± 1.45), which indicated a similar structure formation.

5.4.5 Microstructure formation by solutions combination of biopolymers at ratio 1:1

The TEM micrographs (Figures 5.7 to 5.9) show a variety of particle shapes and sizes formed by α-lactalbumin and WPI alone (Figure 5.7) or in combination with OSA-

modified polysaccharides. The shape and size of particles seem affected by the type of amphiphilic biopolymer interaction characterized previously by the dynamic oscillatory test. Each solution of protein alone or in combination with OSA-modified polysaccharides formed one or more structures, which is in agreement with the relaxation time "λ" slope values determined using rheological method (Figure 5.6).

The results of the λ slope values observed on Figure 5.6 and the analysis of covariance (Table 5.3) confirm in some way the shape and size of particles formed by the different proteins alone or in combination with different OSA-modified polysaccharides. Particles formed by α-lactalbumin were small (~100nm) and big oblate ellipsoids (~1000nm) (Figure 5.7 A), similar to those observed for combination of α-lactalbumin and 7% OSA-modified phytoglycogen (Figures 5.8D).

The geometric aspect ratio of ellipsoids defined as the ratio of the major and minor axes ($r= a_1/a_2$), drastically affects their rotational motion (Goldsmith and Mason, 1962). In previous work, the geometric aspect ratio for anisotropic particles has been assumed as the ratio of the largest to the smallest dimension (Utracki et al., 2010), which seems to be resonable to define rod as r=length/diameter >> 1, and disk or platelets as r=diameter/thickness > 1, and spheroids r= ~1.

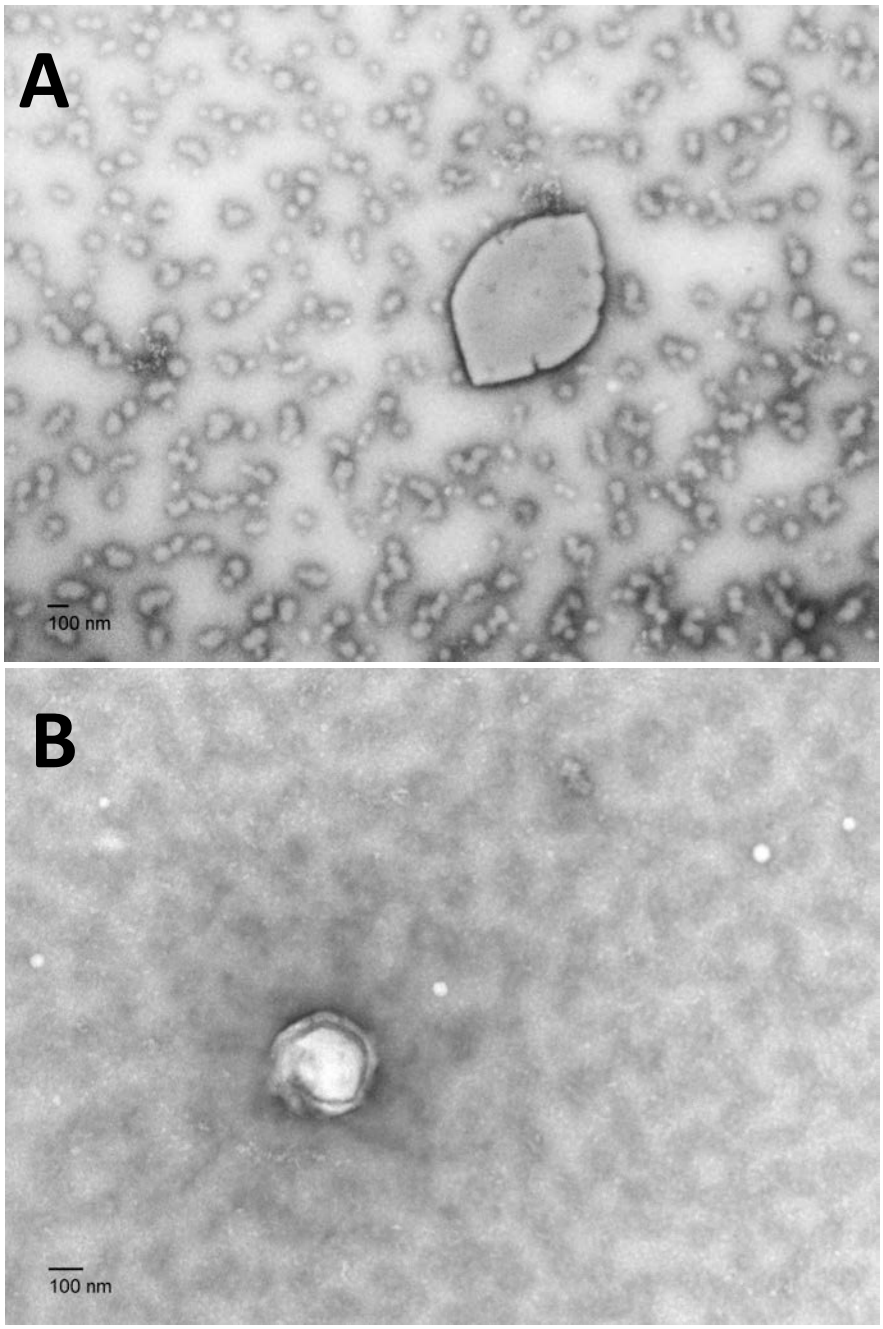

Figure 5.7. Micrographs of electrostatically precipitated particles formed at a concentration of 184 g/L (A) α-lactalbumin (α-L) and (B) Whey protein isolate (WPI). Images were taken at 50,000x magnification.

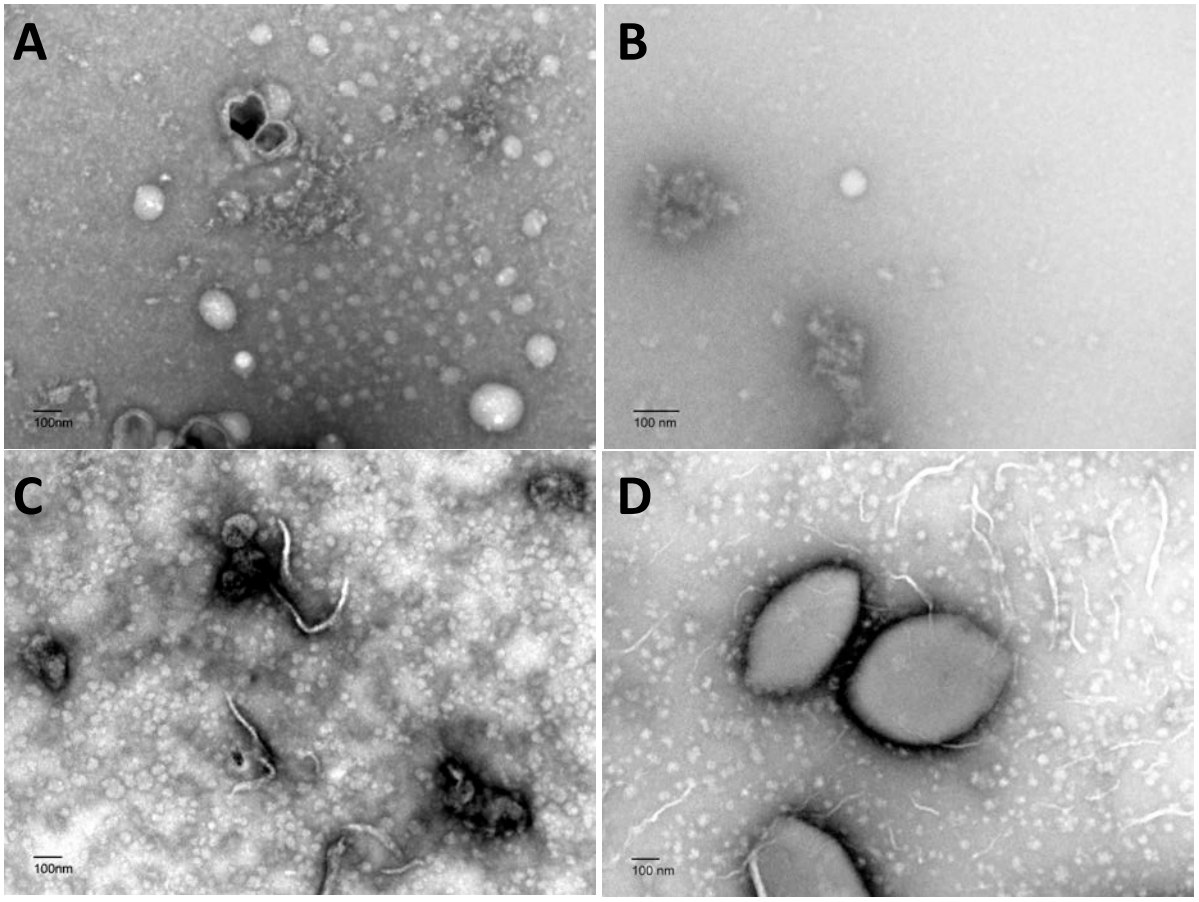

Figure 5.8. Micrographs of electrostatically precipitated particles formed at 1:1 weight ratio to a total concentration of 184 g/L for different combination of α-lactalbumin (α-L) with (A) DWxRc3, (B) DWxRc7, (C) Phytg3, and (D) Phytg7. Images were taken at 50,000x magnification.

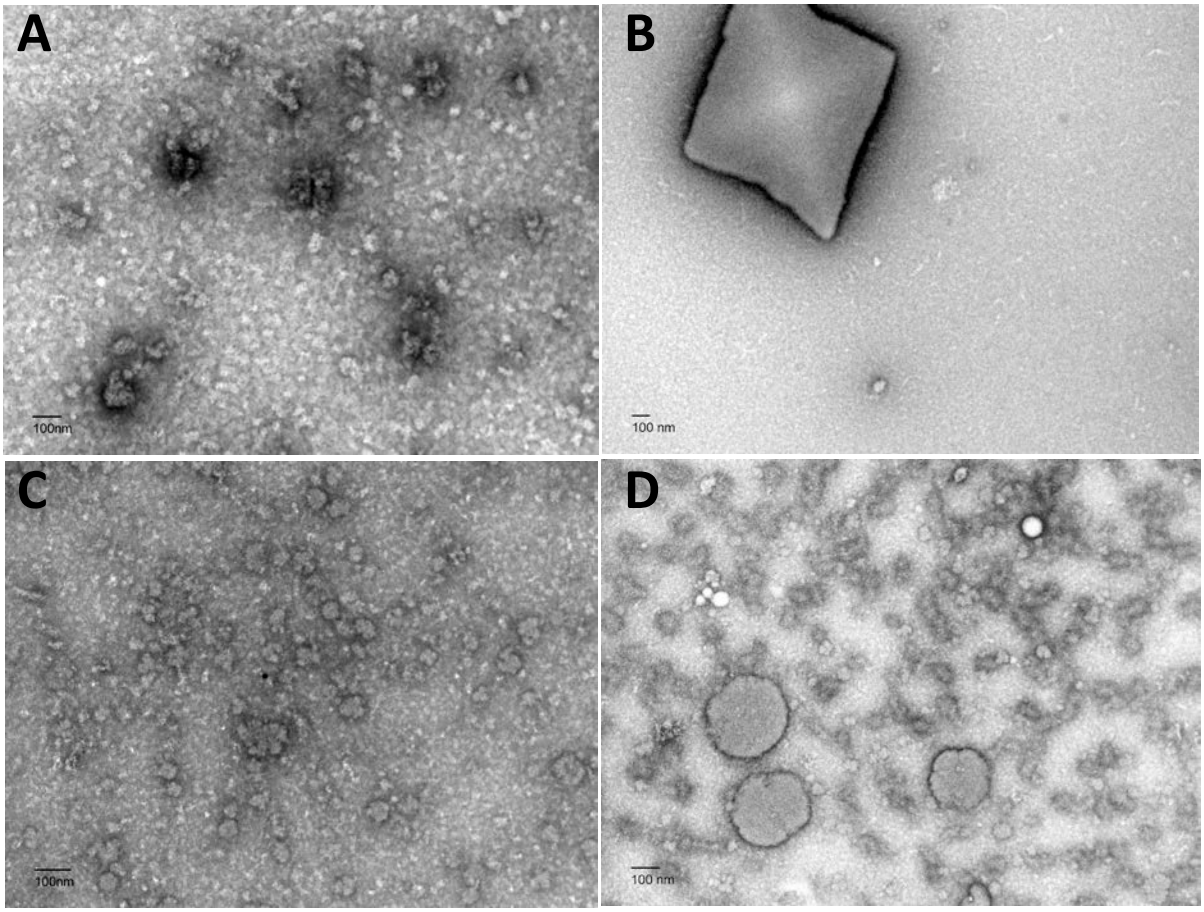

Figure 5.9. Micrographs of electrostatically precipitated particles formed at 1:1 weight ratio to a total concentration of 184 g/L for different combination of whey protein isolate (WPI) with (A) DWxRc3, (B) DWxRc7, (C) Phytg3, and (D) Phytg7. Images were taken at 50,000x magnification.

An interesting observation is the presence of a fiber-type structure (~1000nm) along with spheroid particles formed in the combination of α-lactalbumin with 3% (~300nm) and 7% OSA-modified phytoglycogen (~1000nm) (Figures 5.8C and D). It is possible that the solid-like behavior (Figure 5.6 A) characterized for these combination of biopolymers was influenced by the low rotational motion offered by this type of structure with a geometric aspect ratio r = length/diameter >> 1.

Similarly, small (<100nm) and big spheroid structures (200-400nm) were observed on the combination of WPI with 3% and 7% OSA-modified phytoglycogen (Figures 5.9C and D) with a geometric aspect ratio; r = ~ 1. The combination of WPI with 3% OSA-modified phytoglycogen (Figure 5.9C) presented cluster of particles (~200nm) besides small spheres possibly formed by aggregation of WPI alone. On the other hand, combination of WPI with 7% OSA-modified phytoglycogen presented big disk-type particles of approximately 400nm (aspect ratio; r > 1) besides small spheres (~100nm) possibly formed by aggregation of WPI alone (Figure 5.9 D).

Unlike the spherical structures (200-300nm) formed by WPI alone (Figure 5.7B) or the combination of WPI and α-lactalbumin with 3% OSA-modified DWxRc, the combination of WPI and 7% OSA-modified DWxRc formed a rhomboid type of structure of approximately 1000nm (Figure 5.9 B), which present a similar rotational motion as platelets, due to their similar geometric aspect ratio (aspect ratio; r > 1). Determination of the λ slope values demonstrates the potential of using rheological dynamic properties to ascertain the geometric aspect ratio of structures formed by the molecular interaction between amphiphilic molecules in aqueous solutions.

5.4.6 Particle size of structures formed by combination of biopolymers at ratio 1:1

Disagreements were found between the TEM micrographs (Figures 5.7 to 5.9) and the hydrodynamic diameter of the particles (Figure 5.10). All different particles formed by proteins alone or in combination with OSA-modified polysaccharides were significantly bigger than those observed by the TEM. Figure 5.10A shows that the smallest predominant particle size was found in the combination of α-lactalbumin and 7% OSA-modified DWxRc (~800 nm) followed by the combination with 7% OSA-modified phytoglycogen (~2500 nm), and pure α-lactalbumin (~5000 nm). The biggest particle size was observed in the combinations with 3% OSA-modified DWxRc (~7000 nm) and phytoglycogen (10,000 nm), respectively.

Figure 5.10B shows that the smallest predominant particle size was found on particles formed by pure WPI (~700 nm), followed by combination with 7% OSA-modified DWxRc (~1500) and phytoglycogen (~1500 nm) and the biggest particle size was observed in the combination with 3% OSA-modified phytoglycogen (~2000 nm) and DWxRc (~4000 nm), respectively. Self-assembled amphiphilic molecules can associate into a variety of structures that can be interchanged when the solution conditions change (Israelachvili, 2010). In this regard, the reduction of pH from 7.0 (dynamic oscillatory test conditions) to electrostatic precipitation at pH 4.5 affected the intermolecular forces within each aggregate, thereby modifying the size and shape of the structures ultimate precipitated. This effect was more noticeable in the combination of proteins and the lower percentage (3%) of OSA modification.

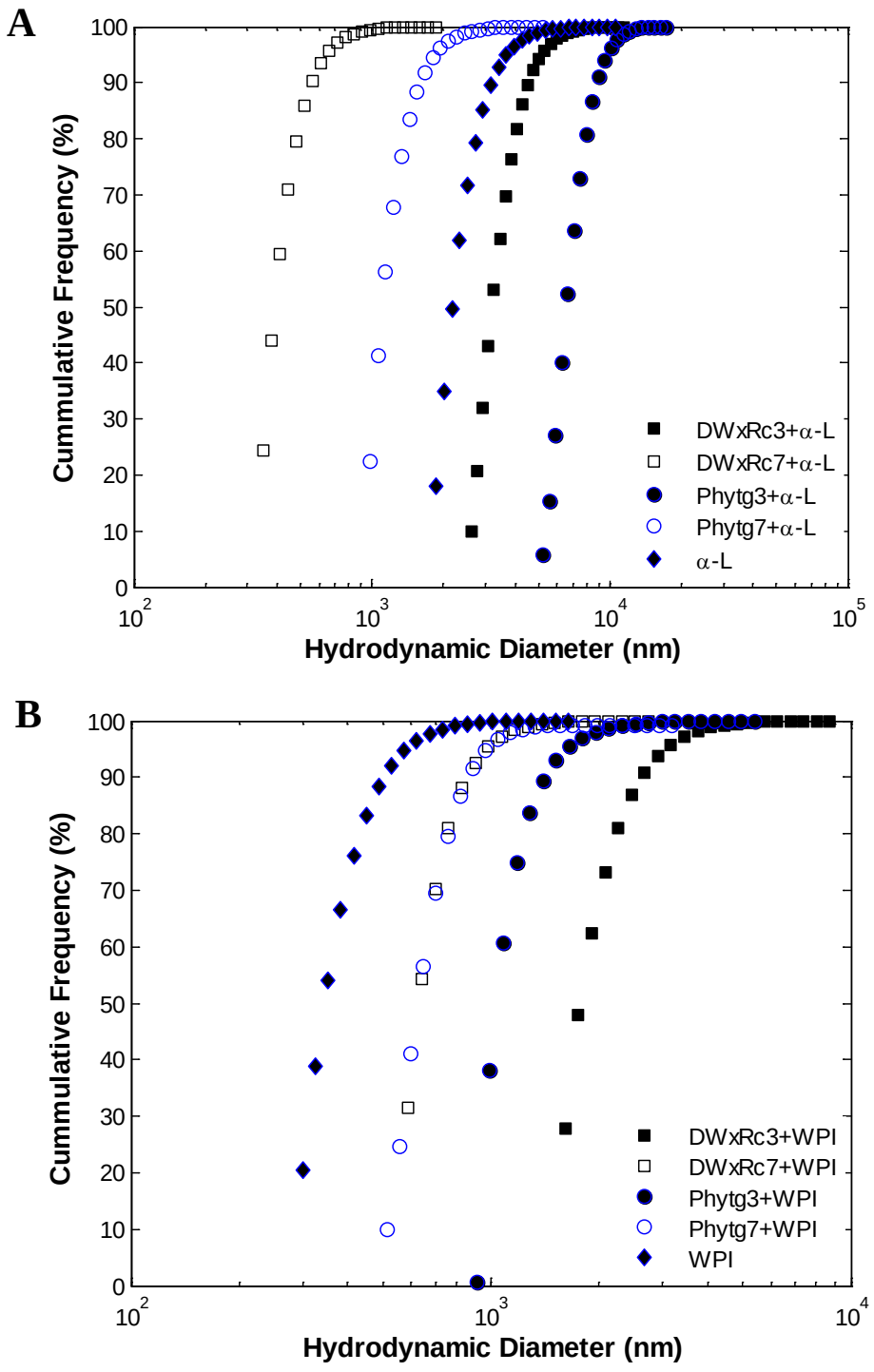

Figure 5.10. Particle size of electrostatically precipitated combination of proteins and OSA-modified polysaccharides at 1:1 weight ratio with a total concentration of 184 g/L.

The electrostatic precipitation induced the aggregation of particles due to reduction of electrostatic repulsion between proteins. Although, more stable particles seem to be formed by protein alone or in combination with higher percentage (7%) or OSA modification.

In previous studies, extensive aggregation of complex between β-lactoglobulin and pectins were attributed to the reduction in net charge between biopolymers at acid pH (Jones et al., 2010a), and more aggregation was observed in combination with higher anionic zeta potential at pH close to the protein pI . The stability of the heated protein/pectin complexes were improved with the addition of 200 mM of sodium chloride (Jones et al., 2010b). Moreover, the aggregation of β-lactoglobulin at low ionic strength solutions resulted from the increment of favorable attractive interactions due to screening effects. This electrostatic aggregation was an indication that hydrophobic attraction is not the only force to take in consideration for the formation of electrostatic precipitation of proteins, but also other type of forces such as electrostatic interaction between of amphiphilic biopolymers molecules should be taken into account according to the process of particle formation and isolation.

5.5 Conclusion

Electrostatic precipitation of protein alone or in combination of OSA-modified polysaccharides is a feasible method to entrap volatile and thermolabile compounds such as essential oils which function as antimicrobials, as well as flavors, vitamins,

polyunsaturated fatty acids, probiotic bacteria, enzymes and other compounds sensitive to degradation or loss of characteristic properties by the action of heat.

Absorbance measurements were in agreement with the total sugar interaction-adsorption of OSA-modified polysaccharides at the electrostatic precipitation of proteins, which in turn were congruent to the entrapment efficiency based on the amount of protein precipitated. These results suggest the use of a spectrophotometric measurement as a rapid, toxic free-solvent, easy and comparative method to evaluate the adsorption interaction between protein and other amphiphilic molecules.

The dynamic oscillatory test should be complemented by an additional analysis of the relaxation time "λ"value, which is the time associated with large scale motion (or changes) in the structure of polymers. The dynamic oscillatory response (solid-like or liquid-like) of proteins alone or in combination with OSA-modified polysaccharides has been related to rotational capability of structures. Structures with high geometric aspect ratio are more difficult to rotational motion compared to small ratio (r = ~1).

The linear decrements of relaxation time "λ"values (slope), which are sensitive to the frequency oscillatory sweep, have been associated as a characteristic for structure formation. Similar characteristic λ slopes values suggest similar structure shape, while the critical frequency, which point out the change of λ slope value, indicated the structure size; therefore, longer critical frequency indicates bigger particles assembled.

TEM visualization of electrostatically precipitated proteins alone or in combination with OSA-modified polysaccharides corroborated in some way the slope values of relaxation time "λ"and the critical frequency values with the shape and size of

structure assembled. It is possible that the structure initially assemble at neutral pH underwent into a change during the electrostatic precipitation at pH close to its pI, influenced by the change in protein native conformation and weakly electrostatic attraction between proteins themselves and with OSA-modified polysaccharides.

To understand the dynamic oscillatory responses in relation to the geometric aspect ratio of native assembled and electrostatically precipitated protein based structures, a visualization method that permits the observation of amphiphilic molecules assembled in their native environment (e.g. Cryo-TEM) must be performed in this regard. Hydrophobic forces, electrostatic interactions and other intermolecular forces must be taken aggregation must be taken in consideration to improve the self-assembly of amphiphilic biopolymers according to the process conditions for particles formation and isolation.

The developed methodology demonstrates the feasibility of using rheological dynamic properties to determine the geometric aspect ratio of anisotropic particles formed from electrostatic precipitation of proteins alone or in combination with OSA-modified polysaccharides. This opens the possibility for a wide range of research to evaluate the effect of shear rate, temperature, and ionic strength on the intermolecular affinity of different amphiphilic compounds in order to design aforetime and engineer particles of diverse size and shapes according to a desired application

CHAPTER VI

CONCLUSIONS

1. Small size dextrin (~15 nm) was produced by enzymatic depolymerization with α-amylase of previous gelatinized waxy corn (20 μm) and waxy rice (2 μm) starch granules.
2. The conversion of small size dextrin (~15 nm) and phytoglycogen (40 nm) to amphiphilic molecules by 3% and 7% octenyl succinate anhydrate (OSA) modification procedure farther the capability to engineer particles of small size characteristics.
3. Water sorption capability and the glass transition temperature (Tg) were reliable characterization techniques that allow prediction of the physical stability of OSA-modified polysaccharides.
4. Depolymerization of waxy starches increased their water sorption capability and reduced the Tg at high relative humidity environment (70% RH) compared to native waxy starches. The OSA modification did not change the adverse effect of depolymerization.
5. The moisture sorption isotherm method did not predict well the effect of adsorbed water on the physical characteristic of proteins like whey protein concentrate 80% (WPC), whey protein isolate (WPI), and α-lactalbumin (α-L), though it was associated with the effect of plasticization by water adsorption on the Tg values of OSA-polysaccharides exposed to higher than 70% RH.

6. The Kwei equation provided better correlation than the Gordon-Taylor equation in predicting the Tg's sensitivity to water sorption in most of the biopolymers evaluated in this study.
7. The critical water activity (Aw 0.25) of whey protein concentrated (WPC) consistently predicted the effect of adsorbed water on its rapid quality deterioration under storage at higher than 25% RH (RH = Aw*100). Mold growth was observed on samples of WPC stored at 97% RH.
8. The Fluorescent spectroscopic method was capable to ascertain formation of a micelle-type structure for WPI (0.6 g/L) and α-lactalbumin (2.5 g/L). Different types of structure were formed by OSA-polysaccharides (10-20 g/L).
9. Rheological characterization by using dynamic oscillatory test at 0.01Pa, 23°C and neutral pH (~7.0) was a suitable method to characterize the intermolecular association of amphiphilic biopolymers. The relaxation time "λ"value (G'/G"∗ω), was very sensitive to type, concentration and combination of biopolymers.
10. The observation of "λ" slope up to a critical frequency value suggest a type and size of structure formation, respectively. This analysis expanded the possibility to evaluate efficient encapsulating methods by self-assemble interaction of pure or combination of amphiphilic biopolymers in aqueous solution.
11. The type of protein under evaluation has a strong influence in the intermolecular associations with OSA-modified polysaccharides, and the percentage of OSA modification in polysaccharides influence to a certain extent, the amount of molecules interacting with the proteins. WPI showed more effective molecular

interaction than α-lactalbumin with all the OSA-modified polysaccharides evaluated in this study.

12. Absorbance measurements (600 nm) were corresponded well with OSA-polysaccharides interaction-adsorption by electrostatic precipitation of proteins and with the entrapment efficiency based on precipitated protein.
13. The "λ"slope and critical frequency value demonstrates the possibility to evaluate the geometric aspect ratio and size of anisotropic particles formed from electrostatic precipitation of proteins alone or in combination with OSA-polysaccharides.
14. Electrostatic precipitation (pH=4.5) of protein alone or combined with OSA-polysaccharides was well-suited and it offers a safer alternative to entrap volatile and thermolabile compounds than the commonly used PLGA (poly (lactic-co-glycolic) acid).

CHAPTER VII

RECOMMENDATIONS FOR FURTHER STUDIES

1. Investigate the effect of water sorption properties and Tg sensitivity to water sorption in biopolymer blends to correlate the entrapped compound release dynamics when it is exposed to different relative humidity environments.
2. Evaluate the effectiveness of Kwei or other equations to predict Tg sensitivity to water sorption in biopolymer blends to design polymeric combinations appropriate for control release of bioactive compounds exposed to different relative humidity environments.
3. Develop a method for visualization of particles formation in aqueous solution to enhance the usefulness of the rheological dynamic properties as they relate to the geometric aspect ratio of anisotropic particles formed at neutral pH (7.0) and after electrostatic precipitation (pH = 4.5) of proteins alone or in combination with OSA-modified polysaccharides.
4. Evaluate the influence of pH, temperature, ionic strength, and type of ion (e.g. monovalent and polyvalent) on the intermolecular affinity, structure geometry, and size of different amphiphilic biopolymers in order to engineer particles of diverse size and shapes according to the desired application.
5. Investigate the applicability of these inexpensive delivery systems (biopolymers blends) in food systems such as oxidative protection of vitamins, polyunsaturated

fatty acid, probiotics, as well as in improving the efficacy of antimicrobial compounds.

REFERENCES

Abiad, M.G., Carvajal, M.T., Campanella, O.H., (2009). A review on methods and theories to describe the glass transition phenomenon: Applicaton in food and pharmaceutical products. Food Engineering Review 1, 105 - 132.

Aminabhavi, T.M., Balundgi, R.H., Cassidy, P.E., (1990). A review on biodegradable plastics. Polymer-Plastics Technology and Engineering 29(3), 235-262.

Astete, C.E., Sabliov, C.M., (2006). Synthesis and characterization of PLGA nanoparticles. Journal of Biomaterials Science - Polymer Edition 17, 247-289.

Bai, Y., (2008). Preparation and structure of octenyl succinic anhydride modified waxy maize starch, microporous starch and maltodextrin, *Grain Science and Industry*. Kansas State University, Manhattan, Kansas, p. 57.

Barbosa-Cánovas, G.V., Fontana, A.J., Jr., Schmidt, S.J.L.T.P., (2007). *Water Activity in Foods - Fundamentals and Applications* (1st ed). John Wiley & Sons, Oxford, UK.

Blazek, J., Gilbert, E.P., (2010). Effect of Enzymatic Hydrolysis on Native Starch Granule Structure. Biomacromolecules 11(12), 3275-3289.

Borde, B., Bizot, H., Vigier, G., Buleon, A., (2002). Calorimetric analysis of the structural relaxation in partially hydrated amorphous polysaccharides. I. Glass transition and fragility. Carbohydrate Polymers 48(1), 83-96.

Bradford, M.A., (1976). A rapid and sensitive for the quantification of microgram quantities of protein utilizing the principle of protein-dye binding. Analytical Biochemistry 72, 248-254.

Brindle, L.P., Krochta, J.M., (2008). Physical properties of whey protein–hydroxypropylmethylcellulose blend edible films. Journal of Food Science 73(9), E446-E454.

Brostow, W., Chiu, R., Kalogeras, I.M., Vassilikou-Dova, A., (2008). Prediction of glass transition temperatures: Binary blends and copolymers. Materials Letters 62(17–18), 3152-3155.

Chae, B., Lane, A.M., Wiest, J.M., (2001). Thermorheological behavior of magnetic dispersions. Journal of Rheology 45(5), 1193-1204.

Chamberlain, E.K., Rao, M.A., (2000). Effect of concentration on rheological properties of acid-hydrolyzed amylopectin solutions. Food Hydrocolloids 14(2), 163-171.

Chen, J., Dickinson, E., (1995). Surface shear viscosity and protein-surfactant interactions in mixed protein films adsorbed at the oil-water interface. Food Hydrocolloids 9(1), 35-42.

Chhabra, R.P., (2010). Non-Newtonian Fluids: An Introduction, in: Deshpande, A., Krishnan , J.M., Kumar, P.B.S. (Eds.), *Rheology of Complex Fluids*. Springer, New York, NY, USA, p. 257.

Chirife, J., Timmermann, E.O., Iglesias, H.A., Boquet, R., (1992). Some features of the parameter k of the GAB equation as applied to sorption isotherms of selected food materials. Journal of Food Engineering 15(1), 75-82.

Clark, D.C., Husband, F., Wilde, P.J., Cornec, M., MillerR., (1995). Evidence of extraneous surfactant adsorption altering adsorbed layer properties of β-

lactoglobulin. Journal of the Chemical Society Faraday Transactions 91(13), 1991-1996.

Copeland, L., Blazek, J., Salman, H., Tang, M.C., (2009). Form and functionality of starch. Food Hydrocolloids 23(6), 1527-1534.

Desmazes, C., Lecomte, M., Lesueur, D., Phillips, M., (2000). A protocol for reliable measurement of Zero-Shear-Viscosity in order to evaluate the anti-rutting performance of binders, *2nd Eurasphalt & Eurobitume Congress* Barcelona, Spain, pp. 203-211.

Dickinson, E., Hong, S.-T., (1994). Surface coverage of β-lactoglobulin at the oil-water interface: Influence of protein heat treatment and various emulsifiers. Journal of Agricultural and Food Chemistry 42(8), 1602-1606.

Dickinson, E., Matsumura, Y., (1994). Proteins at liquid interfaces: Role of the molten globule state. Colloids and Surfaces B: Biointerfaces 3(1–2), 1-17.

Dickinson, E., Woskett, C.M., (1989). Competitive Adsorption Between Proteins And Small-Molecule In Food Emulsions, in: R. D. Bee, P.R., and J. Mingins. (Ed.), *Food Colloids*. Royal Society of Chemistry, London, UK, pp. 74-96.

Dumitriu, S., (2005). *Polysaccharides: Structural Diversity and Functional Versatility*. CRC Press, New York, NY, USA.

Engel, M.F.M., van Mierlo, C.P.M., Visser, A.J.W.G., (2002). Kinetic and structural characterization of adsorption-induced unfolding of bovine α-lactalbumin. Journal of Biological Chemistry 277(13), 10922-10930.

Esmaili, M., Ghaffari, S.M., Moosavi-Movahedi, Z., Atri, M.S., Sharifizadeh, A., Farhadi, M., Yousefi, R., Chobert, J.-M., Haertlé, T., Moosavi-Movahedi, A.A., (2011). Beta casein-micelle as a nano vehicle for solubility enhancement of curcumin; food industry application. LWT - Food Science and Technology 44(10), 2166-2172.

Fanun, M., (2010). Colloids in Drug Delivery, *Surfactant science* CRC Press/Taylor & Francis., Boca Raton, FL, USA.

Fournier, E., (2001). Colorimetric Quantification of Carbohydrates. Current Protocols in Food Analytical Chemistry, E1.1-E1.1.8.

Ganzevles, R.A., Zinoviadou, K., van Vliet, T., Cohen Stuart, M.A., de Jongh, H.H.J., (2006). Modulating surface rheology by electrostatic protein/polysaccharide interactions. Langmuir 22(24), 10089-10096.

Goldsmith, H.L., Mason, S.G., (1962). Particle motions in sheared suspensions XIII. The spin and rotation of disks. Journal of Fluid Mechanics Digital Archive 12(1), 88-96.

Gomes, C., Moreira, R.G., Castell-Perez, E., (2011). Poly (DL-lactide-co-glycolide) (PLGA) nanoparticles with entrappedtrans-cinnamaldehyde and eugenol for antimicrobial delivery applications. Journal of Food Science 76(2), N16-N24.

Gordon, M., Taylor, J.S., (1952). Ideal copolymers and the second order transitions of synthetic rubbers I. Non-crystalline copolymers Journal of Applied Chemistry 2, 493 - 500.

Gunasekaran, S., Ko, S., Xiao, L., (2007). Use of whey proteins for encapsulation and controlled delivery applications. Journal of Food Engineering 83(1), 31-40.

Gurruchaga, M., Silva, I., Goni, I., (2009). Physical blends of starch graft copolymers as matrices for colon targeting drug delivery systems. Carbohydrate Polymers 76(4), 593-601.

Hansted, J.G., Wejse, P.L., Bertelsen, H., Otzen, D.E., (2011). Effect of protein–surfactant interactions on aggregation of β-lactoglobulin. Biochimica et Biophysica Acta (BBA) - Proteins and Proteomics 1814(5), 713-723.

Harrison, R.G., Todd, P., Rudge, S.R., Petrides, D.P., (2003). *Bioseparations Science and Engineering*. Oxford University Press, Oxford, UK.

Hegg, P.O., (1980). Thermal stability of β-lactoglobulin as a function of pH and the relative concentration of sodium dodecylsulphate. Acta Agriculturae Scandinavica 30(4), 401-404.

Hernández-Marín, N.Y., Lobato-Calleros, C., Vernon-Carter, E.J., (2013). Stability and rheology of water-in-oil-in-water multiple emulsions made with protein-polysaccharide soluble complexes. Journal of Food Engineering 119(2), 181-187.

Hoiland, H., Blokhus, A.M., (2003). Solubilization in Aqueous Surfactant System, in: Birdi, K.S. (Ed.), *Surface and Colloid Chemistry*, Second ed. CRC Press, Boca Raton, FL, USA, p. 765.

Ipsen, R., Otte, J., (2007). Self-assembly of partially hydrolysed α-lactalbumin. Biotechnology Advances 25(6), 602-605.

Israelachvili, J.N., (2010). Intermolecular and Surface Forces, 3rd ed. Elsevier Science & Technology, St. Louis, MO, USA.

JECFA, (2011). Compendium of Food Additive Specifications, in: FAO/WHO (Ed.), *Monograph 11*. Joint FAO/WHO Expert Committee on Food Additives, Rome, Italy, p. 139.

JECFA, (2012). Compendium of Food Additive Specifications, in: FAO/WHO (Ed.), *Monograph 13*. Joint FAO/WHO Expert Committee on Food Additives, Geneva, Switzerland, p. 114.

Jones, M.N., Brass, A., (1991). Interaction Between Small Amphiphatic Molecules And Proteins, in: Dickinson, E. (Ed.), *Food, Polymers, Gels, and Colloids*. Royal Society of Chemistry, Cambridge, UK, pp. 65–80.

Jones, O., Decker, E.A., McClements, D.J., (2010a). Thermal analysis of β-lactoglobulin complexes with pectins or carrageenan for production of stable biopolymer particles. Food Hydrocolloids 24(2–3), 239-248.

Jones, O.G., Lesmes, U., Dubin, P., McClements, D.J., (2010b). Effect of polysaccharide charge on formation and properties of biopolymer nanoparticles created by heat treatment of β-lactoglobulin–pectin complexes. Food Hydrocolloids 24(4), 374-383.

Kalogeras, I.M., Brostow, W., (2009). Glass transition temperatures in binary polymer blends. Journal of Polymer Science Part B: Polymer Physics 47(1), 80-95.

Karlson, L., (2002). Hydrophobically modified polymers rheology and molecular associations, *Physical Chemistry*. Lund, Center for Chemistry & Chemical Engineering p. 131.

Kataoka, M., Tokunaga, F., Kuwajima, K., Goto, Y., (1997). Structural characterization of the molten globule of α-lactalbumin by solution X-ray scattering. Protein Science 6(2), 422-430.

Kontopidis, G., Holt, C., Sawyer, L., (2004). Invited review: beta-lactoglobulin: binding properties, structure, and function. J Dairy Sci 87(4), 785-796.

Konuma, T., Sakurai, K., Goto, Y., (2007). Promiscuous binding of ligands by β-lactoglobulin involves hydrophobic interactions and plasticity. Journal of Molecular Biology 368(1), 209-218.

Krieger, I.M., Gougherty, T.J., (1959). A mechanism for non-newtonian flow in suspensions of rigid spheres. Transactions of the Society of Rheology 3, 137-159.

Krstonošić, V., Dokić, L., Milanović, J., (2011). Micellar properties of OSA starch and interaction with xanthan gum in aqueous solution. Food Hydrocolloids 25(3), 361-367.

Kuwajima, K., (1989). The molten globule state as a clue for understanding the folding and cooperativity of globular-protein structure. Proteins: Structure, Function, and Bioinformatics 6(2), 87-103.

Kwei, T.K., (1984). The effect of hydrogen bonding on the glass transition temperatures of polymer mixtures. Journal of Polymer Science. Polymer Letters edition 22(6), 307-313.

Labuza, T.P., (1980). The effect of water activity on reaction kinetics of food deterioration. Food Technology 56(15), 36-43.

Levine, H., Slade, L., (1986). A polymer physico-chemical approach to the study of commercial starch hydrolysis products (SHPs). Carbohydrate Polymers 6(3), 213-244.

Li, S.-P., Ge, Z., Chen, H.-Y., (2005). The relationship between steady shear viscosity and complex viscosity. Journal of Dispersion Science and Technology 26, 415-419.

Liu, Z., Li, Y., Cui, F., Ping, L., Song, J., Ravee, Y., Jin, L., Xue, Y., Xu, J., Li, G., Wang, Y., Zheng, Y., (2008). Production of octenyl succinic anhydride-modified waxy corn starch and its characterization. Journal of Agricultural and Food Chemistry 56(23), 11499-11506.

Livney, Y.D., (2008). Complexes and conjugates of biopolymers for delivery of bioactive ingredients via food, in: Nissim, G. (Ed.), *Delivery and Controlled Release of Bioactives in Foods and Nutraceuticals*. Woodhead Publishing, The Hebrew University of Jerusalem, Israel, p. 464.

Livney, Y.D., (2010). Milk proteins as vehicles for bioactives. Current Opinion in Colloid & Interface Science 15, 73-83.

Madene, A., Jacquot, M., Scher, J., Desobry, S., (2006). Flavor encapsulation and controlled release – A review. International Journal of Food Science and Technology 41(1-21).

Mahler, G.J., Esch, M.B., Tako, E., Southard, T.L., Archer, S.D., Glahn, R.P., Shuler, M.L., (2012). Oral exposure to polystyrene nanoparticles affects iron absorption. Nature Nanotechnology 7(4), 264-271.

Majhi, P.R., Ganta, R.R., Vanam, R.P., Seyrek, E., Giger, K., Dubin, P.L., (2006). Electrostatically driven protein aggregation: β-lactoglobulin at low ionic strength. Langmuir 22(22), 9150-9159.

Maldonado-Valderrama, J., Patino, J.M.R., (2010). Interfacial rheology of protein–surfactant mixtures. Current Opinion in Colloid & Interface Science 15(4), 271-282.

Mattice, W.L., Riser, J.M., Clark, D.S., (1976). Conformational properties of the complexes formed by proteins and sodium dodecyl sulfate. Biochemistry 15(19), 4264-4272.

Meyers, M.A., Chawla, K.K., (2009). *Mechanical Behavior of Materials*. Cambridge University Press Cambridge, UK

Nissim, G., (2008). *Delivery and Controlled Release of Bioactives in Foods and Nutraceutical*. CRC Press Boca Raton, FL, USA.

Noirez, L., Baroni, P., (2012). Identification of a low-frequency elastic behavior in liquid water. Journal of Physics: Condensed Matter 24, 1-6.

Nylander, T., Arnebrant, T., Bos, M., Wilde, P., (2008). Protein/Emulsifier Interactions, in: Hasenhuettl, G., Hartel, R. (Eds.), *Food Emulsifiers and Their Applications*. Springer New York, NY, USA, pp. 89-171.

Osaki, K., Inoue, T., Uematsu, T., (2001). Viscoelastic properties of dilute polymer solutions: The effect of varying the concentration. Journal of Polymer Science Part B: Polymer Physics 39(2), 211-217.

Parfitt, G.D., Rochester, C.H., (1983). *Adsorption From Solution at the Solid/Liquid interface*. Academic Press London, UK.

Pätzold, G., Dawson, K., (1996). Connection of microstructure to rheology in a microemulsion model. Physical Review E 54(2), 1669-1682.

Permyakov, E.A., Berliner, L.J., (2000). α-lactalbumin: structure and function. FEBS Letters 473(3), 269-274.

Prochaska, K., Kędziora, P., Le Thanh, J., Lewandowicz, G., (2007). Surface activity of commercial food grade modified starches. Colloids and Surfaces B: Biointerfaces 60(2), 187-194.

Quintanar-Guerrero, D., Allémann, E., Fessi, H., Doelker, E., (1998). Preparation techniques and mechanisms of formation of biodegradable nanoparticles from preformed polymers. Drug Development and Industrial Pharmacy 24(12), 1113-1128.

Rahman, S., (1999). *Handbook of Food Preservation*. Marcel Dekker, New York.

Recio, I., Ramos, M., Pilosof, A.M.R., (2008). Engineered Food/Protein Structure And Bioactive Proteins and Peptides From Whey, in: Gutiérrez-López, G., Barbosa-Cánovas, G., Welti-Chanes, J., Parada-Arias, E. (Eds.), *Food Engineering: Integrated Approaches*. Springer New York, NY, USA, pp. 399-414.

Rogers, A., Gibon, Y., (2009). Enzyme Kinetics: Theory and Practice, in: Schwender, J. (Ed.), *Plant Metabolic Networks*. Springer, New York, NY, USA, pp. 71-103.

Rojas, E., Torres, G., (2013). Isolation and recovery of glycomacropeptide from milk whey by means of thermal treatment. Food Science and Technology (Campinas) 33, 14-20.

Roland, C.M., (2008). Characteristic relaxation times and their invariance to thermodynamic conditions. Soft Matter 4(12), 2316-2322.

Roos, Y.H., (2010). Glass transition temperature and its relevance in food processing. Annual Review of Food Science and Technology 1(1), 469-496.

Rosen, M.J., Kunjappu, J.T., (2012). *Surfactants and Interfacial Phenomena* (4th ed). John Wiley & Sons, Hoboken, NJ, USA.

Roylance, D., (2001). Engineering Viscoelasticity, Cambridge, MA : Massachusetts Institute of Technology.

Scheffler, S.L., Huang, L., Bi, L., Yao, Y., (2010a). In vitro digestibility and emulsification properties of phytoglycogen octenyl succinate. Journal of Agricultural and Food Chemistry 58(8), 5140-5146.

Scheffler, S.L., Wang, X., Huang, L., San-Martin Gonzalez, F., Yao, Y., (2010b). Phytoglycogen octenyl succinate, an amphiphilic carbohydrate nanoparticle, and ∈-polylysine to improve lipid oxidative stability of emulsions. Journal of Agricultural and Food Chemistry 58(1), 660.

Schramm, G., (2002). *A Practical Approach to Rheology and Rheometry* (2nd ed). Thermo Haake GmbH, Karlsruhe, Germany.

Sekhon, B.S., (2010). Food nanotechnology - An overview. . Nanotechnology, Science and Application. 3, 1-15.

Shaw, K.L., Grimsley, G.R., Yakovlev, G.I., Makarov, A.A., Pace, C.N., (2001). The effect of net charge on the solubility, activity, and stability of ribonuclease Sa. Protein Science 10(6), 1206-1215.

Shpigelman, A., Israeli, G., Livney, Y.D., Thermally-induced protein-polyphenol co-assemblies: beta lactoglobulin-based nanocomplexes as protective nanovehicles for EGCG. Food Hydrocolloids 24(8), 735-743.

Slade, L., Levine, H., (1995). Glass Transitions and Water-Food Structure Interactions, in: John, E.K., Steve, L.T. (Eds.), *Advances in Food and Nutrition Research*. Academic Press, Nabisco Fundamental Science Group East Hanover, NJ, USA pp. 103-269.

Steffe, J.F., (1996). *Rheological Methods in Food Process Engineering* (2nd ed). Freeman Press, East Lansing, MI, USA.

Sunthar, P., (2010). Polymer Rheology, in: Krishnan, J.M., Deshpande, A.P., Kumar, P.B.S. (Eds.), *Rheology of Complex Fluids*. Springer New York, pp. 171-191.

Talwar, S., Scanu, L.F., Khan, S.A., (2006). Hydrophobic interactions in associate polymer/nonionic surfactant systems: Effects of surfactant arquitecture an system parameters. Journal of Rheology 50(6), 831-847.

Tang, C.H., Wu, H., Yu, H.P., Li, L., Chen, Z., Yang, X.Q., (2006). Coagulation and gelation of soy protein isolates induced by microbial transglutaminase. Journal of Food Biochemistry 30(1), 35-55.

Tesch, R., Ramon, O., Ladyzhinski, I., Cohen, Y., Mizrahi, S., (1999). Water sorption isotherm of solution containing hydrogels at high water activity. International Journal of Food Science & Technology 34(3), 235-243.

Tesch, S., Gerhards, C., Schubert, H., (2002). Stabilization of emulsions by OSA starches. Journal of Food Engineering 54(2), 167-174.

Tharanathan, R.N., (2005). Starch — Value addition by modification. Critical Reviews in Food Science and Nutrition 45(5), 371-384.

Timmermann, E.O., (1989). A B.E.T. - like three sorption stage isotherm. Journal of the Chemical Society, Faraday Transactions 1: Physical Chemistry in Condensed Phases 85(7), 1631-1645.

Timmermann, E.O., (2003). Multilayer sorption parameters: BET and GAB values? Colloids and Surfaces A: Physicochemical and Engineering Aspects 220, 235-260.

Timmermann, E.O., Chirife, J., Iglesias, H.A., (2001). Water sorption isotherms of foods and foodstuffs: BET or GAB parameters? Journal of Food Engineering 48(1), 19-31.

Turro, N.J., Kuo, P.-L., (1986). Pyrene Excimer Formation in Micelles of Nonionic Detergents and of Water-Soluble Polymers. Langmuir 2(4), 438-442.

Utracki, L.A., (2004). Clay-containing Polymeric Nanocomposites, *Technology & Engineering*. iSmithers Rapra Publishing, pp. 27-54.

Utracki, L.A., Lyngaae-Jørgensen, J., (2002). Dynamic melt flow of nanocomposites based on poly-ε-caprolactam. Rheologica Acta 41(5), 394-407.

Utracki, L.A., Sepehr, M.M., Carreau, P.J., (2010). Rheology of Polymers with Nanofillers, *Polymer Physics*. John Wiley & Sons, Inc., pp. 639-708.

Varona, S., Martín, Á., Cocero, M.J., (2009). Formulation of a natural biocide based on lavandin essential oil by emulsification using modified starches. Chemical Engineering and Processing: Process Intensification 48(6), 1121-1128.

Verheul, M., Pedersen, J.S., Roefs, S.P.F.M., de Kruif, K.G., (1999). Association behavior of native β-lactoglobulin. Biopolymers 49(1), 11-20.

Viswanathan, A., (1999). Effect of degree of substitution of octenyl succinate starch on enzymatic degradation. Journal of environmental polymer degradation 7(4), 185-190.

Wang, X., Li, X., Chen, L., Xie, F., Yu, L., Li, B., (2011). Preparation and characterisation of octenyl succinate starch as a delivery carrier for bioactive food components. Food Chemistry 126(3), 1218-1225.

Waninge, R., Paulsson, M., Nylander, T., Ninham, B., Sellers, P., (1998). Binding of sodium dodecyl sulphate and dodecyl trimethyl ammonium chloride to β-lactoglobulin: A calorimetric study. International Dairy Journal 8(2), 141-148.

Wolszczak, M., Miller, J., (2002). Characterization of non-ionic surfactant aggregates by fluorometric techniques. Journal of Photochemistry and Photobiology A: Chemistry 147, 45-54.

Wu, B., Degner, B., McClements, D.J., (2013). Microstructure & rheology of mixed colloidal dispersions: Influence of pH-induced droplet aggregation on starch granule–fat droplet mixtures. Journal of Food Engineering 116(2), 462-471.

Wurzburg, O.B., (1972). Starch in food industry, in: Furia, T.E. (Ed.), *Handbook of Food Additives*, 2nd ed. CRC Press, Cleveland, p. 998.

Zhou, Y., Vitkup, D., Karplus, M., (1999). Native proteins are surface-molten solids: application of the lindemann criterion for the solid versus liquid state. Journal of Molecular Biology 285(4), 1371-1375.

APPENDIX A

Table A1.Zero-Shear-Viscosity (ZSV) values for serial dilutions of different biopolymers, calculated from creep test at 0.01Pa and 23°C

	α–Lactalbumin		Whey Protein Isolate		DWxRc-3OSA		DWxRc-7OSA		Phytg-3OSA		Phytg-7OSA	
g/L	Average	Stdev.	Average	Stdev.	Average	Stdev.	Average	Stdev.	Average	Stdev.	Average	Stdev.
36.8	0.042^{a}	0.0025	0.043^{ab}	0.0103	0.034^{b}	0.0042	0.034^{ab}	0.0030	0.035^{a}	0.0027	0.034^{b}	0.0018
18.4	0.031^{abc}	0.0093	0.039^{ab}	0.0052	0.027^{bc}	0.0062	0.026^{b}	0.0039	0.035^{a}	0.0039	0.028^{b}	0.0012
14.72	0.023^{bc}	0.0028	0.032^{ab}	0.0042	0.032^{b}	0.0029	0.029^{ab}	0.0057	0.039^{a}	0.0087	0.022^{c}	0.0037
11.04	0.029^{b}	0.0039	0.026^{bc}	0.0031	0.019^{c}	0.0043	0.031^{b}	0.0027	0.025^{ab}	0.0063	0.026^{bc}	0.0081
7.36	0.021^{c}	0.0035	0.044^{a}	0.0044	0.020^{bc}	0.0059	0.026^{b}	0.0019	0.036^{a}	0.0047	0.020^{c}	0.0014
3.68	0.025^{bc}	0.0042	0.032^{b}	0.0024	0.031^{b}	0.0032	0.029^{ab}	0.0075	0.024^{b}	0.0047	0.024^{bc}	0.0035
1.84	0.033^{ab}	0.0075	0.021^{c}	0.0053	0.027^{bc}	0.0081	0.031^{ab}	0.0070	0.027^{b}	0.0015	0.044^{a}	0.0050
1.472	0.028^{b}	0.0030	0.022^{c}	0.0032	0.030^{b}	0.0042	0.035^{ab}	0.0045	0.031^{ab}	0.0095	0.035^{ab}	0.0085
1.104	0.028^{bc}	0.0059	0.037^{ab}	0.0090	0.028^{ab}	0.0095	0.026^{b}	0.0071	0.029^{ab}	0.0037	0.026^{bc}	0.0081
0.736	0.042^{a}	0.0052	0.036^{ab}	0.0069	0.044^{a}	0.0069	0.043^{a}	0.0081	0.022^{b}	0.0072	0.032^{b}	0.0041
0.368	0.021^{c}	0.0042	0.027^{abc}	0.0072	0.030^{abc}	0.0069	0.031^{ab}	0.0073	0.032^{ab}	0.0036	0.033^{ab}	0.0071
0.184	0.028^{abc}	0.0076	0.025^{abc}	0.0052	0.023^{bc}	0.0048	0.031^{ab}	0.0051	0.029^{ab}	0.0099	0.031^{abc}	0.0092

Values represent mean and standard deviation of three replicates per set of data.
Means values with same letter are not significantly different ($P > 0.05$)